

Universidade Federal de São Carlos
Centro de Ciências Exatas e de Tecnologia
Departamento de Química
Programa de Pós-Graduação em Química

Alana Kelyene Pereira

**Caracterização das interações químicas entre os
microrganismos simbiotes das formigas cortadeiras**

Tese de Doutorado

São Carlos, SP

2021

Universidade Federal de São Carlos
Centro de Ciências Exatas e de Tecnologia
Departamento de Química
Programa de Pós-Graduação em Química

Caracterização das interações químicas entre os microrganismos simbiotes das formigas cortadeiras

Alana Kelyene Pereira*

Tese apresentada como parte dos requisitos para obtenção do título de Doutora em Ciências, na área de concentração de Química Orgânica.

Orientador: Prof. Dr. João Batista Fernandes

*Bolsista FAPESP

São Carlos, SP

2021



Folha de Aprovação

Defesa de Tese de Doutorado da candidata Alana Kelyene Pereira, realizada em 13/01/2021.

Comissão Julgadora:

Prof. Dr. João Batista Fernandes (UFSCar)

Profa. Dra. Fernanda Oliveira das Chagas (UFRJ)

Profa. Dra. Anelize Bauermeister (UCSD)

Profa. Dra. Angela Regina Araujo (UNESP)

Profa. Dra. Simone Possedente de Lira (USP)

O presente trabalho foi realizado com apoio da Fundação de Amparo a Pesquisa do Estado de São Paulo – FAPESP, Processo 2016/12304-2 e da Coordenação de Aperfeiçoamento de Pessoal de Nível Superior – Brasil (CAPES) - Código de Financiamento 001.

O Relatório de Defesa assinado pelos membros da Comissão Julgadora encontra-se arquivado junto ao Programa de Pós-Graduação em Química.

Dedico à mulher mais importante da minha vida, que sempre me ensinou que podem
nos tirar tudo que temos, exceto aquilo que aprendemos.

Minha Vó Cecília.

(in memoriam)

*“Sinto que sou muito mais completa quando não entendo.
Não entender, do modo como falo, é um dom.
Não entender, mas não como um simples de espírito.
O bom é ser inteligente e não entender.
É uma benção estranha, como ter loucura sem ser doida.
É um desinteresse manso, é uma doçura de burrice.
Só que de vez em quando vem a inquietação: quero entender um pouco.
Não demais: mas pelo menos entender que não entendo.”*

Clarice Lispector

Agradecimentos

Sou grata a todos aqueles que estiveram ao meu lado e me ajudaram de diferentes formas durante esses anos do doutorado. Primeiramente, gostaria de agradecer ao prof. Dr. João Batista, pela orientação, paciência e por sempre me permitir tentar minhas ideias.

Nada disso seria possível sem algumas amizades que cruzaram meu caminho e contribuíram com conversas, discussões sobre a vida: Dorai, pela amizade, pelo apoio e por todas as palavras de incentivo. Hocelayne, pela companhia em todos os congressos. Leila, por todos conselhos e sugestões de como melhorar meu trabalho. Táhcita, por todos os desabafos no fim dos dias. Obrigada pela amizade de vocês!

Ao prof. Dr. Dieter Spiteller por me aceitar em seu grupo de pesquisa na Alemanha. Aos colegas em Konstanz, Basanta, Kene, Karin, Darshani, Laetitia, Nico e Ines por terem deixado meus dias muito mais felizes! Vocês me ensinaram bastante! *Dankeschön!*

Muito obrigada pelas valiosas colaborações que fiz durante a execução do projeto: as análises de imageamento por MS do grupo da prof. Dra. Taicia Fill na Unicamp. À Anelize Bauermeister e o prof. Dr. Norberto Pepporine, pelas análises por LC-MS/MS e ajuda com a plataforma GNPS e pelas discussões dos resultados. Aos alunos do NPPS-USP, Ana Paula, Camila e Danielle por me ajudarem com o MZMine e GNPS. Aos prof. Drs. Pagnocca e prof. André, do CEIS-UNESP, por cederem os microrganismos e pelas discussões sobre microbiologia. Aprendi muito com a colaboração de vocês!

Às agências de fomento à pesquisa, Capes, CNPq e, em especial, à Fapesp pelo apoio financeiro (Processos 2016/12304-2 e 2018/21936-8) e pelas oportunidades de apresentar um pouco do meu trabalho em diversas conferências.

Essa tese não seria escrita sem a ajuda de Alexandra Elbakyan, criadora do Sci-Hub! Lutemos por uma ciência de livre acesso e obrigada pela iniciativa!

E por último mas não menos importante, gostaria de agradecer ao meu irmão, Kaique, pelo amor incondicional e por estar sempre ao meu lado! A minha avó Cecília, que não está mais aqui, e meu avô José, que sempre me incentivaram a estudar e a nunca desistir. Ao Zé Claudio, por ser incrível e sempre me lembrar o quanto eu também sou.

Vocês me ajudam a ser um ser humano melhor! Amo vocês.

Lista de abreviaturas e siglas

ACN	Acetonitrile
BCG	Biosynthetic Gene Clusters
BY	Black Yeasts
COSY	^1H - ^1H Correlation Spectroscopy
DESI	Desorption Electrospray Ionization
EDTA	Ethylenediamine tetraacetic acid
DDA	Data Dependent Acquisition
DNA	Deoxyribonucleic Acid
EtAc	Ethyl Acetate
FBMN	Feature-Based Molecular Networking
FPTase	Farnesyl-protein transferase
GC-MS	Gas Chromatography coupled to Mass Spectrometry
GNPS	Global Natural Product Social Molecular Networking
HCA	Hierarchical Cluster Analysis
HMDB	Human Metabolome Database
HMBC	Heteronuclear Multiple Bond Correlation
HPLC	High Pressure Liquid Chromatography
HSQC	Heteronuclear Single Quantum Coherence
HRMS	High Resolution Mass Spectrometry
IMS	Imaging Mass Spectrometry
LCA	Leaf-cutting Ants

LC-MS	Liquid Chromatography - to Mass Spectrometry
LC-HRMS	Liquid Chromatography - High Resolution Mass Spectrometry
MALDI	Matrix Assisted Laser Desorption
MeOH	Methanol
MN	Molecular Networking
MVDA	Multivariate Data Analysis
MQS	Minimum Qualification Score
<i>m/z</i>	Mass-to-charge ratio
NCBI	National Center for Biotechnology Information
NRPS	Nonribosomal Peptide Synthase
OSMAC	One Strain Many Compounds
PCR	Polymerase chain reaction
PCA	Principal Component Analysis
PDA	Potato Dextrose Agar
PKS	Polyketide Synthase
PLS-DA	Partial Least Squares - Discriminant Analysis
SDS	SDS Protein Separation Medium
SFM	Soya Flour Mannitol
SPE	Solid Phase Extraction
SISGEN	Sistema Nacional de Gestão do Patrimônio Genético e do Conhecimento Tradicional Associado
YEME	Yeast and malt medium agar

Resumo

CARACTERIZAÇÃO DAS INTERAÇÕES QUÍMICAS ENTRE OS MICRORGANISMOS SIMBIONTES DAS FORMIGAS CORTADEIRAS. A complexa simbiose do ninho das formigas da tribo Attini inspira a curiosidade em diversos campos de pesquisa desde Microbiologia à Ecologia Química. As formigas dessa tribo se caracterizam por cultivar o fungo mutualista *Leucoagaricus gongylophorus* como alimento há cerca de 50 milhões de anos, em organizações conhecidas como “jardins de fungos”. Em um ambiente extremamente rico em material vegetal, parasitas como fungos do gênero *Escovopsis* surgem e podem prejudicar o formigueiro. Outros microrganismos, como actinobactérias produzem antibióticos que ajudam a protegê-las de parasitas e invasores. A descoberta dos fungos negros, relacionados ao gênero *Phialophora*, presentes no tegumento das formigas cortadeiras foi importante para impulsionar estudos sobre sua relação química-ecológica com outros simbioses. O sistema de agricultura das formigas cortadeiras, englobam os gêneros *Atta* e *Acromyrmex*, que caracterizam por cultivar uma única espécie fúngica que não sobrevivem sem o mutualismo. O presente estudo buscou utilizar de ferramentas analíticas para entender o funcionamento das interações químicas entre os diferentes grupos de simbioses das formigas cortadeiras. A tese foi dividida em três partes principais: **A)** uma abordagem dos cocultivos realizados com os diferentes microrganismos simbioses das formigas cortadeiras, além da discussão sobre as metodologias utilizadas que ajudou a compreender como ocorre a comunicação química entre esses organismos; **B)** a utilização de análise multivariada, mapeamentos moleculares, imageamento por espectrometria de massas e ensaios biológicos na interação entre a levedura negra, *P. capiguarae*, e fungo *Escovopsis* dos ninhos; **C)** a investigação da função ecológica do metabolito bio-ativo da levedura negra nos jardins das formigas cortadeiras relacionado à sua atividade contra a actinobactéria. As discussões desse trabalho colaboram com as pesquisas sobre as interações microbianas existentes no ninho das cortadeiras relacionadas aos fungos negros e sua função químico-ecológica, relatadas aqui pela primeira vez. E, ainda assim, futuros estudos relacionados ao novo simbiote das aténeas mostram-se bastante promissores para compreender um pouco mais sobre essa complexidade microbiana.

Palavras-chaves: Formigas aténeas, Formigas cortadeiras, Fungos negros; Leveduras negras, *Phialophora*; interações microbianas; metabolômica microbiana.

Abstract

CHEMICAL INTERACTIONS AMONG LEAF-CUTTING ANTS SYMBIONT MICROBES.

The complex symbiosis in Attini ant nests inspires curiosity in different fields of research from Microbiology to Chemical Ecology. These ants cultivate their mutualist fungus for approximately 50 million years in structures well-known as fungi gardens. Attini ants need their mutualist fungus to get nutrients and essential enzymes for feeding. Other microorganisms, such as actinobacteria, produce antibiotics, which help to protect the ants against parasites, as *Escovopsis* genus, that harm the whole nest. One of the most important systems of agriculture in the Attine group is the leaf-cutting ants, of genus *Atta* and *Acromyrmex*, which cultivate only a specific species of fungus, *Leucoagaricus gongylophorus*, each one does not survive without the ants' mutualism. They are known as leaf-cutting ants due to their ability in cutting fresh leaves to cultivate the fungus and they have been characterized as an agricultural pest in *Pinus* and *Eucalyptus* forests. The new black yeast discovery in leaf-cutting ants cuticle was important to instigate studies on the chemical-ecological relationship upon other symbionts. Hence, this study aims to use different analytical tools to understand the chemical interactions between the leaf-cutting ants' symbiont microbes. The thesis was divided into three main parts: **A)** an approach over the co-cultures among different symbiont microbes, focusing on different methodologies; **B)** multivariate data analysis, molecular networking, mass spectrometry imaging, and biological assays about the ecological interaction of black yeast and parasite co-culture; **C)** an ecological function investigation of black yeast metabolites correlated to the antimicrobial activity in opposition to the actinobacteria. The findings of this work contribute with relevant information about the microbial interactions existing in leaf-cutting ant nests related to the black yeast, which was reported here for the first time. Nevertheless, next step experiments regarding the black yeasts have been showing promising in understanding more about this microbial complexity.

Key-words: Leaf-cutting ants; black yeasts; *Phialophora*, *Escovopsis*, microbial metabolomics.

Lista de ilustrações

- Figura 2.1 – Filogenia em uma linha do tempo das formigas da tribo Attini e os cinco sistemas de agricultura: agricultura tipo coral (A), agricultura basal (B), agricultura tipo levedura (C), agricultura derivada e agricultura das cortadeiras (D). (Adaptado de [7]). 8
- Figura 2.2 – Cinco diferentes simbioses foram identificados e caracterizados até o momento: as formigas atíneas, o fungo mutualista (cultivar), o fungo que ataca o mutualista, do gênero *Escovopsis*, as actinobactérias do gênero *Pseudonocardia* e *Streptomyces*, e leveduras negras que parasitam o mutualismo entre a formiga e a actinobactérias. (Adaptado de [25]). 11
- Figura 2.3 – (A) Formigas cortadeiras levando o material vegetal para os formigueiros; (B) O jardim de fungos das formigas atíneas, formada pelo fungo mutualista, em uma visão superior do ninho; (C) A biomassa fresca é degradada pelo fungo e organizada em um gradiente de degradação da matéria vegetal [27]; (D) Visão macroscópica do fungo mutualista *Leucogaricus gongylophorus* em meios de cultura batata dextrose agar (BDA), com detalhes do micélio mostrando o grupo de formação (ao centro) e as hifas com um acúmulo de gongilídeos (barra de escala: 200 e 50 μm) (Adaptado de [26]). 12
- Figura 2.4 – (a) Micrografia eletrônica das formigas atíneas, com a presença de bactérias actinobactérias em suas cutículas, mostrando um crescimento padrão nesses insetos; (b) visualização de *Streptomyces* sp. sobre as pernas dianteiras de *Apterostigma* sp e, (c) uma representação de bactérias em operárias de *Acromyrmex octospinosus*. (Adaptado de [11]). . 13
- Figura 2.5 – (a) Jardim de formigas atíneas *Trachymyrmex* sp. saudável; (b) O mesmo jardim de *Trachymyrmex* sp. completamente devastado pela presença do fungo parasita *Escovopsis*; (c) O fungo parasita *Escovopsis weberi* crescido em placas de levedura e malte em meio sólido (Adaptado de [32]). 14

- Figura 2.6 – (a) Formiga atínea *Apterostigma pilosum* de onde as primeiras leveduras negras foram isoladas. (b) Micrografia eletrônica da levedura negra no tórax das formigas [14]. Os microrganismos *P. capiguarae* e *P. attae* em diferentes meios de cultura (c) Corn meal ágar (CMA), (d) Malte ágar (MA), (e) Batata dextrose ágar (BDA) e (f) hifas vegetativas com enrolamento e conídios (barra de escala: 10 μm) (Adaptado de [14, 33]). 15
- Figura 2.7 – Diagrama das interações existentes na microbiota das formigas atíneas. As setas em negrito representam efeitos diretos, enquanto setas tracejadas representam efeitos indiretos. Efeitos positivos são mostrados com (+) e efeitos negativos com (-). (Adaptado de [15]). 16
- Figura 2.8 – (a) Interações do *Escovopsis weberi* com outros organismos dos ninhos das formigas. Metabólitos estão representados por pequenas formas coloridas, mostradas em (b). (b) Metabólitos isolados de *E. weberi*: shearinines D e L, melinacidina, emodina e cicloartropsona (Adaptado de [37]). 18
- Figura 2.9 – (a) Interações químicas entre as actinobactérias com o fungo parasita. Os metabólitos ativos em (b) contra o fungo produzidos pelas actinobactérias, representados por diferentes formas coloridas, são enumeradas e classificadas nos quadros abaixo. (b) Metabólitos produzidos pela *Pseudonocardia* spp. (quadro em azul) e *Streptomyces* spp. (quadro em verde) (Adaptado de [37]). 19
- Figura 2.10–Novos produtos naturais reportados a partir de coculturas de fungos com bactérias ou entre bactérias (Adaptado de [49]). 21
- Figura 2.11–Diferentes abordagens utilizadas no estudo sobre indução metabólica através de coculturas de microrganismos (Adaptado de [55]). 23
- Figura 2.12–Princípio básico da criação das redes moleculares na plataforma GNPS ((Adaptado de [60]). 24

- Figura 3.1 – Schematic representation of the main interactions within leaf cutting ant nests. Black yeasts directly inhibit the growth of the mutualistic actinobacteria of ants, which indirectly benefits the garden parasite by compromising antibiotic defenses. It indirectly decreases the benefit that actinobacteria provide to ants and cultivars. Solid lines indicate direct and dashed lines, indirect effects black yeasts have on the ants' symbionts [6]. Understanding the interaction can be simplified using different approaches: co-cultivations, statistical analysis, molecular networking, and imaging by mass spectrometry. 33
- Figura 3.2 – Experimental design of symbionts co-cultivations according to different experiments (1-10). The first day only the mutualist fungus and the black yeasts were inoculated. After 7 days, the actinobacteria was inoculated and after 21 days, the parasite *Escovopsis* was inoculated. The extractions were made after 28 days. Experiments details: (1) The mutualist and BY *P. attae*, (2) the mutualist and BY *P. capiguarae*, (3). the mutualist and the actinobacteria, (4) the BY *P. attae* and actinobacteria, (5) the BY *P. capiguarae* and actinobacteria, (6) the mutualist and the parasite, (7) the BY *P. attae* and the parasite, (8) the BY *P. capiguarae* and the parasite, (9) the actinobacteria and the parasite and (10) both BYs. 36
- Figura 3.3 – Overview of extraction methodology. The axenic cultures of each microbe was extracted from the hole plate and the co-cultures were extracted in three different zones (A), (B) and (C). 37
- Figura 3.4 – Overall workflow for DESI methodology: 1000 μ L of distilled water is added in the Petri dish, the mycelium is scrapped using a Drigalsky spatula. 5 to 10 μ L of this solution are added in a new Petri dish with a glass slide (26 \times 76 μ m) previously prepared, in 0.75 cm of distance between the strains. The laminules were dried in desiccator for two hours, analyzed directly by DESI and processed using BioMAP. 40

- Figura 3.5 – Co-cultivations among the microbial symbionts of leaf cutting ants. The experiments are organized 1 to 10. (1) The mutualist and black yeast (BY) *P. attae*, (2) the mutualist and BY *P. capiguarae*, (3) mutualist fungus and the actinobacteria, (4) the BY *P. attae* and actinobacteria, (5) the BY *P. capiguarae* and actinobacteria, (6) the mutualist and the parasite, (7) the BY *P. attae* and the parasite, (8) the BY *P. capiguarae* and the parasite, (9) the actinobacteria and the parasite and (10) both BYs. 41
- Figura 3.6 – A: Supervised 2D PLS-Da multivariate data analysis of the co-cultures and mono-cultures fingerprinting. B: Supervised 3D PLS-Da multivariate data analysis. *P. attae* and *Pseudonocardia* sp. (in light pink) and *P. capiguarae* and *Escovopsis* (in light green) are highlighted because of their clear separation related to other groups. 42
- Figura 3.7 – Heat map and grouping analyses of the chemical profiles obtained by LC-MS of co-cultures and mono-cultures samples. Each color means a group of sample related to mono-cultures, *Pseudonocardia* sp. (Bac) in red, *Escovopsis microspora* (EM) in blue, *Leucoagaricus gongyloporus* (LG) in light blue, *Phialophora attae* (PA) in light green and *P. capiguarae* (PC) in light brown, and co-cultures. Clustering result shown as heat map and the differential accumulation of mass features according to the different samples in HCA. HCA was constructed using *Euclidean* distance measure and clustering algorithm using Ward’s method. . . . 44
- Figura 3.8 – Co-cultivation MN among the microbial symbionts of leaf cutting ants. The internal network (A) shows the complete MN: the ions generated in co-cultures are in red, all mono-cultures are in blue and the YEMA are in black. The external information highlights specific spectral families: B) The chemical compound GNPS match to Shearinine D was observed in mono and co-cultures stemming *E. microspora* samples. C) GNPS match to Sesquiterpenoids was detected in co-cultures with the mutualist fungus *Leucoagaricus gongyloporus*. D) and E) GNPS match to indole compound and Coproporphyrin I, respectively, were found in Bac-EM and LG-PA. 45

- Figura 3.9 – Spectral family among the microbial symbionts of leaf cutting ants. All the m/z of this family was found only in the co-cultures samples. The highlighted m/z were also detected in imaging data. The m/z 294.1548 was detected in co-cultures between both black yeasts in pink. The ions m/z 901.7202, 896.4292 and 385.1787 were identified in co-cultures of *L. gongylophorus* and the black yeast, *P. capiguarae*, in orange. 47
- Figura 4.1 – Symbionts microbes interactions of leaf cutting ants: the cultivar *Leucoagaricus gongylophorus*, the actinobacteria that lives in ants cuticle, the parasite, *Escovopsis* sp. and the BYs, isolated from queen ants body, *Phialophora capiguarae*. Main picture was based on photo in NSTA. 53
- Figura 4.2 – (A) Microbial interactions between BY, *P. capiguarae*, and the parasite *Escovopsis*. (B) the parasite *Escovopsis* (LESF016) mycelium is highlighted the co-culture (yellow) and the mono-culture in front of the BY *P. capiguarae* (green). The mycelium areas were calculated based on the media of three replicates. The BY mycelium does not modified after the co-cultivation. (C) Venn diagram with all the m/z present in mono-cultures and co-culture. (D) LC-HRMS profiling of axenic cultures *P. capiguarae* and *Escovopsis* and the co-cultivation zones A, B and C. 59
- Figura 4.3 – (A) Microbial interactions between BY *P. capiguarae* (in dark blue) and the parasite *Escovopsis* (in dark green) and legend of the colors represents the co-culture part provides from the BY (A) in light blue, the yellow is from the parasite (C) and the intersection zone (B) is shown in pink. (B) Unsupervised MVDA (PCA): scores plot between the selected PCs, the explained variance is 50.4%; (C) Hierarchical cluster analysis (HCA) was constructed pondering *Pearson* distance and the average clustering algorithm. (D) Supervised MVDA (PLS-DA) biplot. The scores plot between the selected PCs the explained variances are 42.1%. (E) Selected features m/z 412.1459, 433.2665, 136.0605 and 268.1040 are more expressive present in co-cultures samples. In zone C co-cultures (in yellow) the area is $\geq 10^5$ 61

- Figura 4.4 – (A) Molecular networking of microbial interactions between BY and the parasite and legend of the colors in details: red nodes are related to co-cultures samples and white nodes to mono-cultures. (B) Shearinines spectral family presented three annotated compounds: 1) Shearinine D, 2) Shearinine F and 3) 22,23-dehydro-shearinine A. 64
- Figura 4.5 – (A) Molecular family generated mainly by spectra from co-cultures A, B and C zones samples. Found m/z in imaging-MS are highlighted: 440, 411 and 474. (B) Shearinine "molecular family" was selected to search the ions in the imaging-MS. The found nodes are highlighted m/z 748, 786, and 736. The numbers 1, 2 and 3 are related to the annotated chemical compounds 1) Shearinine D, 2) Shearinine F, and 3) 22,23-dehydro-shearinine A. The imaging-MS shows the spatial distribution of a specific m/z over the co-cultivation surface. The images are plotted on the same color scale from 0 (dark purple) to 2 105 (red). Nodes colors in the molecular networking are regarding to the BY, *P. capiguarae* in dark blue, the parasite fungus, *Escovopsis*, in dark green, and in light blue, pink and yellow are originating from co-cultures zone, A, B, and C, respectively. 66
- Figura 4.6 – Ions detect in imaging-MS related to shearinine compounds: (1) m/z 748 is correlated to the shearinine D. (2) m/z 736 to the shearinine F (3) 22, 23 dehydro-shearinine A is connected to m/z 786. 68
- Figura 4.7 – Shearinines-analogous proposals of m/z 736, 786 and 748 and their relation to the co-culture IMS. 69
- Figura 4.8 – Agar diffusion assay with co-cultivation extracts A-zone, B-zone, C-zone and negative control: (A) the bioassay with *Pseudonocardia* sp. after 5 days of incubation. (B) Statistical analysis of the inhibition zones. (C) the same bioassay after 15 days of incubation. (D) Statistical analysis of the inhibition zones. The comparison was performed using as negative control MeOH. The mono-cultures were also tested and the *Escovopsis* extract showed a similar inhibition than C zone and *P. capiguarae* has not showed bioactivity. 70

- Figura 5.1 – Schematic representation of the experimental part within black yeast symbionts: (1) Black yeasts isolated of leaf-cutting ants cuticle and the electronic microcopy of ants body are represented in the Figure [4]. (2) The black yeast in Petri dishes, *Phialophora* genus, *P. attae* (left) and *P. capiguarae* (right). (3) the bioassays of *P. capiguarae* extract against the actinobacteria *Pseudonocardia* sp. is also showed. 76
- Figura 5.2 – Phylogenetic study of *P. capiguarae*: electrophoresis of PCR amplification with 1000-1500 bp size and plasmide extraction with a concentration of $243.6 \text{ ng} \cdot \mu\text{L}^{-1}$, and a high level of purity A260/A280 of 1.9 and A260/A230 of 1.65. 83
- Figura 5.3 – Black yeasts phylogenetic comparison: phylogenetic analysis of members of *Chaetothyriales* (Class Eurotiomycetes), more details in the *Cyphellophoraceae* family [11]. Different species of black yeasts can be found in different environments: plant endophytes, soil microbiome, wood, water, or ant-associated. *P. attae* and *P. capiguarae* were both found in ant-association and they are quite phylogenetically similar to *Cyphellophora* genus. 84
- Figura 5.4 – Chemical structure of clavarinic acid (terpene) and melanin (PKS-type 1) found in the AntiSMASH analysis of *P. attae* BGC with 100% of similarity. 85
- Figura 5.5 – *P. capiguarae* (PC) strain LC profiling cultivated in different media PDA, YEME and SFM at three different times (7, 14 and 21 days). The highlighted sections show the outstanding chromatographic peaks in the *P. capiguarae* cultivations. 86
- Figura 5.6 – *P. attae* AP399 strain LC profiling cultivated in different media PDA, YEME and SFM at three different times (7, 14 and 21 days). The highlighted sections show the outstanding chromatographic peaks in the *P. attae* cultivations. 87

Figura 5.7 – A) Bioassays against <i>Pseudonocardia</i> sp. using the crude extract (above) and the negative control (MeOH); B) Bioassays against <i>Pseudonocardia</i> sp. using the different fractions 1 to 7. All the bioassays were made in three replicates in different agar plates. The proportion with petroleum ether and ethyl acetate is shown bellow F1 to F7 according to the proportion of petroleum ether and ethyl acetate.	89
Figura 5.8 – Suggested F5-30 compound related to the phomester [25] isolated from the black yeast <i>P. capiguarae</i> . The numbers are related to the Table 5.2 and the COSY and HMBC correlations as well.	91
Figura 5.9 – Fragmentation propose for the isolated compound related from the black yeast <i>P. capiguarae</i>	92
Figura A.1 – Workflow detalhado das etapas utilizadas no processamento dos dados na plataforma do GNPS para a construção dos mapas moleculares. . .	99
Figura A.2 – Workflow detalhado para conversão dos dados utilizando o MSConvert, de qualquer formato para <i>.mzXML</i>	102
Figura A.3 – Workflow detalhado das etapas utilizadas no processamento dos dados no MZMine. Baseado em [1].	106
Figura A.4 – Workflow detalhado das etapas utilizadas no processamento dos dados no site do <i>Metaboanalyst</i>	108
Figura A.5 – Workflow detalhado das etapas utilizadas no processamento dos dados na plataforma GNPS para a construção dos mapas moleculares. . . .	110
Figura B.1 – PCA analysis: Scores plot between the PC 1 (4.3%) and PC 2 (2.9%).	113
Figura B.2 – PLS-DA supervised analysis: Scores plot between the Component 1 (4.3%) and Component 2 (2.9%), with 7.2% of variencie. (1) The mutualist (LG) and BY <i>P. attae</i> (PA), (2) the mutualist (LG) and black yeast (BY) <i>P. capiguarae</i> (PC), (3). the mutualist (LG) and the actinomycete (Bac), (4) the BY <i>P. attae</i> (PA) and actinomycete (Bac), (5) the BY <i>P. capiguarae</i> (PC) and actinomycete (Bac), (6) the mutualist (LG) and the parasite (EM), (7) the BY <i>P. attae</i> (PA) and the parasite (EM), (8) the BY <i>P. capiguarae</i> (PC) and the parasite (EM), (9) the actinomycete (Bac) and the parasite (EM) and (10) both BYs (PA and PC).	114

- Figura B.3 – PLS-DA classification using different number of components. The red star indicates the best classifier in Component 3. In this validated model, R^2 is ~ 0.9 and $Q^2 \leq 0.5$ 115
- Figura B.4 – MolNetEnhancer used to identify the chemical structural information obtained for co-cultures and mono-cultures metabolites. Structural annotation for molecular families was suggested based on MS fragments using the *in silico* tool. The class of metabolites is highlighted and a complete metabolites class overview is summarized at this network. . . 115
- Figura C.1 – PLS-DA classification using different number of components (1, 2 and 3). The red star indicates the best classifier in Component 3. In this validated model, $R^2 \sim 0.9$, $Q^2 \leq 0.85$ and the accuracy $\sim 50\%$ 119
- Figura C.2 – The correlation heatmap analysis can be used to visualize the overall correlations between different features. All the co-cultures samples are correlated (highlighted in a blue square). The mono-cultures are related to the replicates which also means good reproducibility. Dark red squares are related to high similarity and dark blue to high distinction. 119
- Figura C.3 – MolNetEnhancer: Enhanced molecular networks by integrating metabolome mining and annotation tools of LC-HRMS data of interaction between *P. capiguarae*, the black yeast, and the parasite *Escovopsis*. Different natural products classes were categorized: carboxylic acids (in brown), benzothiazoles (in purple), fatty acyls (in blue), flavonoids (in orange), indoles and derivatives (in pink), naphthopyrans (in green) and steroids and derivatives (in yellow). The non-match compounds are in grey. 120
- Figura C.4 – MS/MS comparison of compound 1 shearinine D from the extract of co-culture between AP376 with LESF016 (Silver spectrum) from GNPS spectral library (CCMSLIB00000478066) with 0.63 of cosine. 121
- Figura C.5 – MS/MS comparison of compound 2 shearinine F from the extract of co-culture between AP376 with LESF016 (Silver spectrum) from GNPS spectral library (CCMSLIB00000478461) with 0.65 of cosine. 122

- Figura C.6 – MS/MS comparison of compound 3 22,23-dehydro-shearinine A from the extract of co-culture between AP376 with LESF016 (Silver spectrum) from GNPS spectral library (CCMSLIB00000478065) with 0.92 of cosine. 123
- Figura C.7 – MS/MS fragmentation of compound m/z 748 from the extract of co-culture between PC (AP376) with EM (LESF016). 125
- Figura C.8 – MS/MS fragmentation of compound m/z 736 from the extract of co-culture between PC (AP376) with EM (LESF016). 126
- Figura C.9 – MS/MS fragmentation of compound m/z 786 from the extract of co-culture between PC (AP376) with EM (LESF016). 127
- Figura D.1 – Antismash analysis of *P. attae* strain in NCBI data bank. This strain presents NRPS, terpene and PKS types of secondary metabolites. Metabolites as clavarinic acid and melanin were identified by gene cluster comparison. 128
- Figura D.2 – A) LC-profile of different extractions: ethyl acetate (EA) extraction (1), acid EA extraction (2), basic EA extraction (3), ethyl acetate: dichloromethane: methanol (3:2:1). B) bioactivity against *Streptomyces* sp. The extracts were solubilized in methanol (MeOH) and the negative control was performed in this solvent. 128
- Figura D.3 – Differences between the bioassay against *Streptomyces* 28.2 and *Pseudonocardia* W3 according to the time. The inhibition disappeared in 3 days in the bioassay against *Streptomyces* 28.2 (in the left) and the inhibition zone remained the same even after a month of incubation (in the right). This kind of bioactivity means that extract activity does not change or degrade over time. 129
- Figura D.4 – A) The bioassays against *Pseudonocardia* W3 sp. using the different fractions 1 to 7. B) Statistic analysis based in inhibition zone area observed on AP376 extracts bioassays. Bioassays shows a clear inhibition zone in F5 and F7. The material referent of F7 was not enough to proceed with purification. 129

- Figura D.5–A) Base peak and UV (250 nm) chromatogram of the RP C18 HPLC separation of bioactive silica column F5. The red and blue sections is related to the collecting time using semi-prep-HPLC. B) The subfractions were tested against the actinomycete. C) Statistical analysis of the subfractions. 130
- Figura D.6–A) Bioassays of the three different sub-fractions of fraction 5 (F5) and statistical analysis of bioactivity against *Pseudonocardia* sp. W3. F5-A2 was collected in 2 min, F5-B30 in 30 and F5-32 in 32 min over LC-run. B) Statistic analysis based in inhibition zone area observed on different sub-fractions of F5 bioassays. *The inhibitions are showed based on the area of inhibition. The samples names are based on the retention time (min) and the M means the media of the inhibition zone area. 130
- Figura D.7–Compound F5-30 isolated of black yeast *P. capiguarae*. A) HRMS info can be seen in m/z 393. B) LC profile of the compound. C) MSI between the black yeast (PC) and parasite *Escovopsis* (EM) D) MSI between the black yeast (PC) and actinobacterium *Pseudonocardia* sp. (Bac). 131
- Figura D.8– ^1H NMR spectrum of F5-B30 in methanol- d_4 (600 MHz). The spectra above is the complete 0 to 6 ppm. (A) Detail view from spectrum region of 0 to 2.5 ppm and (B) Detail view from spectrum region of 3 to 5.6 ppm. 132
- Figura D.9– ^{13}C NMR spectrum of F5-B30 in methanol- d_4 (150 MHz). The complete spectra is shown above. (A) Detail view from spectrum region of 0 to 35 ppm. (B) Detail view from spectrum region of 60 to 78 ppm. (C) Detail view from spectrum region of 174 to 175 ppm. 133
- Figura D.10– ^1H - ^1H COSY NMR spectrum of F5-B30 in methanol- d_4 (600 MHz). . . 134
- Figura D.11–HSQC NMR 2D spectrum of F5-B30 in methanol- d_4 (600 MHz). Expansion HSQC NMR spectrum of F5-B30 of the aliphatic part. . . . 135
- Figura D.12–HMBC NMR 2D spectrum of F5-B30 in methanol- d_4 (600 MHz). (A) Expansion of HMBC NMR spectrum of F5-B30 of the aliphatic part. . 136

Sumário

1	CONTEXTUALIZAÇÃO	1
1.1	Introdução Geral	1
1.2	Motivação do estudo	3
1.3	Estrutura da tese	4
1.4	Referências	4
2	INTERAÇÕES DOS SIMBIONTES DAS FORMIGAS CORTADEI- RAS DE FOLHAS: UMA BREVE REVISÃO	7
2.1	As formigas da tribo Attini	7
2.2	Histórico das descobertas sobre os ninhos das atíneas	8
2.3	A complexa simbiose das formigas atíneas	10
2.3.1	<i>Leucoagaricus gongylophorus</i> e o mutualismo obrigatório	11
2.3.2	A proteção das actinobactérias nos ninhos das atíneas	12
2.3.3	O invasor <i>Escovopsis</i> nos jardins de fungos	13
2.3.4	Os novos simbiontes: leveduras e fungos negros	14
2.4	Correlação das interações simbióticas das formigas atíneas	15
2.5	Guerra química entre os microrganismos das formigas atíneas	17
2.6	Interações microbianas e cocultivo entre microrganismos	20
2.7	Ferramentas analíticas em estudos de ecologia química	22
2.7.1	Análise multivariada dos dados obtidos por LC-MS	22
2.7.2	Redes moleculares na plataforma GNPS	24
2.8	Referências	25
3	DIFFERENT TOOLS TO INVESTIGATE CHEMICAL INTERAC- TIONS AMONG LEAF-CUTTING ANTS SYMBIONTS	32
3.1	Abstract	32
3.2	Introduction	33
3.3	Experimental part	35
3.3.1	Biological Material	35
3.3.2	Experimental settings of culture and co-culture conditions	35

3.3.3	Extraction and sample preparation for LC-MS	37
3.3.4	LC-MS data acquisition	37
3.3.5	LC-MS data processing	38
3.3.5.1	Multivariate data analysis	38
3.3.5.2	Molecular networking data analysis	38
3.3.6	Imaging-MS sample preparation and data analysis	39
3.4	Results and discussion	40
3.4.1	Morphological patterns in co-culture of symbiont microbes	40
3.4.2	Chemical diversity of co-cultures in MVDA	42
3.5	Diversity of annotated metabolites in molecular networking	44
3.6	Search for metabolite induction in fungal co-culture by data mining using imaging-MS	46
3.7	Outlook and remarks	48
3.8	Referências	48
4	CHEMICAL WARFARE BETWEEN LEAF-CUTTING ANTS PA- RASITES AND BLACK YEASTS	52
4.1	Abstract	52
4.2	Introduction	53
4.3	Material and methods	54
4.3.1	Microbial samples	54
4.3.2	Co-culture experiments	55
4.3.3	Crude extraction and sample preparation	55
4.3.4	Mass spectral data acquisition	55
4.3.5	LC-MS data process and analysis	56
4.3.5.1	Multivariate data analysis	56
4.3.5.2	Classical molecular MS/MS network analysis	56
4.3.5.3	Feature based molecular MS/MS network analysis	57
4.3.6	DESI imaging on co-cultivations	57
4.3.7	Antimicrobial assays with extracts	58
4.4	Results and discussion	58
4.4.1	Co-culture and interaction of black yeast <i>versus</i> parasite <i>Escovopsis</i> sp.	58
4.4.2	Multivariate data analysis in microbial interactions	60

4.4.3	Classical molecular networking of black yeast and parasite interactions	63
4.4.4	DESI-IMS of spectral families of the microbial interaction	65
4.4.5	Network annotation propagation of induced chemical compound in co-cultures	67
4.4.6	Fragmentation studies of shearinines-analogous compounds	69
4.4.7	Antimicrobial assays against actinobacterias	70
4.5	Outlook	71
4.6	Referências	71
5	BLACK YEAST <i>PHIALOPHORA</i> GENUS ECOLOGICAL FUNCTION ASSOCIATED WITH LEAF-CUTTING ANTS	75
5.1	Abstract	75
5.2	Introduction	76
5.3	Experimental part	78
5.3.1	Biological material	78
5.3.2	Phylogenetic analysis of black yeast strains	78
5.3.2.1	Genomics DNA from black yeasts from a agar culture	78
5.3.2.2	DNA extraction of the strain	78
5.3.2.3	PCR condition - 18S rDNA	78
5.3.2.4	Transformation with cloning vector pJET 1.2	79
5.3.2.5	Sequencing of DNA (18S)	79
5.3.3	Initial screening of black yeasts isolates for biological activity	79
5.3.3.1	Optimization of the growth conditions of <i>Phialophora</i> black yeasts	79
5.3.3.2	LC-MS analysis	80
5.3.3.3	Bioassays with extracts	80
5.3.4	Cultivation of black yeasts and isolation of bioactive metabolites	80
5.3.4.1	Scale-up growth, silica column and data analysis	80
5.3.4.2	Bioactive compounds isolation	81
5.3.4.3	NMR Spectroscopy	81
5.3.4.4	Bioassays against actinobacteria	81
5.3.5	DESI imaging analysis on co-cultivations	82
5.4	Results and discussion	82
5.4.1	Black yeast <i>P. capiguarae</i> phylogenetic comparison	82
5.4.2	Chemical profiling comparison of the black yeasts: LC profile and bioassays	85

5.4.2.1	Growth optimization of black yeasts: LC-profiling and bioactivity analysis	85
5.4.2.2	Different extraction procedures	87
5.4.3	Bioactive compound isolation of black yeast	88
5.4.3.1	Silica column chromatography	88
5.4.3.2	Bioactive metabolite: isolation and elucidation	89
5.5	Outlook	92
5.6	Referências	93
6	CONSIDERAÇÕES E PERSPECTIVAS	96
	 ANEXOS	 97
	ANEXO A – PROCESSAMENTO DE DADOS DE LC-MS	98
A.1	Instalação de softwares e aberturas de contas	98
A.2	Preparo básico de amostra para LC-MS	100
A.3	Aquisição de dados de LC-MS/MS	100
A.4	Organização dos dados para análises	101
A.5	Convertendo os dados para mzXML ou mzML	101
A.6	Processamento dos dados de LC-MS utilizando o MZMine	102
A.7	Organização dos dados para análises estatísticas no <i>Metaboanalyst</i>	106
A.8	Construção dos mapas moleculares na plataforma GNPS	109
A.9	Organização dos mapas moleculares utilizando o Cytoscape	111
A.10	Análise geral das informações obtidas	112
A.11	Referências	112
	 ANEXO B – SUPPLEMENTARY INFORMATION - CHAPTER 3	 113
	 ANEXO C – SUPPLEMENTARY INFORMATION - CHAPTER 4	 119
	 ANEXO D – SUPPLEMENTARY INFORMATION - CHAPTER 5	 128

1 Contextualização

1.1 Introdução Geral

As formigas atíneas (subfamília Myrmicinae, tribo Attini) caracterizam um grupo de cerca de 230 espécies diferentes de formigas, localizadas principalmente em regiões neotropicais do continente americano. A principal característica dessa tribo de formigas é a sua completa dependência do fungo mutualista, que elas cultivam como principal fonte de alimento. Esse mutualismo é um exemplo de simbiose moldada por milhões de anos de coevolução [1].

As formigas da tribo Attini cultivam o fungo basidiomiceto (*Leucocoprineae* e *Pterulaceae*) como fonte de nutrientes essenciais para as larvas e rainha [2] em organizações conhecidas como jardim de fungo. As formigas dos gêneros *Acromyrmex* e *Atta* utilizam material vegetal fresco recém-cortado para cultivar o fungo mutualista, e por isso, são conhecidas como formigas cortadeiras de folhas.

O fungo mutualista é difundido para a nova colônia através de transmissão vertical durante o período de reprodução [3]. Quando uma fêmea alada (içá) deixa o ninho para realizar o voo nupcial ela carrega uma pequena porção do fungo em sua cavidade infrabucal, e, após o acasalamento com os machos alados (bitus), as rainhas retornam ao solo para estabelecerem novas colônias. Com o passar do tempo, outros microrganismos aderiram à essa simbiose e tornou a microbiota da colônia cada vez mais complexa.

Como as formigas Attini dependem diretamente do fungo mutualista, sua manutenção e proteção são de fundamental importância. Assim, esses insetos utilizam diferentes mecanismos para defender seus jardins de fungos de outros microrganismos indesejáveis [4]. Dentre os mecanismos de defesa estão a retirada dos organismos invasores das colônias e o mutualismo com as actinobactérias do gênero *Pseudonocardia* e *Streptomyces*, encontradas nas cutículas de formigas Attini. As actinobactérias produzem substâncias antimicrobianas que inibem o crescimento de fungos parasitas, como o gênero *Escovopsis* e *Fusarium* [5], [6]. Entretanto, o parasita *Escovopsis* também possui mecanismos de defesa contra as actinobactérias e contra o mutualista [7], [8].

Como um novo grupo de simbiontes, as leveduras e os fungos negros (*Chaetothyriales* e *Capnodiales*) tem sido frequentemente isolados do exoesqueleto de atíneas. A presença

desses microrganismos em associação com as formigas tem sido considerada de extrema relevância, pois esse nicho ainda é desconhecido e existem diversos relatos de fungos negros ocasionando severas infecções em humanos [9].

Por ser um tema pouco explorado, o papel químico e ecológico dos fungos negros na simbiose das formigas cortadeiras ainda é desconhecido. Little e Currie isolaram colônias de leveduras negras (filogeneticamente próximas a fungos do gênero *Phialophora*; Ascomycota) do tegumento de formigas *Apterostigma* sp. (tribo Attini) [10]. Segundo esse estudo, as leveduras negras mantêm uma associação com as atíneas ao longo do período evolutivo e, portanto, são classificadas como simbiontes. Adicionalmente, eles também propõem que a levedura negra possui uma relação de antagonismo com a *Pseudonocardia* sp., diretamente competindo por nutrientes e suprimindo o crescimento das actinobactérias [11].

Porém, outros estudos têm revelado que a diversidade de leveduras negras e actinobactérias no tegumento das formigas Attini é muito maior do que se pensava [12], [13] colocando em questionamento a classificação das leveduras negras *Phialophora* como simbiote.

O foco principal da tese foi verificar as interações microbianas com microrganismos simbiontes das formigas cortadeiras, incluindo fungo mutualista, actinobactérias, fungos parasitas e leveduras negras através da utilização de diferentes ferramentas analíticas e abordagens de análises dos dados, incluindo análise multivariada dos dados, redes moleculares, imageamento por espectrometria de massas e ensaios biológicos. O estudo de um sistema complexo, como é o caso dos jardins de fungos das formigas cortadeiras, exige a utilização de diversas ferramentas de análise associadas a técnicas clássicas para melhor interpretação dos dados obtidos.

Os resultados provenientes das interações microbianas sugerem uma complexidade de produção e indução de metabólitos. A relação antagônica das leveduras negras com o parasita *Escovopsis* sp. contribuem para uma maior compreensão das interações ecológicas existentes nos jardins, além de fomentar a necessidade de estudos mais profundos em relação a esses simbiontes. Estudos *in vivo* ainda precisam ser realizadas para definição de conclusões decisivas baseadas nos resultados obtidos até agora.

1.2 Motivação do estudo

Diversos motivos podem ser listados para influenciar a atual pesquisa e os principais estão listadas a seguir:

(A) Devido a necessidade de identificar as interações químicas entre alguns dos simbiontes das formigas cortadeiras, especialmente relacionados ao quinto simbionte das atíneas: **as leveduras negras**. Esse grupo de microrganismos tem poucos estudos relacionados a seu arsenal metabólico e sua função química nos ninhos ainda não foi definida na literatura.

(B) Novas tecnologias analíticas surgem diariamente e aprender a lidar com grande número de dados em novos softwares tem se tornando um desafio constante nas pesquisas. Diante disso, um resumo detalhado das metodologias utilizadas no trabalho é apresentado no Anexo A para auxiliar outros estudantes que desejam realizar estudos similares. Nesse trabalho consta abordagens relacionadas a LC-MS, como mapeamentos moleculares, processamento de dados para análise estatísticas, imageamento por espectrometria de massas e análises de bioensaios. Associar diferentes técnicas é de extrema importância para uma análise coerente dos dados. A ausência de um tutorial adequado para o grupo de pesquisa tem dificultado o andamento de projetos e por isso torna-se extremamente necessário a organização desse guia para futuros trabalhos.

(C) Nos últimos vinte anos, a resistência aos antibióticos tem sido um tópico relevante relacionado à saúde humana. Essa realidade impulsiona a necessidade de estudos relacionados a novos potenciais antibióticos que possam ser utilizados para doenças humanas [14]. As formigas cortadeiras apresentam uma simbiose com actinobactérias, produtoras de antibióticos, e a sua inibição pode ser importante para o controle agrícola das pragas e, possivelmente para a química medicinal. Nesse trabalho, buscou-se entender quais os principais metabólitos produzidos pelos simbiontes das formigas com atividade contra as actinobactérias do formigueiro.

(D) As formigas cortadeiras são potentes pragas agrícolas e seu controle racional ainda é um desafio. Esse trabalho buscou entender os mecanismos de simbioses entre os diversos microrganismos a fim de estabelecer alternativas para o controle dessa praga. Uma vez entendendo como as interações químicas ocorrem, o planejamento para o controle desses insetos torna-se bastante facilitado.

Essas quatro grandes motivações para o estudo estão presentes ao longo dos próximos capítulos e serão ressaltados nos objetivos de cada seção.

1.3 Estrutura da tese

A tese foi dividida em seis capítulos com o objetivo de organizar os resultados em diferentes tópicos e facilitar o entendimento do conteúdo pelo leitor. O capítulo 1 resume o trabalho com uma breve introdução ao principal tema da tese, assim como a motivação para a execução do trabalho e como a tese está organizada.

No capítulo 2 é apresentada uma revisão da literatura sobre os principais tópicos estudados: a simbiose das formigas, uma breve explicação sobre as metodologias utilizadas no trabalho e um histórico sobre as diversas pesquisas relacionadas às formigas atíneas. O motivo para esse capítulo ser em português deve-se principalmente ao fato de ser um conteúdo introdutório para estudantes que desejam estudar o tema e, muitas vezes, não encontram um material em detalhes na literatura.

Os demais capítulos estão escritos em inglês e em formato de artigo científico para a futura submissão em periódicos da área. O capítulo 3 detalha as metodologias de análise dos cocultivos dos microrganismos simbiotes e a importância do delineamento experimental para dar sequência aos demais estudos realizados. Junto a esse capítulo, um material suplementar no anexo A apresenta as metodologias utilizadas para poder servir de guia para alunos do grupo de pesquisa que desejam realizar estudos similares.

O capítulo 4 aborda principalmente a interação entre a levedura negra, *Phialophora capiguarae*, e o parasita *Escovopsis* sp. Nessa sessão discutem-se análises multivariada de dados obtidos por LC-MS, mapas moleculares e monitoramento por imageamento. Esses estudos trazem pela primeira vez a interação de um ponto de vista químico entre esses dois simbiotes. Ensaio biológicos frente a actinobactéria *Pseudonocardia* sp. são abordados nessa sessão.

O capítulo 5 traz o estudo detalhado da função química e ecológica de metabólitos produzidos pelas leveduras negras do gênero *Phialophora*, abordando a otimização dos cultivos guiados pela atividade biológica frente às actinobactérias.

O capítulo 6 enumera as principais contribuições desse estudo e as perspectivas para futuros trabalhos.

1.4 Referências

- [1] Willis JC. The fungus gardens of certain south with a thick mass of weathered pieces of leaves and twigs, American Ants. Nature. 1893;48(1243):392–394.

-
- [2] Weber NA. The Fungus-culturing Behavior of Ants. *American Zoologist*. 2015;12(3):577–587.
- [3] Mueller U, Schultz T, Currie C, Adams R, Malloch D. The Origin of the Attini ant-fungus mutualism. *The Quarterly Review of Biology*. 2001;76:169–197.
- [4] Currie CR. A community of ants, fungi, and bacteria: a multilateral approach to studying symbiosis. *Annual Review of Microbiology*. 2001;55:357–380.
- [5] Chevrette M, Carlson C, Ortega H, Thomas C, Ananiev G, Barns K, et al. The antimicrobial potential of *Streptomyces* from insect microbiomes. *Nature Communications*. 2019 01;10.
- [6] Currie CR, Scottt JA, Summerbell RC, Malloch D. Fungus-growing ants use antibiotic-producing bacteria to control garden parasites. *Nature*. 1999;398(6729):701–704.
- [7] Heine D, Holmes NA, Worsley SF, Santos ACA, Innocent TM, Scherlach K, et al. Chemical warfare between leafcutter ant symbionts and a co-evolved pathogen. *Nature Communications*. 2018;9:2208.
- [8] Dhodary B, Schilg M, Wirth R, Spiteller D. Secondary metabolites from *Escovopsis weberi* and their role in Attacking the garden fungus of leaf-cutting ants. *Chemistry - A European Journal*. 2018;24:4445–4452.
- [9] Teixeira M, Moreno L, Stielow B, Muszewska A, Hainaut M, Gonzaga L, et al. Exploring the genomic diversity of black yeasts and relatives (Chaetothyriales, Ascomycota). *Studies in Mycology*. 2017 01;86:1–28.
- [10] Little A, Currie CR. Symbiotic complexity: discovery of a fifth symbiont in the Atinne ant-microbe symbiosis. *Biology Letters*. 2007;3:501–504.
- [11] Little A, Currie C. Black yeast symbionts compromise the efficiency of antibiotic defenses in fungus-growing ants. *Ecology*. 2008;89:1216–1222.
- [12] Attili-Angelis D, Duarte A, Pagnocca F, Nagamoto N, Vries M, Stielow B, et al. Novel *Phialophora* species from leaf-cutting ants (tribe Attini). *Fungal Diversity*. 2014;65:65–75.

- [13] Duarte APM, Attili-Angelis D, Baron NC. Leaf-cutting ants: an unexpected micro-environment holding human opportunistic black fungi. *Antonie van Leeuwenhoek*. 2014;106:465–473.

- [14] Hofer U. The cost of antimicrobial resistance. *Nature Reviews Microbiology*. 2019;17.

2 Interações dos simbiosomas das formigas cortadeiras de folhas: uma breve revisão

2.1 As formigas da tribo Attini

Com o processo de evolução, a maioria dos insetos desenvolveram habilidades e comportamentos extremamente especializados na natureza. As formigas, que conseguem sobreviver em diversos ecossistemas terrestres, apresentam peculiaridades em sua vivência que contribuem para questionar e fomentar diversos grupos de estudo, no quesito ambiental, ecológico, entomológico e bioquímico [1, 2, 3].

As formigas da tribo Attini ou formigas atíneas (Formicidae: Myrmicinae) estão localizadas, restritamente no continente americano, que estende-se do Brasil até o México e em algumas áreas do sul dos Estados Unidos [4]. As atíneas vivem em mutualismo obrigatório com o fungo basideomiceto que elas cultivam como fonte de alimento. A origem desse mutualismo pode ter se dado ao acaso, na qual fungos saprofíticos se desenvolveram nos ninhos e, com o tempo, se tornaram alimento para as formigas, que se adaptaram e aprenderam a cultivá-los. A relação é mutualística, portanto, apresenta benefícios aos fungos que utilizam a segurança dos ninhos para facilitar sua reprodução e também para as formigas que se beneficiam de alimentação proveniente do fungo [5].

Para organizar o estudo, as formigas atíneas foram classificadas de acordo com dados de sequenciamento de genes nucleares e seus fósseis, categorizando-as em cinco diferentes grupos baseados em seus sistemas de agricultura ou fungicultura [6]: (A) **Agricultura basal**: condição ancestral das atíneas; (B) **Agricultura tipo coral**: único grupo das atíneas que cultivam fungo que não pertence à tribo *Leucocoprinae*; (C) **Agricultura tipo levedura**: membros desse grupo crescem os cultivares como nódulos, semelhantes a células de leveduras, em uma fase unicelular, diferente das outras atíneas que cultivam fungos pluricelulares; (D) **Agricultura derivada**: são consideradas atíneas de nível superior e não são cortadeiras de folhas e (E) **Agricultura das cortadeiras**: *Atta* e *Acromyrmex* são os principais gêneros desse grupo, essas formigas são conhecidas como cortadeiras por terem capacidade de cortar folhas e flores frescas para o cultivo do fungo, *L. gongylophorus* que é incapaz de viver fora do mutualismo com as atíneas [1, 7, 8]. A figura 2.1 mostra a filogenia das formigas da tribo Attini e os cinco tipos de agricultura.

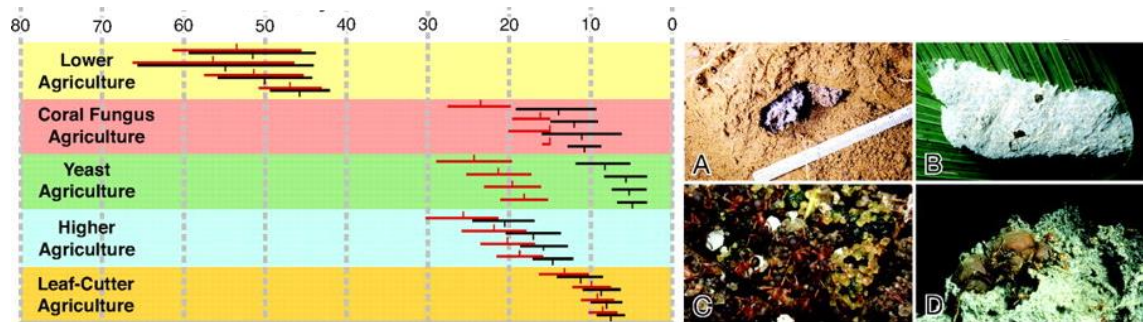


Figura 2.1 – Filogenia em uma linha do tempo das formigas da tribo Attini e os cinco sistemas de agricultura: agricultura tipo coral (A), agricultura basal (B), agricultura tipo levedura (C), agricultura derivada e agricultura das cortadeiras (D). (Adaptado de [7]).

2.2 Histórico das descobertas sobre os ninhos das atíneas

A simbiose das formigas cortadeiras e sua complexidade chamam a atenção de diversas áreas de pesquisa há mais de um século de estudos. Inúmeras pesquisas foram e ainda são realizadas a fim de compreender melhor a microbiota das formigas atíneas.

O primeiro trabalho sobre as formigas aparece na literatura em 1893. Nesse ano, o estudo sobre a simbiose foi publicado (em alemão) por Dr. Fritz Möller e descreve com detalhes os estudos microbiológicos sobre o mutualismo das formigas com seu fungo cultivar [9]. Estudos aprofundados para compreender melhor a simbiose do fungo mutualista e sua relação com as formigas começaram a ser realizados apenas 62 anos depois do primeiro estudo [2].

No início do século XX, pouco era conhecido sobre a complexidade dos ninhos, e o fungo parasita *Escovopsis* foi citado pela primeira vez por Muchovej e Della Lucia em 1990, porém nenhuma informação sobre simbiose é discutida no trabalho. Depois da sua identificação como patógeno dos ninhos, o microfungo foi estudado *in situ* pela primeira vez por Fisher [10], porém não foi um estudo que discutia o possível novo simbionte nos jardins.

Os estudos de Currie durante seu doutorado (1995-1999) trouxeram informações extremamente válidas para a compreensão da simbiose das formigas. Em 1999, ele realizou diversos estudos que contribuíram para o entendimento dos jardins das cortadeiras: a) o isolamento de actinobactérias das cutículas das formigas e a atividade delas contra o *Escovopsis* em ensaios de confronto em placas [11], b) isolamento de *Escovopsis* em diferentes ninhos das formigas cortadeiras na América Central comprovou que ele se trata

de um simbioss recorrente às formigas cortadeiras [12].

Todos os estudos realizados no final do século XX possibilitaram que diversas áreas do conhecimento pudessem perceber a importância de entender as relações simbióticas das formigas com o fungo mutualista, as actinobactérias e seu fungo parasita. Em 2001, o primeiro artigo de revisão aborda as interações entre os quatro indivíduos envolvidos na microbiota das atíneas [13].

Apenas em 2007 houve a descoberta por Currie e Little do quinto simbioss dos ninhos das formigas atíneas, os fungos e leveduras negras. Inicialmente esses simbioss foram relacionados ao gênero *Phialophora* [14]. Em estudos seguintes, os extratos das leveduras negras mostraram uma inibição do crescimento das actinobactérias. Com esse trabalho pode-se inferir que as leveduras negras são indiretamente prejudiciais ao ninho, uma vez que impede a produção de antibióticos pelas actinobactérias para proteção do jardim de fungos [15].

Com o desenvolvimento das técnicas espectroscópicas no início do século XXI, surgem os primeiros trabalhos que realizaram o isolamento dos metabólitos das actinobactérias. A substância dentigerumcina, com significativa atividade contra o *Escovopsis*, foi isolada pela primeira vez [16], comprovando hipóteses anteriores [11]. Em outros estudos, Haeder e colaboradores fizeram o isolamento da candicidina que também se mostrou ativa contra o fungo parasita dos ninhos [17].

O conhecimento pelo metabolismo das actinobactérias gera curiosidade e investigação. Diversos estudos realizaram o isolamento de metabólitos secundários de actinobactérias provenientes de diferentes ambientes, uma vez que estes apresentam uma fonte promissora de novos antibióticos para doenças humanas [18, 19].

Mais recentemente, Duarte e colaboradores identificaram uma variedade de leveduras negras isoladas do tegumento das formigas cortadeiras. Gêneros de fungos e leveduras até então não descritos puderam ser detectados nas cutículas das rainhas, porém sua função nos ninhos não era ainda totalmente compreendida [20].

Com novas abordagens analíticas, percebeu-se que para entender o micro-ambiente das formigas atíneas seria necessário entender as interações entre os microrganismos simbioss. Nessa vertente, Boya e colaboradores estudaram a comunicação entre actinobactérias e o fungo parasita através da análise por imageamento de MALDI de cocultivos. A indução metabólica foi verificada através de redes moleculares quando a actinobactéria *Streptomyces* era cultivada frente ao *Escovopsis*. Contribuições importantes relacionadas

à anotação de novos metabólitos produzidos pelo fungo parasita e isolamento de antimicrobianos produzidos pelas actinobactérias foram discutidas nesse estudo [21].

Em trabalhos mais recentes, as substâncias anotadas anteriormente para o fungo parasita foram isoladas e confirmadas. Dentre elas, diferentes shearininas, emodina e cicloartropsona foram identificadas e ensaiadas frente ao fungo mutualista e a cicloartropsona apresentou expressiva atividade inibitória [22]. Durante o mesmo período, outro estudo isolou os mesmos compostos e comprovou atividade antibiótica da shearinine D frente a *Pseudonocardia* [23].

A discussão da linha do tempo dos estudos realizados evidencia a necessidade de entender as relações entre os microrganismos simbioss das formigas cortadeiras presentes em uma complexa microbiota. Estudar os indivíduos separadamente pode não colaborar com o entendimento da comunicação entre eles. Portanto, a associação entre aspectos biológicos e químicos são de extrema importância para compreender o funcionamento das interações dentro nos ninhos das formigas atíneas.

2.3 A complexa simbiose das formigas atíneas

As formigas atíneas vivem em um mutualismo obrigatório com o fungo, *L. gongylophorus*. O fungo degrada o material vegetal fresco e o transforma em fonte de nutrientes assimiláveis pelas formigas [24]. Além do fungo mutualista, conhecido como cultivar, outros microrganismos são encontrados nos jardins das atíneas. O fungo parasita *Escovopsis*, as actinobactérias produtoras de antimicrobianos, *Pseudonocardia* e *Streptomyces*, e as leveduras negras também integram o ambiente das formigas. Com uma vasta complexidade, diversas áreas de pesquisas são impulsionadas a entender essa temática, como por exemplo a Ecologia química, Ecologia de comportamento, Ecologia microbiana, Co-evolução, Estabilidade de mutualismo, Patogênese, Inovação evolucionária, entre outras áreas do conhecimento. Um resumo da composição da microbiota e as diversas áreas do conhecimento está enumerado na figura 2.2 [25].

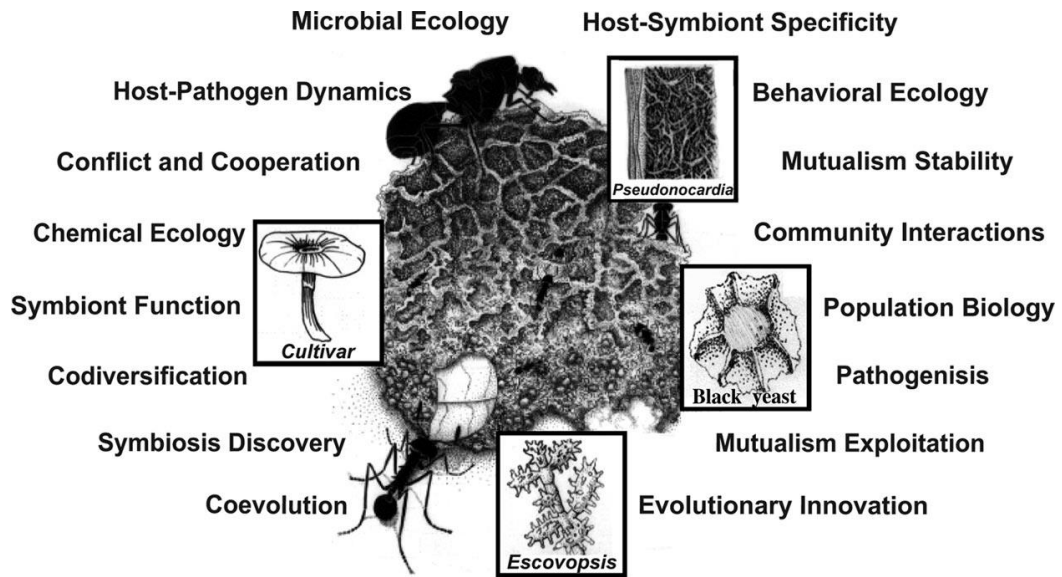


Figura 2.2 – Cinco diferentes simbioss foram identificados e caracterizados até o momento: as formigas atíneas, o fungo mutualista (cultivar), o fungo que ataca o mutualista, do gênero *Escovopsis*, as actinobactérias do gênero *Pseudonocardia* e *Streptomyces*, e leveduras negras que parasitam o mutualismo entre a formiga e a actinobactérias. (Adaptado de [25]).

O entendimento de cada um desses grupos é essencial para compreender a comunicação entre eles, por isso os detalhes de cada simbiote serão discutidos nas sessões seguintes.

2.3.1 *Leucoagaricus gongylophorus* e o mutualismo obrigatório

O mutualismo entre formigas atíneas e o fungo *L. gongylophorus* (Fungi: Basidiomycota) que elas cultivam para alimentação é muito bem estudado [13, 26]. O fungo vive em uma simbiose obrigatória com as formigas devido principalmente à cooperação bioquímica entre os indivíduos: as formigas levam o material vegetal para o formigueiro e o fungo mutualista degrada-o produzindo metabólitos primários assimiláveis pelos insetos através das estruturas formadas pelas hifas, os gongilídeos, constituindo, assim, o jardim de fungos [27] (fig. 2.3). O principal fundamento dessa simbiose está na inabilidade das formigas degradarem a celulose e a pectina das plantas. Essa fonte de nutrientes é assimilada pelo fungo mutualista e, então, utilizada pelas formigas [28]. Por isso, essa simbiose é de extrema importância para o desenvolvimento das espécies de atíneas. De outro lado, as formigas oferecem proteção ao fungo e material vegetal como fonte de alimento.

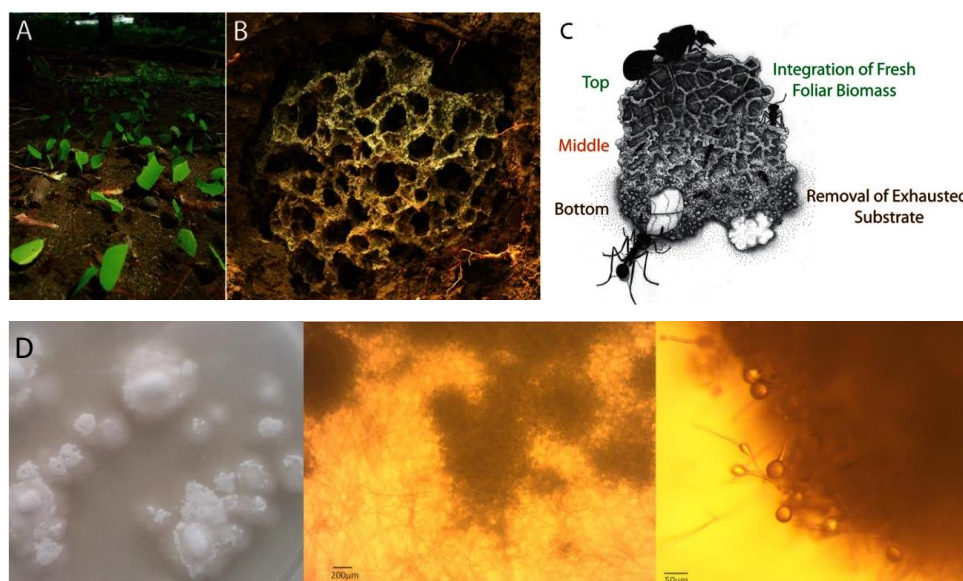


Figura 2.3 – (A) Formigas cortadeiras levando o material vegetal para os formigueiros; (B) O jardim de fungos das formigas atíneas, formada pelo fungo mutualista, em uma visão superior do ninho; (C) A biomassa fresca é degradada pelo fungo e organizada em um gradiente de degradação da matéria vegetal [27]; (D) Visão macroscópica do fungo mutualista *Leucogaricus gongylophorus* em meios de cultura batata dextrose agar (BDA), com detalhes do micélio mostrando o grupo de formação (ao centro) e as hifas com um acúmulo de gongilídeos (barra de escala: 200 e 50 μm) (Adaptado de [26]).

2.3.2 A proteção das actinobactérias nos ninhos das atíneas

As actinobactérias dos jardins das formigas atíneas são encontradas sobre a cutícula desses insetos, formando uma camada esbranquiçada principalmente sob o exoesqueleto das formigas *Acromyrmex* (Fig 2.4a). A produção de substâncias antimicrobianas, como a dentigerumcina, por exemplo, é a principal função quimio-ecológica das bactérias nos ninhos, sendo capazes de impedir a proliferação de outros organismos parasitas nos jardins de fungo [1, 11]. A actinobacteria, *Pseudonocardia* sp., foi inicialmente identificada e isoladas do exoesqueleto das formigas. Depois, diversas *Streptomyces* sp. são também descritas como produtora de compostos antifúngicos, como a candidicina [29]. Possivelmente, as actinobactérias coevoluiram com as formigas atíneas para especificamente controlar o fungo parasita *Escovopsis* sp, e conseqüentemente, proteger o formigueiro [12].

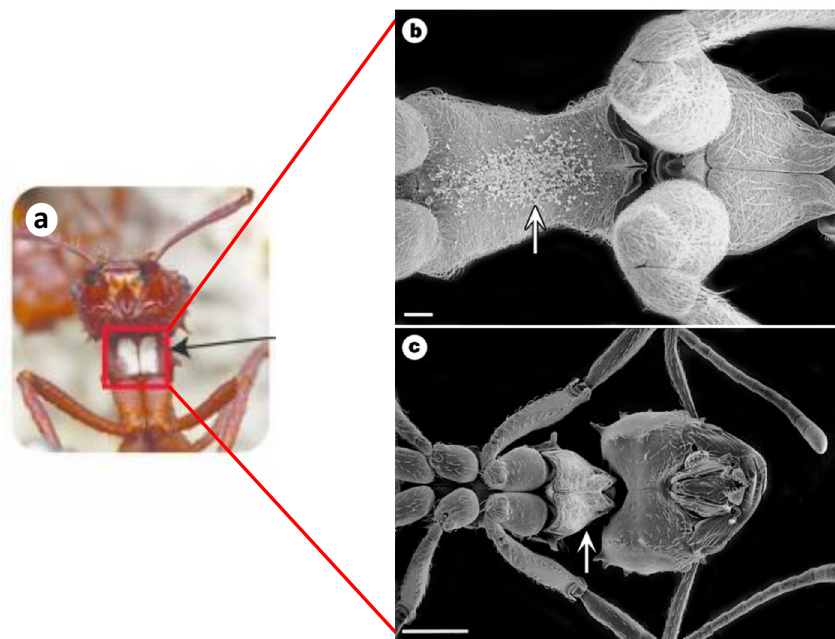


Figura 2.4 – (a) Micrografia eletrônica das formigas atíneas, com a presença de bactérias actinobactérias em suas cutículas, mostrando um crescimento padrão nesses insetos; (b) visualização de *Streptomyces* sp. sobre as pernas dianteiras de *Apterostigma* sp e, (c) uma representação de bactérias em operárias de *Acromyrmex octospinosus*. (Adaptado de [11]).

2.3.3 O invasor *Escovopsis* nos jardins de fungos

Fungos do gênero *Escovopsis* são comumente encontrados nos ninhos das formigas cortadeiras, atuando como parasita altamente virulento, podendo levar à devastação de todo o formigueiro, além de competir por substrato com o fungo mutualista (Fig 2.5). Ninhos de atíneas com a presença do *Escovopsis* sp. apresentaram menor acúmulo do jardim de fungo e também uma diminuição na produção de operárias, mostrando um impacto negativo sobre a simbiose. Esse gênero de fungo ainda não foi encontrado fora do jardim das atíneas, nem mesmo no solo adjacente aos ninhos. A transmissão desse fungo parasita é exclusivamente horizontal, sendo que outros microrganismos que vivem nos ninhos das formigas podem ser responsáveis por dispersá-lo [30, 31].

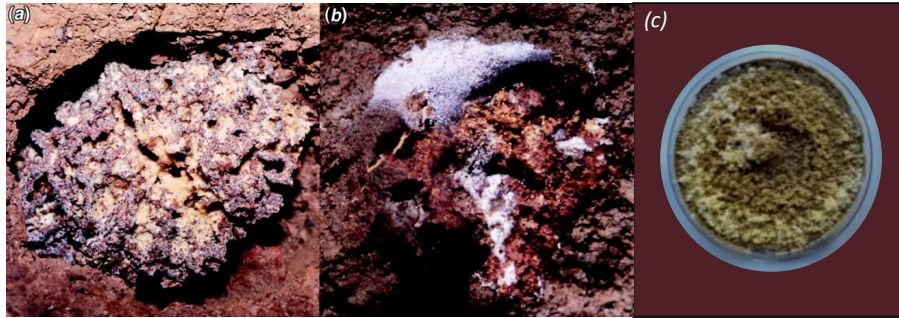


Figura 2.5 – (a) Jardim de formigas atíneas *Trachymyrmex* sp. saudável; (b) O mesmo jardim de *Trachymyrmex* sp. completamente devastado pela presença do fungo parasita *Escovopsis*; (c) O fungo parasita *Escovopsis weberi* crescido em placas de levedura e malte em meio sólido (Adaptado de [32]).

2.3.4 Os novos simbiossantes: leveduras e fungos negros

Um novo grupo de microrganismos foi classificado como o quinto simbiossante das formigas atíneas, esses simbiossantes estariam filogeneticamente próximos ao gênero *Phialophora*. Esses microrganismos foram denominados como leveduras e fungos negros. Embora tenha controvérsias quanto a sua classificação simbiótica, algumas evidências as caracterizam como simbiossantes: eles são geralmente encontrados em associações com as atíneas em diferentes ninhos e esses microrganismos estão sempre localizados nas cutículas dos corpos das formigas, mesma região onde as actinobactérias são encontradas buscando entender melhor a morfologia e a biologia das cepas (Fig 2.6A e B) [14].

Os microrganismos do gênero *Phialophora* foram os primeiros a serem isolados e caracterizados como simbiossantes (Chaetothyriales: Herpotrichiellaceae). As leveduras adquirem os nutrientes necessários a partir das actinobactérias, suprimindo o crescimento destas e comprometendo a proteção do ninho, devido à diminuição da proteção antimicrobiana. Até o momento, diversos gêneros de leveduras e fungos negros foram isolados do tegumento das formigas cortadeiras de folhas incluindo os gêneros *Aureobasidium* sp., *Exophiala* sp., *Pyrenochaeta* sp., *Phialophora* sp. [14, 15]. Este trabalho realizou diferentes estudos com *P. capiguarae* e *P. attae* (Fig 2.6D-F).

Na natureza, as leveduras negras são encontradas nos solos, em plantas, na água e em madeira em decomposição. Algumas leveduras negras causam doenças em humanos e em plantas [34]. Essa diversidade dificulta entender a verdadeira origem das leveduras negras como simbiossantes das formigas. Baseados em estudos, devido à relação desses microrganismos com plantas como endofíticos ou fitopatógenos, eles poderiam ter sido

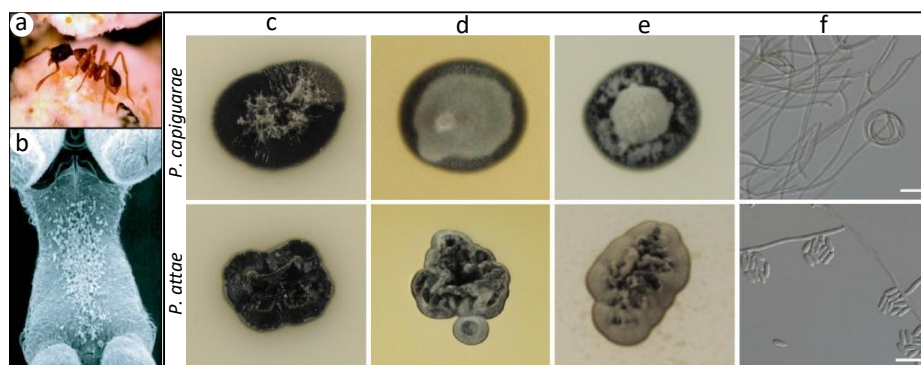


Figura 2.6 – (a) Formiga atínea *Apterostigma pilosum* de onde as primeiras leveduras negras foram isoladas. (b) Micrografia eletrônica da levedura negra no tórax das formigas [14]. Os microrganismos *P. capiguarae* e *P. attae* em diferentes meios de cultura (c) Corn meal ágar (CMA), (d) Malte ágar (MA), (e) Batata dextrose ágar (BDA) e (f) hifas vegetativas com enrolamento e conídios (barra de escala: 10 μm) (Adaptado de [14, 33]).

levados para dentro dos ninhos através do transporte de folhas frescas para o cultivo do mutualista. Alguns fungos da ordem Chaetothyriales apresentam capacidade de utilizar hidrocarbonetos como fontes de carbono, o que pode ter os auxiliado na sobrevivência no tegumento das formigas. Os estudos sobre a relação dos fungos negros com as formigas ainda são iniciais e podem revelar interessantes aspectos sobre a ecologia e interações entre os diversos microrganismos presentes nos ninhos das atíneas [20, 33].

2.4 Correlação das interações simbióticas das formigas atíneas

O termo simbiose refere-se à convivência de diferentes espécies de organismos em um mesmo ambiente e é encontrada na maioria dos ecossistemas, em diversas relações ecológicas. As várias interações existentes entre as formigas cortadeiras e os diversos microrganismos existentes nos jardins de fungos tornaram-se um grande modelo de estudo de simbiose [13].

As formigas beneficiam desse sistema, pois os fungos produzem enzimas que degradam os tecidos das plantas e desintoxicam certos metabólitos secundários das plantas que podem atuar com propriedades inseticidas e os fungos são mantidos em um ambiente praticamente livre de competição com outros microrganismos. Diferentes microrganismos parasitas são encontrados nos jardins, como do gênero *Escovopsis*, porém, na maioria dos casos, eles são controlados pelas actinobactérias produtoras de substâncias antimicrobi-

anas. Entretanto, as leveduras negras podem prejudicar esse equilíbrio, afetando a ação antimicrobiana das bactérias.

As leveduras negras podem comprometer a eficiência da atividade dos antibióticos, uma vez que inibem o crescimento das actinobactérias, o que resulta em uma supressão menos eficiente dos parasitas, como o *Escovopsis*, e diminui os benefícios das bactérias para o jardim de fungo (indicado pelo X em vermelho). As leveduras negras, indiretamente, beneficiam os parasitas do jardim, prejudicando o desenvolvimento do formigueiro (setas em verde) O resumo das interações é detalhado na Figura 2.7.

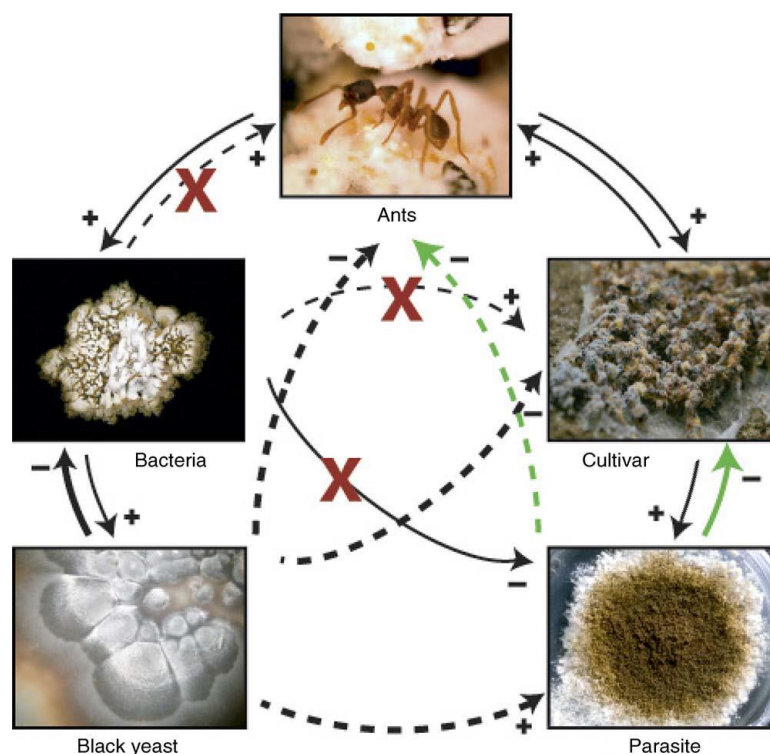


Figura 2.7 – Diagrama das interações existentes na microbiota das formigas atíneas. As setas em negrito representam efeitos diretos, enquanto setas tracejadas representam efeitos indiretos. Efeitos positivos são mostrados com (+) e efeitos negativos com (-). (Adaptado de [15]).

Um sistema de simbiose bastante complexo, como é o caso dos ninhos das formigas atíneas, precisa ser estudado por diferentes abordagens analíticas. Dessa forma, as interações não podem ser realizadas de forma unilateral com um dos simbiontes e sim, em associação com os demais microrganismos.

2.5 Guerra química entre os microrganismos das formigas atíneas

Na natureza, as interações entre os organismos são mediadas por diferentes substâncias químicas [35]. Pesquisas recentes em ecologia microbiana tem revelado uma grande diversidade quimio-ecológica entre as comunidades de microrganismos de diferentes ecossistemas. Entretanto, entender os fundamentos da comunicação química entre esses organismos tem sido um desafio para pesquisadores de diversas áreas, porém necessário para aprofundar o conhecimento de uma microbiota específica [36].

Dentre os microrganismos simbioss das formigas atíneas, estudos sobre a comunicação química entre eles revelaram informações importantes sobre essa microbiota e sobre a função ecológica dos metabólitos produzidos por esses microrganismos. Pesquisas relacionadas aos microrganismos presentes nos ninhos das formigas permeiam a literatura há mais de um século. As classificações para os microrganismos simbioss é bem estabelecida, porém o conhecimento dos metabólitos envolvidos nessa comunicação apenas foi descoberta recentemente [37].

Estudos recentes sobre o potencial químico do fungo *Escovopsis* mostraram uma diversidade na produção de metabólitos secundários, o que confirmou os estudos do genoma do fungo. Diferentes alcalóides terpeno-indólicos shearininas D e L foram isolados e mostraram efeitos sobre o comportamento das operárias e aumentaram a mortalidade das formigas nas colônias. A shearinina D ainda se mostrou ativa contra a *Pseudonocardia*. A dicetopiperazina melinacidina também se mostrou efetiva contra a actinobactéria. Esses compostos também foram evidenciados e superexpressos quando o fungo parasita era cultivado juntamente com o mutualista, porém não mostraram atividade contra o fungo [23].

Outros metabólitos também foram isolados do parasita, a antroquinona emodina e o policetídeo cicloartropsona, e ambos mostram atividade antifúngica frente ao mutualista *L. gongylophorus*. A substância cicloartropsona também foi testada contra a actinobactéria *Streptomyces*, apresentando atividade antibiótica frente a bactéria [22]. Os detalhes dos metabólitos isolados e sua comunicação frente aos outros organismos simbioss estão mostrados na figura 2.8.

A mais efetiva estratégia de defesa dos ninhos das formigas atíneas é a ação antimicrobiana realizada pelas bactérias actinobactérias. Além de proteger contra o ataque do *Escovopsis*, as actinobactérias também protegem contra microrganismos invasores nos

jardins. As diversas bactérias que vivem nas cutículas das formigas são uma importante barreira para a proliferação de organismos que prejudicariam todo o equilíbrio da colônia, tornando-se assim, uma simbiose essencial para a preservação do ninhos das formigas atíneas [11].

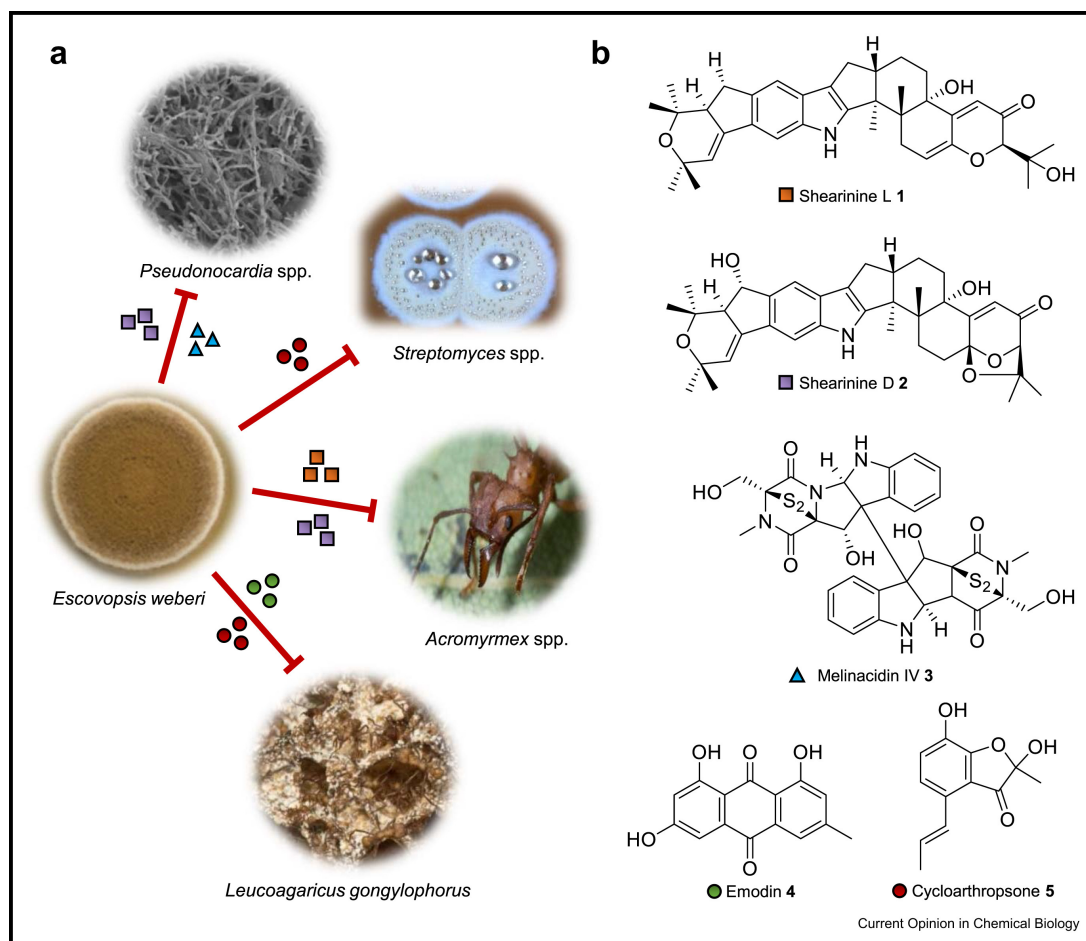


Figura 2.8 – (a) Interações do *Escovopsis weberi* com outros organismos dos ninhos das formigas. Metabólitos estão representados por pequenas formas coloridas, mostradas em (b). (b) Metabólitos isolados de *E. weberi*: shearinines D e L, melinacidina, emodina e cicloartropsona (Adaptado de [37]).

As actinobactérias são muito estudadas por serem produtoras de antibióticos. Muitas substâncias bioativas produzidas pela *Pseudonocardia* e *Streptomyces* já foram identificadas e a maioria deles apresentaram uma significativa atividade contra o parasita *Escovopsis*. *Pseudonocardia* produz diversos depsipeptídeos cíclicos e macrolídeos políenos: o policetídeo não ribossomal peptídeo dentigerumicina A apresentou atividade contra o patógeno *Escovopsis* [16]. Substâncias análogas a dentigerumicina também foram isoladas da actinobactéria porém não apresentaram atividade antifúngica [38] (Fig 2.9b).

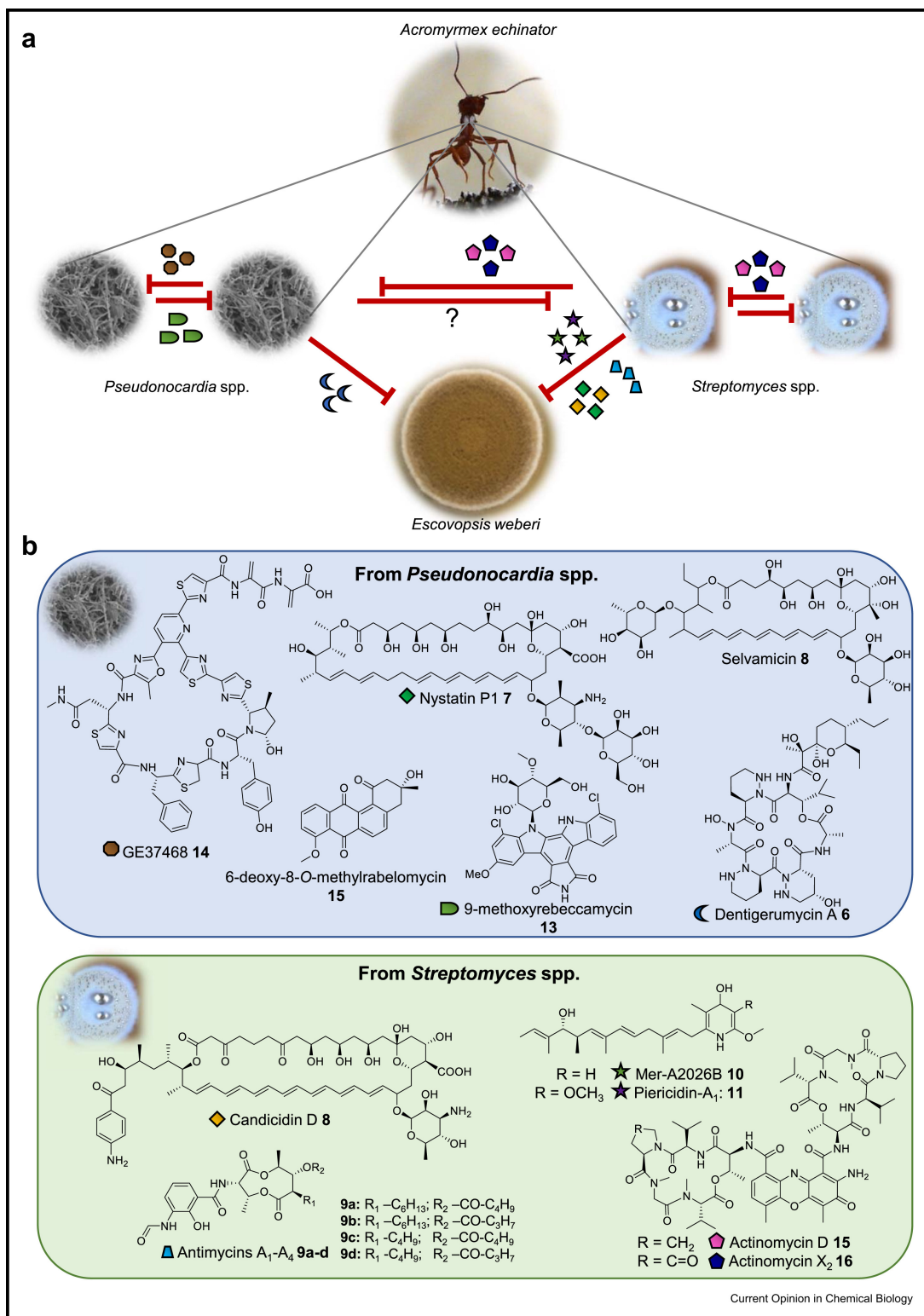


Figura 2.9 – (a) Interações químicas entre as actinobactérias com o fungo parasita. Os metabólitos ativos em (b) contra o fungo produzidos pelas actinobactérias, representados por diferentes formas coloridas, são enumeradas e classificadas nos quadros abaixo. (b) Metabólitos produzidos pela *Pseudonocardia* spp. (quadro em azul) e *Streptomyces* spp. (quadro em verde) (Adaptado de [37]).

Outros compostos isolados da *Pseudonocardia* sp. foram testados frente ao parasita, como o polieno niastatina P1, elucidado a partir de informações de MS/MS e do sequen-

ciamento do genoma da bactéria e apresentou atividade contra o *Escovopsis* [29], e a selvamicina, que não apresentou atividade antifúngica [39] (Fig 2.9b).

No exoesqueleto das formigas encontram-se também bactérias do gênero *Streptomyces*, que produz diversos antifúngicos como a candicidina D [17] e antimicina A1-A4 [40] que apresentaram expressiva atividade contra o *Escovopsis* porém nenhuma inibição contra o fungo mutualita, expressando, assim, alta seletividade. Já o metabólito actinomicina D-X2 apresentou atividade contra os dois fungos [41]. E recentemente, dois monohidroxipiridinas Mer-A2026B e piericidina apresentaram inibição do crescimento do fungo parasita e também atividade antileishmaniose [42].

Diante da comprovação da atividade desses metabólitos frente ao parasita *Escovopsis*, fortes evidências são traçadas de que essas substâncias são também produzidas na natureza como metabólitos de defesa dentro do ninho das atíneas.

2.6 Interações microbianas e cocultivo entre microrganismos

Microrganismos são encontrados em todos ambientes e, por isso, assumem uma grande possibilidade de interações. Este complexo de comunidades microbianas é definido como microbioma. O termo inclui as bactérias, vírus, protistas, leveduras e fungos que vivem em um ambiente particular [43, 44]. Os microrganismos vivem em constante interação, competindo por nutrientes limitados, sendo assim, eles desenvolveram mecanismos para a sobrevivência, para se protegerem e defenderem, a partir da produção de metabólitos secundários [45].

A coexistência de vários microrganismos em um mesmo nicho pode afetar o seu desenvolvimento e crescimento, além de afetar a capacidade de sintetizar metabólitos primários e secundários [46]. Dessa forma, rotas biossintéticas podem ter seus genes silenciados quando um organismo é cultivado de forma axênica, já que ele se encontra em um ambiente sem competição [47].

Estudos prévios mostraram que cocultivos ou culturas mistas de microrganismos resultam no aumento de atividade biológica de extratos brutos, devido principalmente a uma indução de novos metabólitos, consequência de uma expressão de rotas metabólicas anteriormente silenciadas [48].

Diferentes classes de substâncias foram induzidas através de cocultivos [49]. Cocultura entre o fungo *Aspergillus fumigatus* e bactéria *Streptomyces* sp. produziram diversos

dicetopiperazinas e o novo metabólito 11-O-methylpseurotina A2 (**1**), e policetídeos da classe fumiciclina A e B (**2** e **3**) [50]. Novos derivados da fumiformamida (**4**), ácido 2-(carboximetilamino) benzóico (**6**), (+)-citreoisocoumarinol (**7**) também foram produzidos através do cocultivo entre *Fusarium tricinctum* com *Bacillus subtilis* [51] (Fig. 2.10).

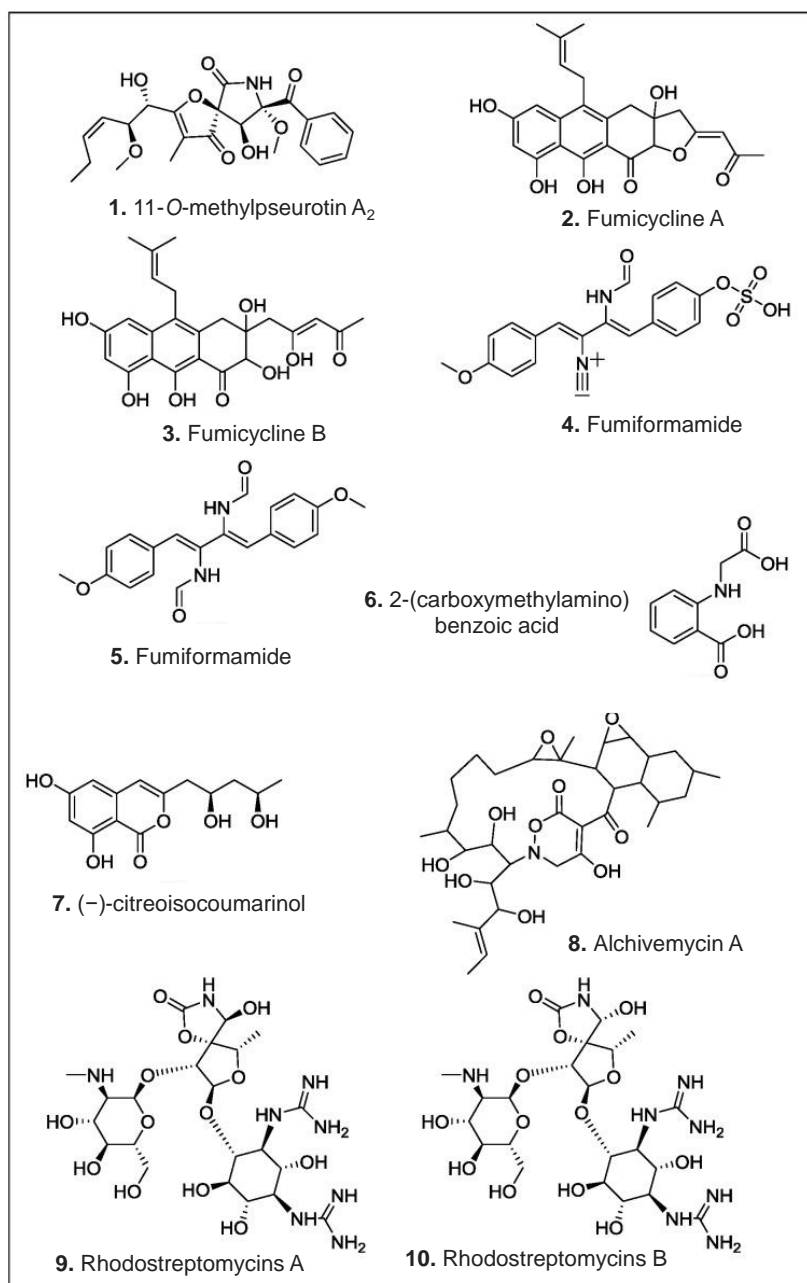


Figura 2.10 – Novos produtos naturais reportados a partir de coculturas de fungos com bactérias ou entre bactérias (Adaptado de [49]).

Cocultivos entre *S. endus* com *Tsukamurella pulmonis* induziram a produção do antibiótico alchivemicina A (**8**) [52]. Cocultivos entre a bactéria *Rhodococcus fascians*, que não produz nenhuma substância antibiótica, junto a *S. padanus* produziram novos anti-

bióticos aminoglicosídeos rodostreptomycinas A e B (**9** e **10**) [53]. A lista de metabólitos produzidos através de cocultivos é extensa e, colaboram para que novos trabalhos dentro da temática sejam realizados (Fig. 2.10).

As técnicas de cocultura tem sido aplicadas para diferentes objetivos: i) como forma de compreender as comunidades microbianas na agricultura, microrganismos existentes na rizosfera ou endofíticos; ii) investigar as interações da microbiota no corpo humano; iii) induzir a produção de algum metabólito secundário de interesse; iv) potencializar a produção de produtos específicos e, no caso do presente trabalho, v) entender os fenômenos de simbiose na natureza [54, 55].

Na busca por substâncias bioativas produzidas por esses microrganismos, cultivar um microrganismo em presença de outro, os chamados cocultivos, como uma estratégia para mimetizar o ambiente microbiológico natural do formigueiro constitui uma ferramenta válida. O jardim de fungo constitui uma microbiota de complexa interação de fungos, leveduras e bactérias, mantendo, assim, a estabilidade dos ninhos das formigas. A tentativa de mimetizar esse ambiente pode ser aproximada da realidade através da utilizações de coculturas.

2.7 Ferramentas analíticas em estudos de ecologia química

2.7.1 Análise multivariada dos dados obtidos por LC-MS

Estudos envolvendo LC-MS geram uma grande quantidade de dados de várias dimensões e a análise desses dados exige, portanto, abordagens mais sofisticadas, envolvendo ferramentas quimiométricas, como a análise multivariada de dados [56].

A busca pela detecção de indução metabólica em coculturas fornece grande quantidade de dados que exigem um tratamento e processamento adequado e diferentes ferramentas podem ser utilizadas. Cocultivos precisam ser comparados com as culturas axênicas, para verificar a indução ou supressão metabólica. Geralmente, os dados de LC-MS obtidos são complexos e não permitem que uma comparação visual seja suficiente e eficaz. A análise de dados ocorre após o processamento dos dados através do “*peak peaking*”, do inglês.

Dessa forma, os dados brutos podem ser comparados, através de diferentes metodologias: (I) busca por íons induzidos apenas nas coculturas [57], (II) estudos de PCA (análise de componentes principais) e PLS-DA (análise discriminante por mínimos quadrados par-

ciais) para verificar o grau de similaridade que possui entre as amostras e saber quais as variáveis responsáveis por essa separação [54] e (III) a nova abordagem POChEMon (Monitoramento projetado do contorno químico ortogonal) que revela toda a competição bioquímica alterada nos cocultivos [58]. A Figura 2.11 mostra os detalhes dessas abordagens [55].

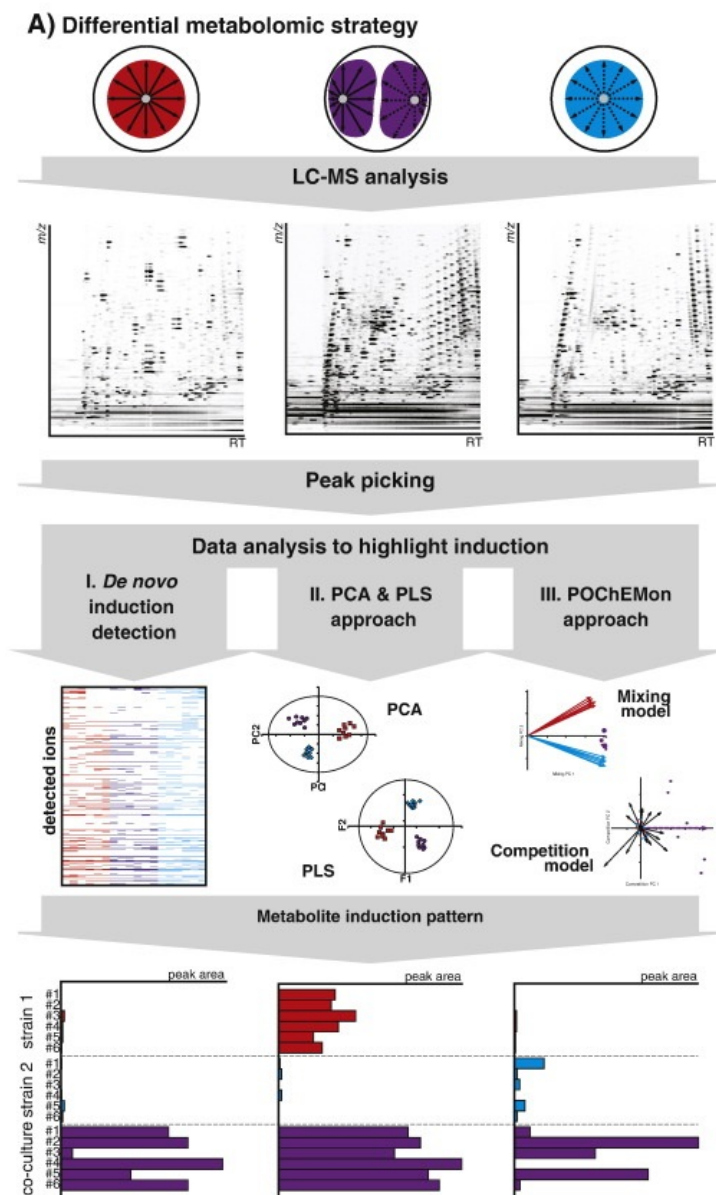


Figura 2.11 – Diferentes abordagens utilizadas no estudo sobre indução metabólica através de coculturas de microrganismos (Adaptado de [55]).

Por fim, as informações adquiridas pelas análises multivariadas de dados fornecem íons relevantes que foram induzidos nos cocultivos ou que estejam mais relacionados à essas amostras. Os diversos métodos de análises multivariadas podem ser utilizados separadamente ou em conjunto, mas a interpretação dos dados também pode ser desafiadora.

2.7.2 Redes moleculares na plataforma GNPS

A identificação de metabólitos por LC-MS sempre foi uma etapa desafiadora na área de produtos naturais [59]. Antes, apenas a comparação com base de dados, raramente disponíveis, era realizada. Para facilitar a anotação de metabólitos e a organização dos dados obtidos por espectrometria de massas, foi criado o *Global Natural Products Social Molecular Networking*, o GNPS, que consiste em um banco de dados gratuito, onde os usuários podem organizar seus dados brutos de LC-MS e comparar os espectros de fragmentação das amostras com uma biblioteca de metabólitos primários e secundários [60].

A construção de mapas ou redes moleculares são uma das principais funções dentro do GNPS. As redes são construídas através do alinhamento dos espectros de fragmentação e comparados com as bibliotecas presentes na plataforma. Quando um espectro possui uma semelhança com os fragmentos de alguma substância da biblioteca, tem-se um “*match*”, combinação em português, e uma consequente anotação do metabólito. Uma comparação entre os espectros também é realizada, sendo agrupadas pela similaridade dos padrões de fragmentação. O valor de cosseno varia de 0-1 (na qual 1 é 100% de similaridade) e determina o grau de similaridade entre os espectros das amostras comparados à biblioteca (Fig. 2.12).

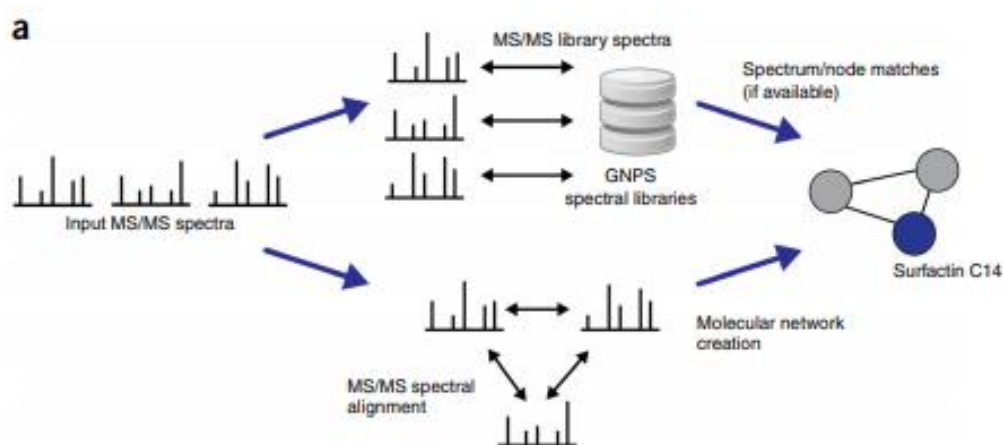


Figura 2.12 – Princípio básico da criação das redes moleculares na plataforma GNPS ((Adaptado de [60])).

As redes moleculares são muito úteis para a organização de muitos dados, pois permitem uma visualização completa dos dados em apenas uma rede. Para amostras mais

estudadas, a plataforma pode fornecer anotações importantes e decisivas para a continuação do trabalho. Para amostras menos conhecidas, de espécies de plantas ou microrganismos pouco estudados, essa ferramenta pode colaborar com o direcionamento do estudo. Sendo assim, a plataforma pode ser muito útil na área de produtos naturais se for bem explorada.

Atualmente, a versatilidade da plataforma acompanha os mais diferentes projetos e ideias, propagação de anotação *in silico* e predição de fragmentação podem ser realizadas e a distinção quantitativa dos dados também estão presentes em alguns trabalhos [61]. As ferramentas presentes na plataforma GNPS contribuem para estudos de comparação de cocultivos e facilitam a visualização, organização e análise dos dados obtidos por LC-MS.

2.8 Referências

- [1] Marchiori AC. Diversidade e evolução na simbiose entre bactérias e formigas Attini. Tese de Doutorado Universidade Estadual Paulista Júlio de Mesquita Filho, Instituto de Biociências de Rio Claro.
- [2] Weber NA. Pure Cultures of Fungi Produced by Ants. *Science*. 1955;121(3134):109.
- [3] Hervey A, Rogerson CT, Leong I. Studies on fungi cultivated by ant. *Brittonia*. 1977;29(2):226–236.
- [4] Mead MI, Khan A, Nickless G, Grealley BR, Tainton D, Pitman T, et al. Leaf cutter ants: A possible missing source of biogenic halocarbons. *Environmental Chemistry*. 2008;5:5–10.
- [5] Mueller U, Schultz T, Currie C, Adams R, Malloch D. The origin of the Atinneant-fungus mutualism. *The Quarterly review of biology*. 2001;76:169–197.
- [6] Mehdiabadi NJ, Schultz T. Natural history and phylogeny of the fungus-farming ants (Hymenoptera: Formicidae: Myrmicinae: Attini). *Myrmecological News*. 2010;13:37–55.
- [7] Schultz TR, Brady SG. Major evolutionary transitions in ant agriculture. *Proceedings of the National Academy of Sciences*. 2008;105(14):5435–5440.

- [8] Mehdiabadi N, Schultz T. Natural history and phylogeny of the fungus-farming ants (Hymenoptera: Formicidae: Myrmicinae: Attini). *Myrmecological News*. 2010;13:37–55.
- [9] Willis JC. The fungus gardens of certain south with a thick mass of weathered pieces of leaves and twigs, *American Ants*. *Nature*. 1893;48(1243):392–394.
- [10] Fisher PJ, Stradling DJ, Sutton BC, Petrini LE. Microfungi in the fungus gardens of the leaf-cutting ant *Atta cephalotes*: A preliminary study. *Mycological Research*. 1996;100(5):541–546.
- [11] Currie CR, Scottt JA, Summerbell RC, Malloch D. Fungus-growing ants use antibiotic-producing bacteria to control garden parasites. *Nature*. 1999;398(6729):701–704.
- [12] Currie CR, Mueller UG, Malloch D. The agricultural pathology of ant fungus gardens. *Proceedings of the National Academy of Sciences of the United States of America*. 1999;96(14):7998–8002.
- [13] Currie CR. A community of ants, fungi, and bacteria: a multilateral approach to studying symbiosis. *Annual Review of Microbiology*. 2001;55:357–380.
- [14] Little A, Currie CR. Symbiotic complexity: discovery of a fifth symbiont in the Atinne ant-microbe symbiosis. *Biology Letters*. 2007;3:501–504.
- [15] Little A, Currie C. Black yeast symbionts compromise the efficiency of antibiotic defenses in fungus-growing ants. *Ecology*. 2008;89:1216–1222.
- [16] Oh DC, Poulsen M, Currie CR, Clardy J. Dentigerumycin: a bacterial mediator of an ant-fungus symbiosis. *Nature Chemical Biology*. 2009;5(6):391–393.
- [17] Haeder S, Wirth R, Herz H, Spiteller D. Candicidin-producing *Streptomyces* support leaf-cutting ants to protect their fungus garden against the pathogenic fungus *Escovopsis*. *Proceedings of the National Academy of Sciences*. 2009;106(12):4742–4746.
- [18] Solecka J, Zajko J, Postek M, Rajnisz A. Biologically active secondary metabolites from Actinomycetes. *Open Life Sciences*. 2012;7(3):373–390.

- [19] Fiedler HP, Bruntner C, Bull A, Ward A, Goodfellow M, Potterat O, et al. Marine actinomycetes as source of novel secondary metabolites. *Antonie van Leeuwenhoek*. 2005;87:37–42.
- [20] Duarte APM, Ferro M, Rodrigues A, Bacci M, Nagamoto NS, Forti LC, et al. Prevalence of the genus *Cladosporium* on the integument of leaf-cutting ants characterized by 454 pyrosequencing. *Antonie van Leeuwenhoek, International Journal of General and Molecular Microbiology*. 2016;109(9):1235–1243.
- [21] Boya CA, Fernandez-Marin H, Mejia LC, Spadafora C, Dorrestein PC, Gutierrez M. Imaging mass spectrometry and MS/MS molecular networking reveals chemical interactions among cuticular bacteria and pathogenic fungi associated with fungus-growing ants. *Scientific Reports*. 2017;7(1):1–13.
- [22] Dhodary B, Schilg M, Wirth R, Spiteller D. Secondary metabolites from *Escovopsis weberi* and their role in Attacking the garden fungus of leaf-cutting ants. *Chemistry - A European Journal*. 2018;24:4445–4452.
- [23] Heine D, Holmes NA, Worsley SF, Santos ACA, Innocent TM, Scherlach K, et al. Chemical warfare between leafcutter ant symbionts and a co-evolved pathogen. *Nature Communications*. 2018;9(2208):1–11.
- [24] Aylward F, Khadempour L, Tremmel D, McDonald B, Nicora C, Wu S, et al. Enrichment and broad representation of plant biomass-degrading enzymes in the specialized hyphal swellings of *Leucoagaricus gongylophorus*, the fungal symbiont of leaf-cutter ants. *PLoS ONE*. 2015;10(9):0134752.
- [25] Caldera EJ, Poulsen M, Suen G, Currie CR. Insect symbioses: A case study of past, present, and future fungus-growing ant research. *Environmental Entomology*. 2009;38(1):78–92.
- [26] Viguera G, Paredes-Hernández D, Revah S, Valenzuela J, Olivares-Hernández R, Le Borgne S. Growth and enzymatic activity of *Leucoagaricus gongylophorus*, a mutualistic fungus isolated from the leaf-cutting ant *Atta mexicana*, on cellulose and lignocellulosic biomass. *Letters in Applied Microbiology*. 2017;65(2):173–181.
- [27] Aylward FO, Burnum-Johnson KE, Tringe SG, Teiling C, Tremmel DM, Moeller JA, et al. *Leucoagaricus gongylophorus* Produces Diverse Enzymes for the Degradation

- of Recalcitrant Plant Polymers in Leaf-Cutter Ant Fungus Gardens. *Applied and Environmental Microbiology*. 2013;79(12):3770–3778.
- [28] Gomes De Siqueira C, Bacci M, Pagnocca FC, Bueno OC, Hebling MJ. Metabolism of plant polysaccharides by *Leucoagaricus gongylophorus*, the symbiotic fungus of the leaf-cutting ant *Atta sexdens* L. *Applied and Environmental Microbiology*. 1998;64(12):4820–4822.
- [29] Barke J, Seipke R, Grünschow S, Heavens D, Drou N, Bibb M, et al. A mixed community of actinomycetes produce multiple antibiotics for the fungus farming ant *Acromyrmex octospinosus*. *BMC Biology*. 2010;8:109.
- [30] Currie CR, Wong B, Stuart AE, Schultz TR, Rehner SA, Mueller UG, et al. Ancient tripartite coevolution in the Atinneant-microbe symbiosis. *Science*. 2003;299(5605):386–388.
- [31] Aksenov AA, Da Silva R, Knight R, Lopes NP, Dorrestein PC. Global chemical analysis of biology by mass spectrometry. *Nature Reviews Chemistry*. 2017;1(7):1–20.
- [32] Currie C, Mueller U, Malloch D. The agricultural pathology of ant fungus gardens. *Proceedings of the National Academy of Sciences*. 1999;96:7998–8002.
- [33] Toledo APMD. Fungos negros presentes no integumento de formigas cortadeiras (Tribo Attini). Tese de Doutorado Universidade Estadual Paulista Júlio de Mesquita Filho, Instituto de Biociências de Rio Claro. 2016.
- [34] Teixeira M, Moreno L, Stielow B, Muszewska A, Hainaut M, Gonzaga L, et al. Exploring the genomic diversity of black yeasts and relatives (Chaetothyriales, Ascomycota). *Studies in Mycology*. 2017 01;86:1–28.
- [35] Mithofer A, Boland W. Do you speak chemistry? Small chemical compounds represent the evolutionary oldest form of communication between organisms. *EMBO Reports*. 2016;17.
- [36] Schmidt R, Ulanova D, Wick L, Bode H, Garbeva P. Microbe-driven chemical ecology: past, present and future. *The ISME Journal*. 2019;13.

- [37] Batey SFD, Greco C, Hutchings MI, Wilkinson B. Chemical warfare between fungus-growing ants and their pathogens. *Current Opinion in Chemical Biology*. 2020;59:172–181.
- [38] Sit C, Ruzzini A, Arnam E, Ramadhar T, Currie C, Clardy J. Variable genetic architectures produce virtually identical molecules in bacterial symbionts of fungus-growing ants. *Proceedings of the National Academy of Sciences of the United States of America*. 2015;112(43):13150–13154.
- [39] Van Arnam EB, Ruzzini AC, Sit CS, Horn H, Pinto-Tomas AA, Currie CR, et al. Selvamycin, an atypical antifungal polyene from two alternative genomic contexts. *Proceedings of the National Academy of Sciences*. 2016;113(46):12940–12945.
- [40] Seipke R, Barke J, Brearley C, Hill L, Yu D, Goss R, et al. A Single *Streptomyces* symbiont makes multiple antifungals to support the fungus farming ant *Acromyrmex octospinosus*. *PLoS one*. 2011;6:22028.
- [41] Schoenian I, Spiteller M, Ghaste M, Wirth R, Herz H, Spiteller D. Chemical basis of the synergism and antagonism in microbial communities in the nests of leaf-cutting ants. *Proceedings of the National Academy of Sciences of the United States of America*. 2011;108:1955–1960.
- [42] Ortega H, Ferreira L, Melo W, Oliveira A, Alvarenga R, Lopes N, et al. Antifungal compounds from *Streptomyces* associated with Atinneants also inhibit *Leishmania donovani*. *PLoS Neglected Tropical Diseases*. 2019;13:e0007643.
- [43] Aly A, Debbab A, Chaidir C. Fungal endophytes: Unique plant inhabitants with great promises. *Applied Microbiology and Biotechnology*. 2011;90:1829–1845.
- [44] Pace NR. A Molecular View of Microbial Diversity and the Biosphere. *Science*. 1997;276(5313):734–740.
- [45] Knight V, Sanglier JJ, DiTullio D, Braccili S, Bonner P, Waters J, et al. Diversifying microbial natural products for drug discovery. *Applied Microbiology and Biotechnology*. 2003;62:446–458.
- [46] Ross-Davis A, Stewart J, Shaw J, Kim MS, Klopfenstein N. Metagenomic approaches for surveying forest soil microbial communities on permanent plots. *Phytopathology*. 2013;103:139–142.

- [47] Pettit R. Mixed fermentation for natural product drug discovery. *Applied Microbiology and Biotechnology*. 2009;83:19–25.
- [48] Brakhage A, Schroeckh V. Fungal secondary metabolites - strategies to activate silent gene clusters. *Fungal genetics and biology*. 2010;48:15–22.
- [49] Marmann A, Aly A, Lin W, Wang B, Proksch P. Co-Cultivation A Powerful Emerging Tool for Enhancing the Chemical Diversity of Microorganisms. *Marine Drugs*. 2014;12(2):1043–1065.
- [50] König C, Scherlach K, Schroeckh V, Horn F, Nietzsche S, Brakhage A, et al. Bacterium induces cryptic meroterpenoid pathway in the pathogenic fungus *Aspergillus fumigatus*. *Chembiochem: a European Journal of Chemical Biology*. 2013;14.
- [51] Ola A, Thomy D, Lai D, Broetz-Oesterhelt H, Chaidir C. Inducing secondary metabolite production by the endophytic fungus *Fusarium tricinctum* through co-culture with *Bacillus subtilis*. *Journal of natural products*. 2013;76:2094–2099.
- [52] Onaka H, Mori Y, Igarashi Y, Furumai T. Mycolic acid-containing bacteria induce natural-product biosynthesis in *Streptomyces* species. *Applied and Environmental Microbiology*. 2011;77:400–406.
- [53] Kurosawa K, Ghiviriga I, Sambandan TG, Lessard P, Barbara J, Rha C, et al. Rhodostreptomycins, antibiotics biosynthesized following horizontal gene transfer from *Streptomyces padanus* to *Rhodococcus fascians*. *Journal of the American Chemical Society*. 2008;130:1126–1127.
- [54] Bertrand S, Schumpp O, Bohni N, Bujard A, Azzollini A, Monod M, et al. Detection of metabolite induction in fungal co-cultures on solid media by high-throughput differential ultra-high pressure liquid chromatography-time-of-flight mass spectrometry fingerprinting. *Journal of Chromatography A*. 2013;1292:219–228.
- [55] Bertrand S, Bohni N, Schnee S, Schumpp O, Gindro K, Wolfender JL. Metabolite induction via microorganism co-culture: A potential way to enhance chemical diversity for drug discovery. *Biotechnology Advances*. 2014;32(6):1180 – 1204.
- [56] Gorrochategui E, Jaumot J, Lacorte S, Tauler R. Data analysis strategies for targeted and untargeted LC-MS metabolomic studies: Overview and workflow. *Trends in Analytical Chemistry*. 2016;82:425–442.

- [57] Bertrand S, Azzollini A, Schumpp O, Bohni N, Schrenzel J, Monod M, et al. Multi-well fungal co-Culture for *de novo* metabolite-induction in time series studies based on untargeted metabolomics. *Molecular BioSystems*. 2014;10:2289–2298.
- [58] Jansen J, Blanchet L, Buydens L, Bertrand S, Wolfender JL. Projected Orthogonalized CHEMical Encounter MONitoring for microbial interactions in co-culture. *Metabolomics*. 2015;11:908–919.
- [59] Oberlies N, El-Elimat T. High resolution MS, MS/MS, and UV database of fungal secondary metabolites as a dereplication protocol for bioactive natural products. *ACS National Meeting Book of Abstracts*. 2013:1709–1716.
- [60] Wang M, Carver J, Phelan V, Sanchez L, Garg N, Peng Y, et al. Sharing and community curation of mass spectrometry data with Global Natural Products Social Molecular Networking. *Nature Biotechnology*. 2016 05;34:828–837.
- [61] Nothias LF, Petras D, Schmid R, Duhrkop K, Rainer J, Sarvepalli A, et al. Feature-based molecular networking in the GNPS analysis environment. *Nature Methods*. 2020;17(9):905–908.

3 Different tools to investigate chemical interactions among leaf-cutting ants symbionts

Nesse capítulo é realizado um estudo detalhado dos cocultivos de microrganismos simbiotes das formigas cortadeiras. Ferramentas analíticas, como análise multivariada de dados, redes moleculares e imageamento por espectrometria de massas foram utilizadas para compreender melhor as interações estudadas. Dez diferentes coculturas foram realizadas e utilizados como um guia para futuras análises de estudos de interações entre microrganismos.

3.1 Abstract

Leaf-cutting ants live in a mandatory mutualism with the basidiomycete fungus, *Leucoagaricus gongylophorus*. During the evolution, other symbiont microbes joined to the ants garden. Different parasites were raised, as such as the parasite *Escovopsis* and actinobacteria. Actinobacteria also protect the mutualist fungus with antimicrobial compounds to preserve the equilibrium. The black yeasts can damage this antimicrobial control. Due to the complex relationship among Attini ants with their symbiont microbes, different studies were done in the last century. Different analytical tools have been used to try to understand the microbial interactions in leaf cutting ants nests. In this study, one of each of symbionts, mutualist and parasite fungus, actinobacteria and black yeasts, were exposed in co-cultures to verify induction or production of metabolites. Here we investigate the metabolic profiles of these co-cultivations using mass-spectrometry-based metabolomic approaches and molecular networking. Furthermore, the induced m/z were compared to imaging co-cultivations to recognize the present ion precisely in the interaction. In this way, our results represented a large number of metabolites, as such as shearinines, sesquiterpenoids, indoles and coproporphyrin I, which can be induced in co-cultures with different kind of symbionts. Besides, this sort of study is simplified when different approaches are employed.

Key-words: Microbial interactions, *Leucoagaricus gongylophorus*, *Escovopsis*, *Pseudonocardia*, *Phialophora* leaf cutting ants symbionts, metabolomics, molecular network, imaging mass spectrometry.

3.2 Introduction

Tribe Attini ants have an ancient mandatory association with fungi that they cultivate for food. As such, the ants have developed various mechanisms to defend their fungus garden, including hygienic behaviors to rid the garden of foreign microbes and management of harmful garden waste [1, 2, 3]. Despite these defensive mechanisms, the system mutualism is parasitized by a specialized pathogen of the genus *Escovopsis*.

The ants engage in a second mutualism with actinobacteria of the genus *Pseudonocardia* to help protect their fungal crops from the specialized pathogen, which produces antibiotics that specifically inhibit *Escovopsis* and other parasites [4]. The mutualist bacteria typically occur on ants' cuticle structures, which produce nutrients to support bacterial growth [5]. In recent studies, black yeasts have also been found in ants' cuticle. These microbes compete for nutrients and inhibit the actinobacteria growth [6]. Thus, each member of the fungus-growing ant community is directly and indirectly influenced by one another in both positive and negative ways [7]. The interactions within leaf-cutting ant nests and an overview of this study is illustrated in Fig. 3.1.

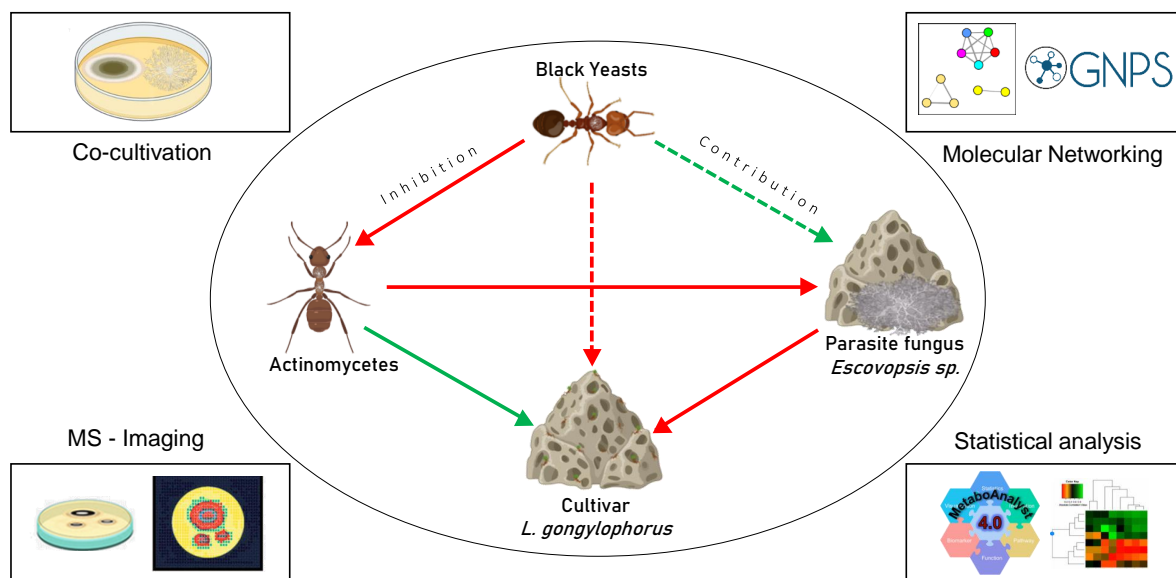


Figura 3.1 – Schematic representation of the main interactions within leaf-cutting ant nests. Black yeasts directly inhibit the growth of the mutualistic actinobacteria of ants, which indirectly benefits the garden parasite by compromising antibiotic defenses. It indirectly decreases the benefit that actinobacteria provide to ants and cultivars. Solid lines indicate direct and dashed lines, indirect effects black yeasts have on the ants' symbionts [6]. Understanding the interaction can be simplified using different approaches: co-cultivations, statistical analysis, molecular networking, and imaging by mass spectrometry.

Mass spectrometry (MS) approaches are useful to understand biological systems. To understand complex data sets, with thousands of ions measured per sample, the use of multivariate data analysis (MVDA) is necessary. Many clustering and classification methods are currently used successfully to create concise summaries of the data, as well as to represent linear and non-linear relationships between features [8]

As previously mentioned, different analytical tools have been used to understand the interactions within leaf-cutting ant symbionts, for instance co-cultivation [9, 10], imaging-MS [10, 11] and molecular networking [9, 10]. Those studies have evidenced the necessity to use more than one analytical tool to acquire a complete overview of metabolomic data of symbiont microbes. For this reason, an interdisciplinary approach combined biology, analytical and organic chemistry and chemometrics, is fully appropriated to explore the symbiont interaction in the garden of leaf-cutting ants [12].

Molecular networking (MN) is one of the main analysis tools used within the Global Natural Product Social Molecular Networking (GNPS) platform. GNPS platform is an important metabolites library of MS/MS spectra of previously reported metabolites. When a spectrum acquired for a sample is highly similar to a MS/MS spectrum from the GNPS library, it is recognized and annotated. The platform provides the ability to analyze LC/MS data and compares it with public libraries' data setting [13]. Also, MN is a useful alternative when there is a large number of samples to compare or classify them. This kind of analysis can simplify the visualization of the chemical space present in MS experiments [13].

Here, we report an alternative approach to co-cultivating symbiont microbes isolated from leaf-cutting ant nests. Five different microbes were previously isolated and identified as symbiont strains. The interactions were classified according to the visual morphology such as medium color, inhibition, or overgrowth. Mono and co-cultures were evaluated by comparative metabolomics analysis such as MVDA, MN, and imaging mass spectrometry (IMS). Thus, the combination of those analytical tools could help to understand the communication among leaf-cutting ants symbionts.

3.3 Experimental part

3.3.1 Biological Material

The symbiont microbes strains used in this study were isolated from leaf cutting ants (*Atta* and *Acromyrmex*) and registered in the Sistema Nacional de Gestão do Patrimônio Genético e do Conhecimento Tradicional Associado (SISGEN - Brazil). The strains were stored at 4°C in vials containing a diluted Yeast and malt medium agar (YEMA) (3 g yeast extract, 5 g peptone, 3 g of malt extract, 10 g of D-glucose, 15 g of agar (Acumedia) in 1000 mL of dd-water) and maintained in new Petri dishes every 15 days. The complete information about the strains is described in Table 3.1, such as the microbe information, the strain code, the source of isolation and the location information.

Tabela 3.1 – Microbes information used in this study: the group of symbionts, the name, the code and the strain, and information about the isolation such as species of ants, city, and year. All the strains were collected in Brazil.

Group	Mutualistic fungus	Black yeast	Parasite	actinobacteria
Microbe	<i>Leocoagaricus gongylophorus</i>	<i>Phialophora attae</i> and <i>P. capiguarae</i>	<i>Escovopsis weberi</i>	<i>Pseudonocardia</i> sp.
Strain Code	FF2006 LG	AP399/376 PA/PC	LESF019 EM	TCP30 Bac
Isolation	<i>Atta sexdens</i> gardens	gynes of <i>A. capiguara</i>	<i>A. sexdens rubropilosa</i>	workers of <i>Acromyrmex subterraneus</i>
Place, year	Corumbataí-SP, 2006	Botucatu-SP, 2012	Botucatu-SP, 2013	Viçosa-MG, 2016

3.3.2 Experimental settings of culture and co-culture conditions

For all mono-cultures, a 5 mm agar plug of a microbial pre-culture was inoculated in the centre of a 9 cm Petri dish containing 20 mL of YEME media. Similarly, for co-culture two 5 mm agar plugs of a pre-culture of the two different microbial species on the opposite sides of the plate with 2 cm of distance. Bacteria was spreaded in Petri dishes and incubated at 25°C.

Blank samples (only YEME agar) were prepared. The cultures were incubated at 25°C in the dark. The mutualist, *L. gongylophorus*, and the black yeasts (BY), *P. attae* and *P. capiguarae*, were inoculated in the beginning of the experiment, then the actinobacteria,

Pseudonocardia sp. was inoculated after 14 days, and the parasite, *E. microspora*, after 21 days. Three replicates of each single culture and co-culture in the same conditions were cultivated for 28 days of growth. The inoculation time was stipulated based on each strain. The co-cultivation was performed according to the Figure 3.2.

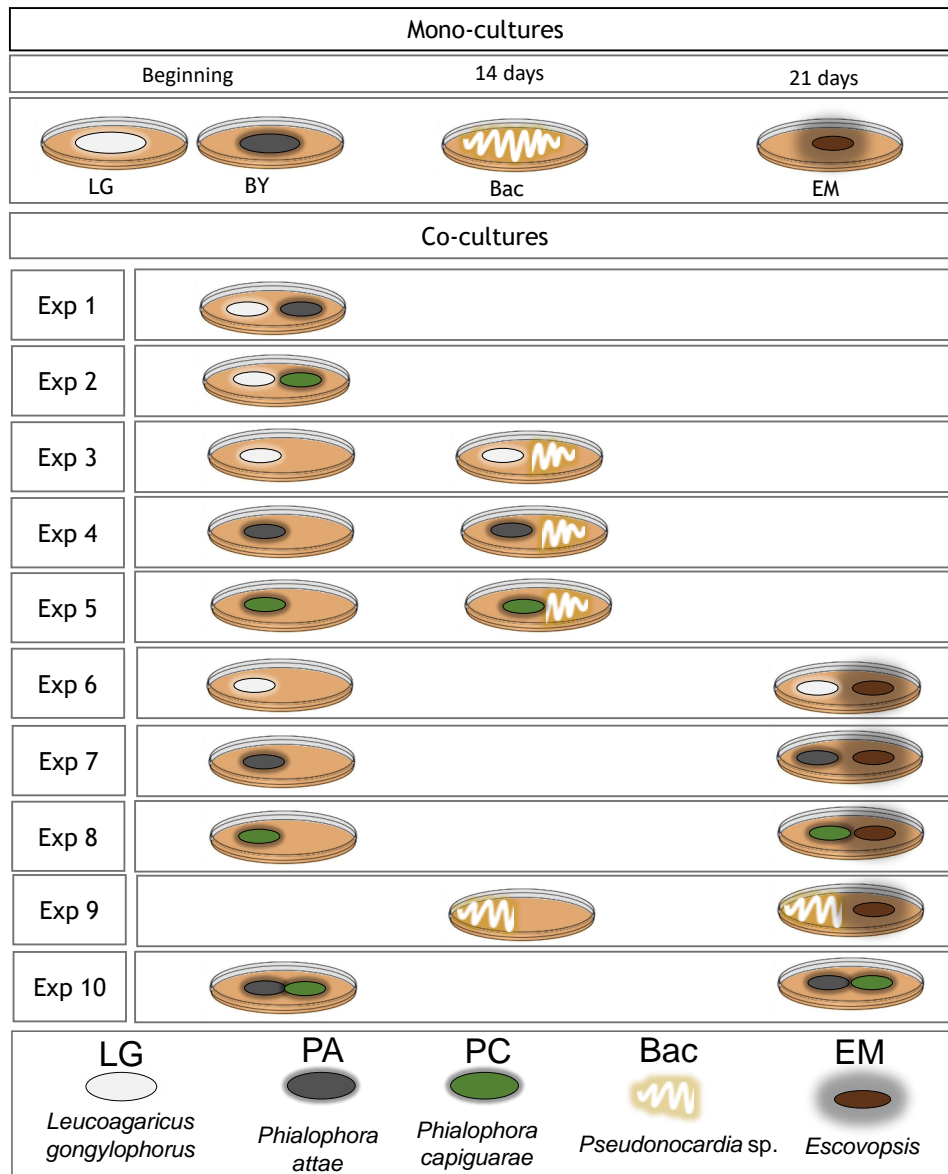


Figura 3.2 – Experimental design of symbionts co-cultivations according to different experiments (1-10). The first day only the mutualist fungus and the black yeasts were inoculated. After 7 days, the actinobacteria was inoculated and after 21 days, the parasite *Escovopsis* was inoculated. The extractions were made after 28 days. Experiments details: (1) The mutualist and BY *P. attae*, (2) the mutualist and BY *P. capiguarae*, (3). the mutualist and the actinobacteria, (4) the BY *P. attae* and actinobacteria, (5) the BY *P. capiguarae* and actinobacteria, (6) the mutualist and the parasite, (7) the BY *P. attae* and the parasite, (8) the BY *P. capiguarae* and the parasite, (9) the actinobacteria and the parasite and (10) both BYs.

3.3.3 Extraction and sample preparation for LC-MS

Small pieces of different co-cultures, the axenic cultures of each microbial pure strain culture and non-inoculated YEME agar dish (blank) were sliced and placed in different flasks. The interactions of microbial co-cultures were divided in 3 sections, splitting in zone (A) relating to the first inoculated microbe, (B) the confrontation zone and (C) the second inoculated microbe (Fig. 3.3).

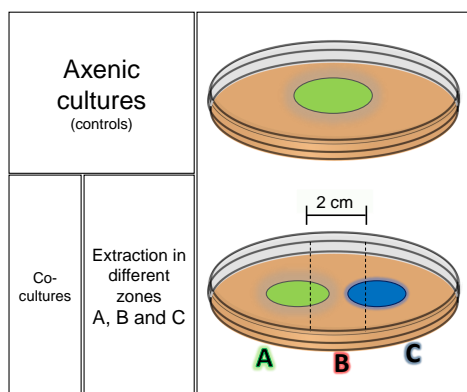


Figura 3.3 – Overview of extraction methodology. The axenic cultures of each microbe was extracted from the hole plate and the co-cultures were extract in three different zones (A), (B) and (C).

The fresh material was transferred into an extraction vessel with 100 mL of ethyl acetate per approximately 50 mg of biological material. The extractions were performed in a water-bath sonicator (Soni-tech TDR force) at room temperature for 15 min. The sonicated samples were filtered through filter paper and cotton. Finally, the extracts were dried under vacuum using a centrifugal evaporator (Büchi, Brazil). Uninoculated plates and mono-cultures were used as blanks and controls, respectively. The dry extracts were dissolved in 100% acetonitrile (ACN) and filtered through 0.45 μm filters at a concentration of 2 mg/mL. In total, 105 samples and blanks were measured.

3.3.4 LC-MS data acquisition

Experiments were performed using a Quadruple-Time of flight high-resolution ESI (Bruker-Daltonics) mass spectrometer coupled to a LC Model UFLC system (Shimadzu), which included an in-line degasser, binary pump, and refrigerated autosampler. A 5 μm C18 column with 250 mm \times 4,6 mm (Phenomenex Luna), maintained at 25°C, was operated using a gradient elution of H₂O and ACN (both with 0.1% formic acid) running at 1.0 mL \cdot min⁻¹. The gradient program was as follows: 5 to 100% ACN over 25 min,

100% ACN for 10 min using 15 μL of injection volume at 40°C. All of the mass spectra were recorded in the positive-ion mode in a DDA mode acquisition. MS parameters were a spray voltage of 3.5 kV, a capillary temperature of 220°C, a dry gas in 9 L \cdot min⁻¹ at 40 psi. The m/z range was 50 to 1500, detecting the signals below $1.0 \cdot 10^3$. For internal calibration, a solution of sodium trifluoroacetic acid (10 mg \cdot mL⁻¹) was used.

3.3.5 LC-MS data processing

3.3.5.1 Multivariate data analysis

MS raw data .d (Bruker) were converted into .mzXML data using MS Convert software (ProteoWizard). The feature detection was performed between the retention time from 2 to 30 min with MZMine 2.34 (MZmine VTT, Finland) using parameters according to the qTOF-MS detector for data processing. For mass detection a range of 50 to 1500 Da was used, during 2 to 35 min and $1.0 \cdot 10^3$ noise level. Peaks with a width of at least 0.2 s and an intensity greater than $6.0 \cdot 10^3$ were selected with a 10 ppm m/z tolerance. Chromatogram deconvolution was performed using the local minimum search algorithm (minimum peak height of $2.1 \cdot 10^3$, peak duration of 0.05 to 5 and baseline level of $2.0 \cdot 10^3$). Deisotope filtering was applied using the isotopic peaks grouper module with tolerance parameters adjusted to 0.001 s and 10 ppm. Feature alignment and gap filling were achieved with an m/z tolerance of 10 ppm and a retention-time (RT) tolerance of 0.1 min. The exported feature lists were exported in CVS file format and organized using Microsoft Excel, and multivariate data analyses (MVDA) were performed using Metaboanalyst 4.0 [14]. The data scaling was performed using auto-scaling (mean-centered and divided by standard deviation of each variable). Principal component analysis (PCA), partial least squares regression (PLS-DA) and hierarchical cluster analysis (HCA) in a heat map form applied after unit variance scaling was used for sample discrimination (scores) as well as the generation of biplots and the list of features (loadings).

3.3.5.2 Molecular networking data analysis

A molecular network was created using the online workflow on the GNPS website [13]. The data was filtered by removing all MS/MS fragment ions within ± 17 Da of the precursor m/z . MS/MS spectra were filtered by choosing only the top 4 fragment ions in the ± 50 Da window throughout the spectrum. The precursor ion mass tolerance was set

to 0.8 Da and a MS/MS fragment ion tolerance of 0.1 Da. A network was then created where edges were filtered to have a cosine score above 0.65 and more than 4 matched peaks. Further, edges between two nodes were kept in the network if and only if each of the nodes appeared in each other's respective top 10 most similar nodes. Finally, the maximum size of a molecular family was set to 100, and the lowest scoring edges were removed from molecular families until the molecular family size was below this threshold. The spectra in the network were then searched against GNPS spectral libraries. The library spectra were filtered in the same manner as the input data. All matches kept between network spectra and library spectra were required to have a score above 0.65 and at least 4 matched peaks. To enhance chemical structural information within the molecular network, information from *in silico* structure annotations from GNPS Library Search were incorporated into the network using the GNPS MolNetEnhancer workflow on the GNPS website. Chemical class annotations were performed using the ClassyFire chemical ontology [15].

3.3.6 Imaging-MS sample preparation and data analysis

The strains were inoculated using water suspension in the agar plates with the microscope slides, photographed and put in a vacuum desiccator for complete agar dehydration at room temperature [16]. MS imaging was performed using a ProSolia DESI source (Model OS-3201) coupled to a Thermo Scientific Q Exactive Hybrid Quadrupole-Orbitrap Mass Spectrometer. The DESI configuration was set with an emitter height of 2.5 mm, mass spectrometer inlet height of 0.1 mm, inlet to emitter distance of 3.8 mm, 58°C spray angle, 5.0 kV spray voltage, inlet capillary temperature of 320°C, 100 V S-lens, 160 psi ultrapure nitrogen nebulizing gas pressure, and a sprayed solvent of methanol at a $3.0 \mu\text{L} \cdot \text{min}^{-1}$ flow rate. Images were collected from m/z 200 to 1500 with a step sized of 200 μm , a scan rate of $741 \mu\text{m} \cdot \text{s}^{-1}$, and a pixel size of $200 \mu\text{m} \cdot 200 \mu\text{m}$. In short, major conditions were as follows: $3 \text{ L} \cdot \text{min}^{-1}$ of solvent flow rate, nebulizing gas backpressure of 100 psi, and $2 \text{ mL} \cdot \text{min}^{-1}$ gas flow rate. The DESI-IMS data was converted into imaged files using Firefly data conversion software (version 2.1.05) and viewed using the BioMAP software (version 3.8.04). In BioMAP software the data were opened in an m/z 200 to 1000 range, and the false-color scaling were adjusted to a fixed value to enable a relative comparison between experiments. The MS spectra were opened using X-Calibur software (Thermo Scientific). The overall workflow is shown in Fig. 3.4.

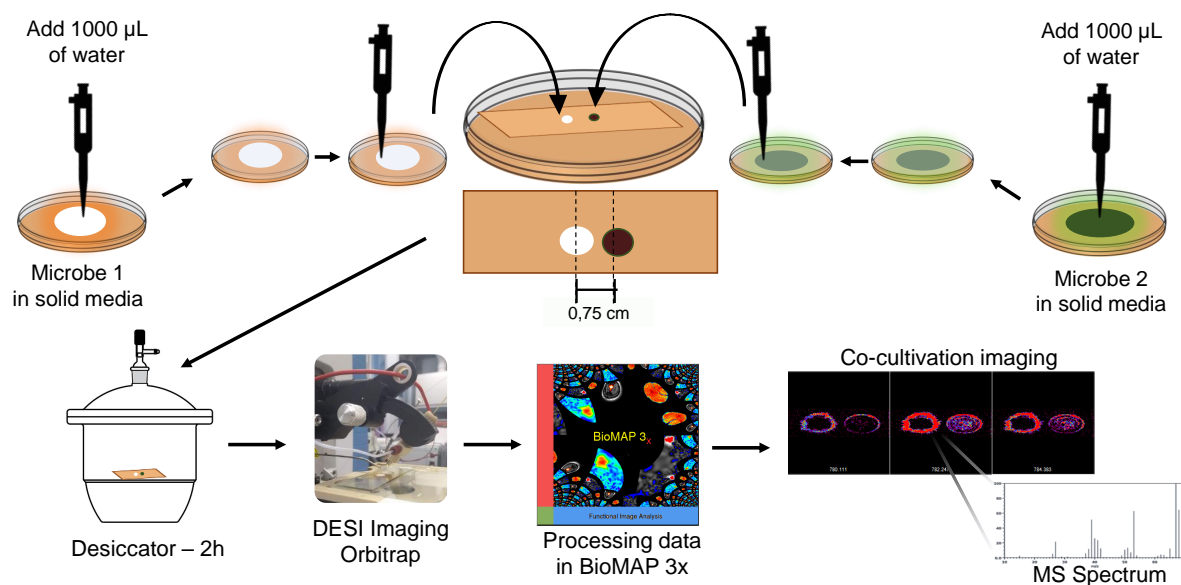


Figura 3.4 – Overall workflow for DESI methodology: $1000\mu\text{L}$ of distilled water is added in the Petri dish, the mycelium is scrapped using a Drigalsky spatula. 5 to $10\mu\text{L}$ of this solution are added in a new Petri dish with a glass slide ($26 \cdot 76\mu\text{m}$) previously prepared, in 0.75 cm of distance between the strains. The laminules were dried in desiccator for two hours, analyzed directly by DESI and processed using BioMAP.

3.4 Results and discussion

3.4.1 Morphological patterns in co-culture of symbiont microbes

Cultivations were performed in solid media because of a fungal ecology perspective, solid media better mimics the natural growth conditions of filamentous fungi. The visualization in solid media makes it easier to cut a part of the agar media for further analysis of the location of fungal confrontations [17].

The microbial interactions were observed over a period of four weeks. After the incubation time, symbiont microbial co-cultures were classified according to four patterns: zone line, distance inhibition, contact inhibition, and overgrowth [17, 18]. Different kinds of interactions were observed in those co-cultures (Fig. 3.5). The interaction between mutualist fungus, *L. gongylophorus*, and black yeast, *P. attae* and *P. capiguarae* (Exp. 1 and 2) presented a zone line interaction formation. New substances may have been produced due to the dark color in the medium in those co-cultures. The experiments between the mutualist fungus, *L. gongylophorus*, and actinobacteria *Pseudonocardia* sp. (Exp. 3), between both black yeasts *P. attae* and *P. capiguarae* and parasite *E. microspora* (Exp.

7 and 8), between the parasite fungus and actinobacteria (Exp. 9) had a small inhibition zone between the strains. This interaction suggests the production of antimicrobial compounds. The co-culture between both black yeasts and the actinobacteria (Exp. 4 and 5) showed a contact inhibition and each one has grown in its space but no evidence of compound production. The same situation was verified for the co-culture between both black yeast (Exp. 10). The only co-culture expressed as an overgrowth was between the mutualist fungus, *L. gongylophorus* with the parasite fungus *E. microspora* (Exp. 6). The parasite invades completely the mutualist space and it is not possible to recognize a split between them.

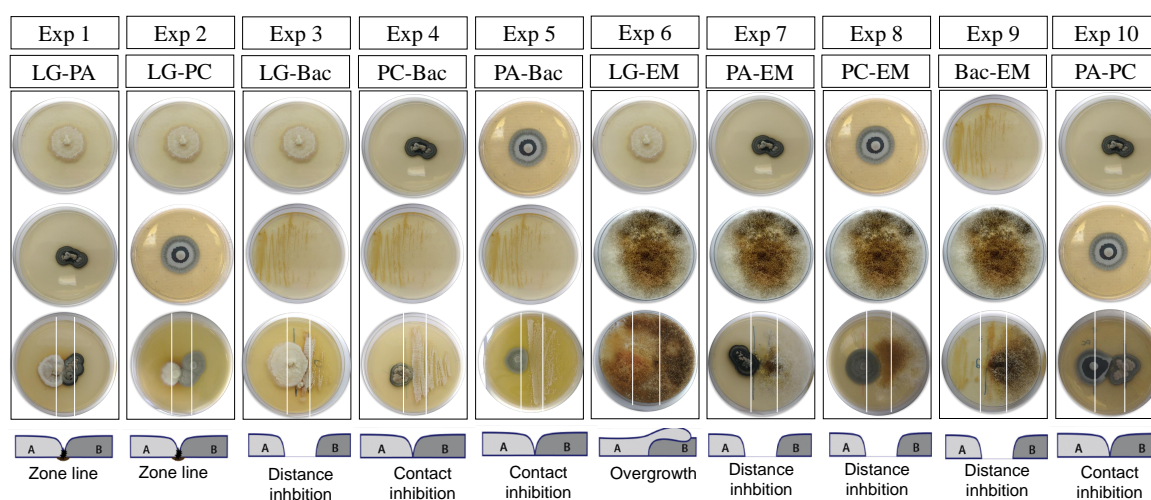


Figura 3.5 – Co-cultivations among the microbial symbionts of leaf cutting ants. The experiments are organized 1 to 10. (1) The mutualist and black yeast (BY) *P. attae*, (2) the mutualist and BY *P. capiguarae*, (3) mutualist fungus and the actinobacteria, (4) the BY *P. attae* and actinobacteria, (5) the BY *P. capiguarae* and actinobacteria, (6) the mutualist and the parasite, (7) the BY *P. attae* and the parasite, (8) the BY *P. capiguarae* and the parasite, (9) the actinobacteria and the parasite and (10) both BYs.

In the attempt to verify whether the types of patterns in the interactions could be related to the differences between the mono and co-cultures, all experiments were performed using LC-MS fingerprint screening as well as the different zones in the plate (A), (B), and (C). The different zones were analyzed to verify the metabolic induction in the confrontation zone (B) or to try to recognize the source of the induction. The reproducibility was checked in three biological replicates to assure sample repeatability.

3.4.2 Chemical diversity of co-cultures in MVDA

As a first step, we performed a complete overview of statistic analysis (PCA, PLS, HCA) on these 114 samples. In this part, the different sections of the Petri dish (A, B, and C) were labeled only as co-cultures. The PLS-Da (Fig. 3.6A) resulted in better-resolved clustering between the co-cultures than PCA (Fig. B.1). The individual PLS-Da of each experiment is indicated in Fig. B.2. The method was validated with $Q^2 > 0.5$ and $R^2 \sim 0.9$ (Fig. B.3).

PLS-Da is a supervised analysis and the separation between the mono and co-cultures samples was clearer. The model has low variance (Component 1 with 2.8% and component 2 with 2.9%) due to the large number of samples (105) and variables ($\sim 30,000$) (Fig. 3.6A). The metabolic profile data setting of co-cultures and mono-cultures contained a large number of loadings (variables). The experiments co-cultures between *P. attae* and *Pseudonocardia* sp. (PA-Bac) and *P. capiguarae* and *Escovopsis* (PC-EM) demonstrated differences between mono and co-cultures. The experiment in details between the black yeast *P. capiguarae* and the parasite (PC-EM) is detailed in chapter 4.

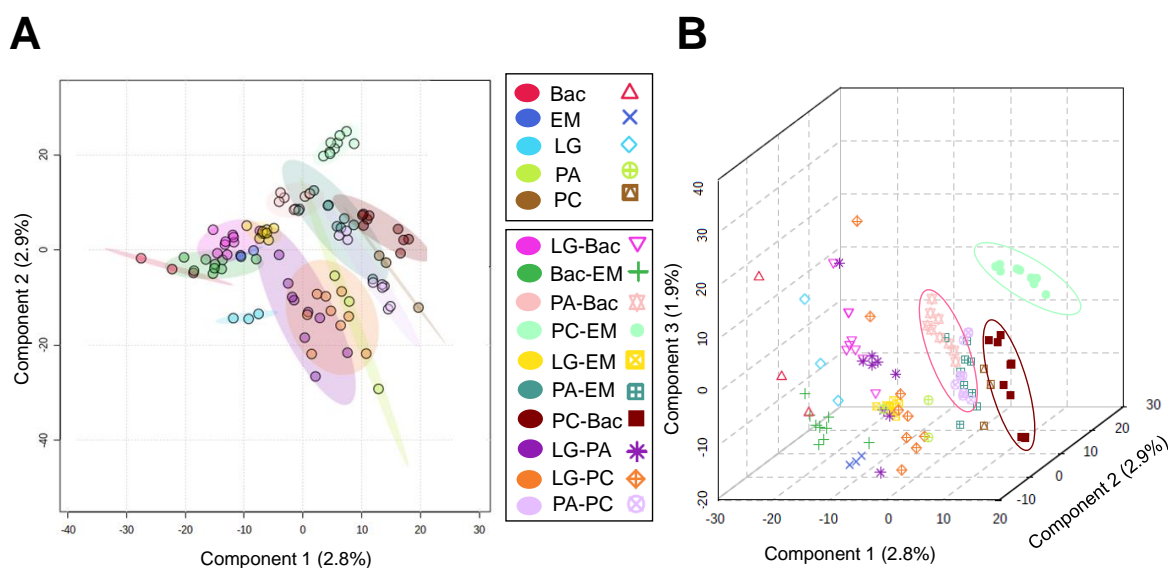


Figura 3.6 – A: Supervised 2D PLS-Da multivariate data analysis of the co-cultures and mono-cultures fingerprinting. B: Supervised 3D PLS-Da multivariate data analysis. *P. attae* and *Pseudonocardia* sp. (in light pink) and *P. capiguarae* and *Escovopsis* (in light green) are highlighted because of their clear separation related to other groups.

Supervised analysis of the data via PLS was used to detect over-expressed compounds in the co-cultures. The individual PLS-Da shows an apparent separation between some co-cultures experiments (Fig. B.2), in special experiments 4: *Phialophora attae* and

Pseudonocardia sp. and 8: *P. capiguarae* and *Escovopsis* sp. These experiments help to understand the kinds of microbial interaction: 1) the compound production only in co-cultures; 2) the compound production only in mono-cultures and 3) the compound production in both kinds of cultures. The third one is represented when the samples are closer to PLS-Da graphic representation. In the ten microbial interactions studied under this statistical methodology, only two represented a variation between mono and co-cultures. This observation indicates the importance of having a large initial data set. These observations can support the hypotheses of the metabolite induction in microbial co-cultures [18, 19, 20]. Some co-cultures cannot induce different metabolites due to the type of interaction. Those chemical interactions stimulate the metabolite induction because the same microbes live in a full confrontation in nature. Co-cultures systems help to mimic what happens in the leaf-cutting ants' microbiome.

The heat-map analysis was used to highlight the chemical diversity of co-cultures in comparison to mono-cultures, in addition, each cultivation has specific m/z more or less intense than in the other samples. Two different clusters were created in the heat-map, i) the first one with co-culture LG-Bac, mono-culture Bac and EM, Bac-EM, PC-EM, and LG-EM, ii) the second group was composed of PA-EM, PC-Bac and PA-PC and the mono-cultures LG, PA and PC (Fig. 3.7B).

We recognize the metabolic variation in mono and co-cultures samples in heat-map visualization. Even with a large number of variables (ions) the separation in two different groups contribute to establish the similar groups to their mono-cultures. The co-culture between the mutualist fungus and actinobacteria is more related to the mono-culture of *Pseudonocardia* sp. This feature means the metabolites from *L. gongylophorus* do not present prominence in this specific interaction. On the other hand, the opposite occurs in co-cultures between the black yeast and the mutualist fungus. However, all co-cultures with the *Escovopsis* are similar to the same parasite mono-culture.

In the light of these results, we consider that HCA associate to a heat map visualization facilitate the interpretation of convoluted data and lead to understand the similarities and differences between mono and co-cultures. In addition, we verify which of microbes in these interaction produces the most relevant metabolites that contribute to the differentiation of co-cultivations.

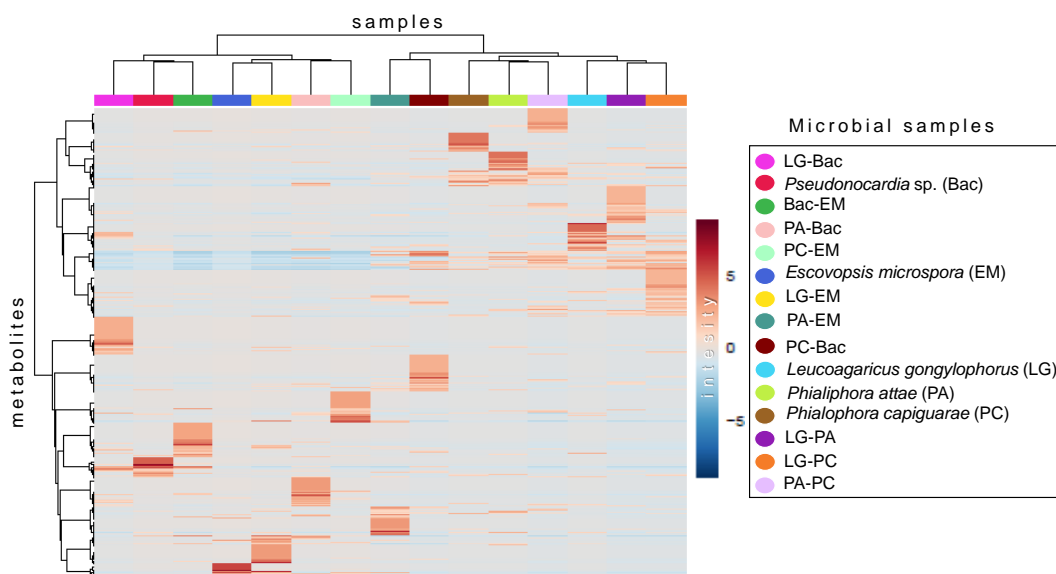


Figura 3.7 – Heat map and grouping analyses of the chemical profiles obtained by LC-MS of co-cultures and mono-cultures samples. Each color means a group of sample related to mono-cultures, *Pseudonocardia* sp. (Bac) in red, *Escovopsis microspora* (EM) in blue, *Leucoagaricus gongylophorus* (LG) in light blue, *Phialophora attae* (PA) in light green and *P. capiguarae* (PC) in light brown, and co-cultures. Clustering result shown as heat map and the differential accumulation of mass features according to the different samples in HCA. HCA was constructed using *Euclidean* distance measure and clustering algorithm using Ward's method.

3.5 Diversity of annotated metabolites in molecular networking

The raw LC-MS data were submitted to GNPS platform in a MN data analysis. In total, the library annotated 166 primary and secondary metabolites. Only 58 hits had the cosine higher than 0.8, which means possible similarity. The complete information, highlighting the chemical compounds, the instrument where the data were collected, the precursor ion, Minimum Qualification Score (MQS) or cosine score and the metabolite class is presented in Table B.1 (Supplementary information). Twelve different classes as such as fatty acids, flavin nucleotides, steroids derivatives, diazanaphlens, imidazopyridines, carboxylic acids, indoles and derivatives, benzene and substituted derivatives, benzofurans and naphthopyrans were annotated in the samples.

The other analysis in GNPS platform, the MolNetEnhacer integrated metabolome mining and used the annotation tools to classify the spectral families in groups according to the metabolite class. Fatty acids, flavin nucleotides, glycerophospholipids, steroids,

diazonophtalens, carboxylic acids, naphthopyrans, purine nucleosides, indole and derivatives, organonitrogen, benzene and derivatives and benzofurans metabolite class were classified in the MolNetEnhacer organization. The full network can be visualized in Fig. B.4 (Supplementary information).

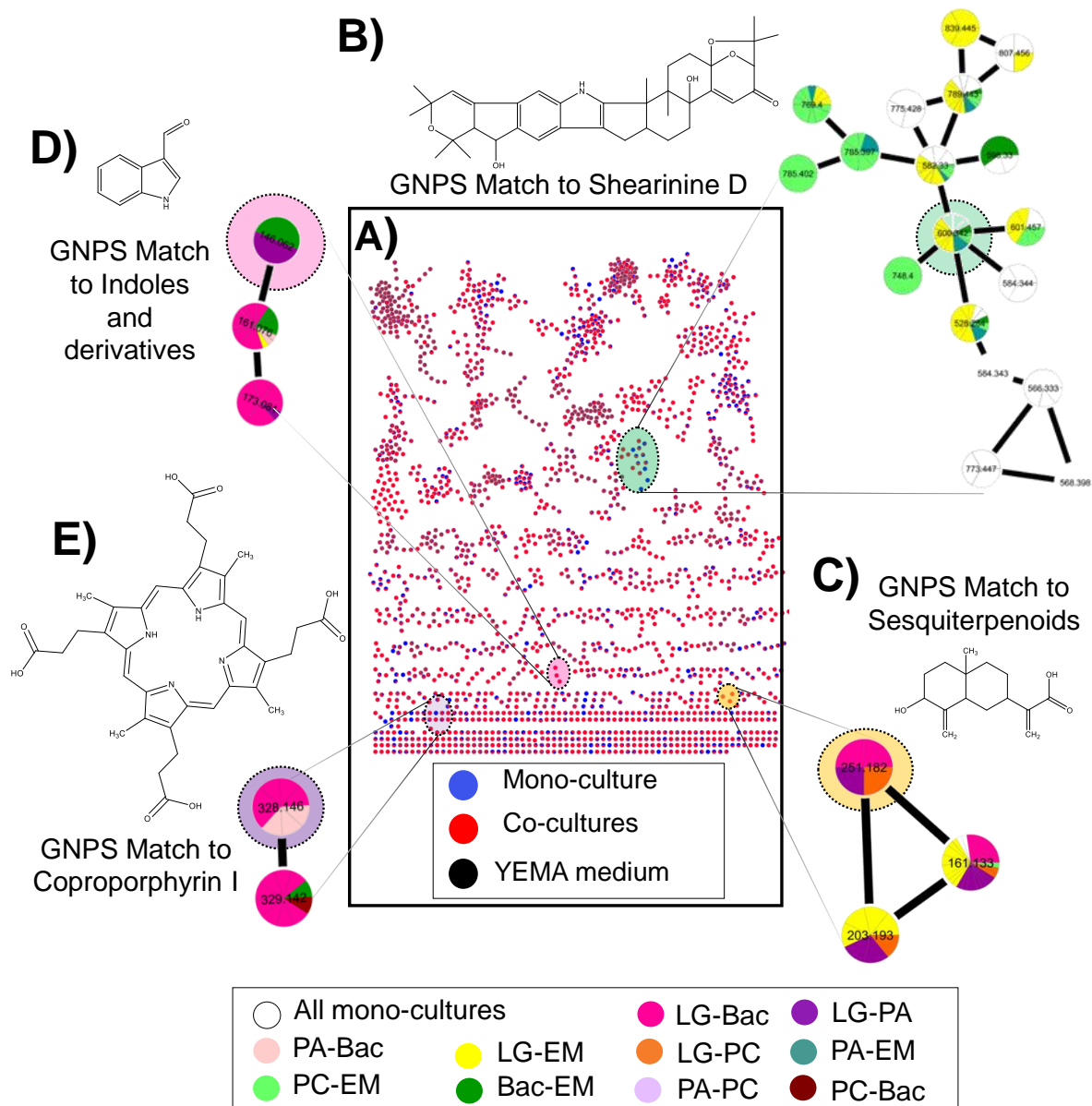


Figure 3.8 – Co-cultivation MN among the microbial symbionts of leaf cutting ants. The internal network (A) shows the complete MN: the ions generated in co-cultures are in red, all mono-cultures are in blue and the YEMA are in black. The external information highlights specific spectral families: B) The chemical compound GNPS match to Shearinine D was observed in mono and co-cultures stemming *E. microspora* samples. C) GNPS match to Sesquiterpenoids was detected in co-cultures with the mutualist fungus *Leucoagaricus gongyloporus*. D) and E) GNPS match to indole compound and Coproporphyrin I, respectively, were found in Bac-EM and LG-PA.

Most molecular families in the network were not annotated or classified in a metabolite class by the GNPS library, which means that the metabolites produced by the co-cultures investigated in this study have not been deposited in all libraries at the platform or they are unknown metabolites. The global network shows a large number of MS spectrum that were observed in the co-cultures (red nodes) samples (Fig. 3.8A).

Indole triterpenoids, Shearinine D (m/z 600.3) was found in mono-cultures from *Escovopsis* and also in co-cultures with black yeast and parasite (PC-EM and PA-EM), mutualist fungus with parasite (LG-EM), actinobacteria with parasite (Bac-EM) and in the mono-culture of parasite (EM) as well. A sesquiterpenoids metabolite (m/z 251.2) was annotated in co-cultures of mutualist fungus and actinobacteria (LG-Bac), mutualist fungus and both black yeasts (LG-PA and LG-PC). An indole compound (m/z 146) was observed in co-cultivation of actinobacteria with parasite (Bac-EM) and in mutualist and black yeast co-culture (LG-PA). Coproporphyrin I (m/z 328.1) was annotated in co-cultures of actinobacteria with mutualist fungus (LG-Bac) and with black yeast as well (PA-Bac). The complete hits of GNPS library are described in Table B.1.

In previous studies, shearinines D, E, and F produced by *Penicillium janthinellum* have presented potential anticancer activity [21]. Other studies showed the bioactivity of those class of compounds against the actinobacteria and to mutualist fungus, *L. gongylophorus* [9, 22]. Coproporphyrin compounds are produced by *Bacillus thuringiensis* [23] and *Glutamicibacter arilaitensis* [24]. However, the corproporphyrin was never associated with the actinobacteria *Pseudonocardia* sp. or on the studied fungi.

Overall, the co-cultures samples were more predominant than ions from mono-cultures samples and it suggests the metabolic induction of chemical compounds.

3.6 Search for metabolite induction in fungal co-culture by data mining using imaging-MS

Molecular network can facilitate the data organization of a large list of co-cultures and mono-cultures samples. The experiment generated a special spectral family with m/z only observed in co-culture samples. The m/z rations were searched in imaging MS data and correlated to some co-cultures: some of them (m/z 294, 896, 901 and 385) were observed in co-culture with mutualist fungus *L. gongylophorus* and the black yeast *P. capiguarae*. Unfortunately, the highlighted m/z in the spectral family were not annotated

in GNPS library. On the other hand, the non-annotation suggest that the metabolites are unknown, or they are not described in the online metabolite libraries so far (Fig. 3.9).

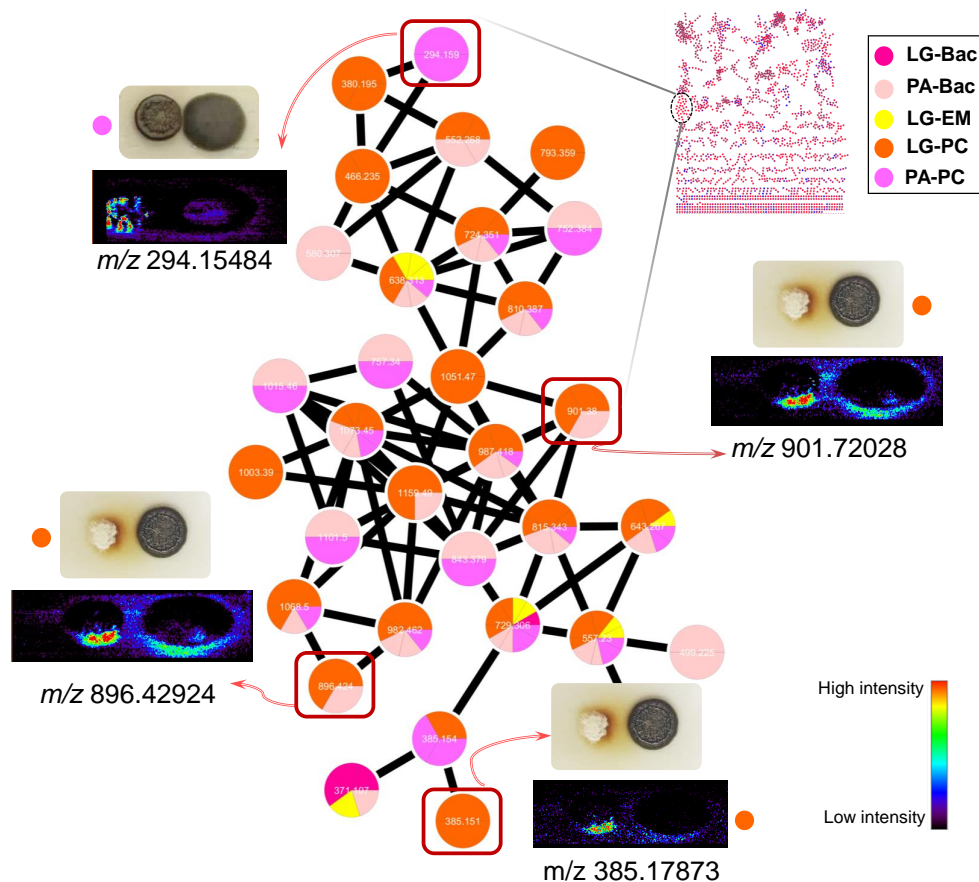


Figura 3.9 – Spectral family among the microbial symbionts of leaf cutting ants. All the m/z of this family was found only in the co-cultures samples. The highlighted m/z were also detected in imaging data. The m/z 294.1548 was detected in co-cultures between both black yeasts in pink. The ions m/z 901.7202, 896.4292 and 385.1787 were identified in co-cultures of *L. gongylophorus* and the black yeast, *P. capiguarae*, in orange.

The imaging using MS showed the visual induction of some ions. We still do not know what kind of compounds they are, and deep investigation is necessary. The metabolites in co-cultures are highlighted in the mutualist fungus zone, which can suggest the induction of those ions by the *L. gongylophorus*. It is important to observe the utility of the imaging-MS as guiding tool of induced metabolites in co-cultures.

Different studies using microbial symbionts of leaf-cutting were made based on the GNPS library, mainly related to actinobacteria [10] and the parasite [9], which can mean that most of the chemical compounds produced in co-cultivation between the symbionts are unknown and new metabolites. Boya and coworkers [10] have found a large diversity of chemical compounds produced by the bacteria to reduce the growth of the pathogen.

They also suggest that bacterial metabolites are not induced by *Escovopsis*, because the same metabolite was found in the absence and presence of the parasite. The production of shearinines is also observed in mono and co-cultures, which does not mean metabolite induction in those situations. These studies were based on MALDI-IMS.

Different from previous studies, our co-cultures showed a high chemical diversity when compared to the mono-cultures: i) the most different co-cultures (PA-Bac and PC-EM) were classified in separate clusters in PLS-Da analysis; ii) the majority of nodes originated of the co-cultures at the network view and iii) the classical network originated an exclusive cluster formed only for co-culture samples.

3.7 Outlook and remarks

Microbial interactions are important source of induction of new compounds. The dereplication of natural products is a powerful alternative to try to find relevant metabolites, using multivariate data analysis and MN tools as a orientation of the study. However, these tools present some limitations: i) only the intense peaks are emphasized in MVDA, and the less intense peaks are ignored; and ii) the MS/MS fragmentation can variate according to source ionization or MS analyser and the match cannot be relevant even with more than 5-6 peaks matched. In addition, isolation and characterization of those metabolites are required to complete the study. Moreover, the analysis tool combination was relevant to guide the next steps of this current study and the methodology can lead students that intend to make this sort of investigation in microbial interactions environments for different reasons i) use of different approaches to understand the sample complexity, ii) MVDA can lead the choice of promising co-cultures experiments, iii) MN made on GNPS platform can guide the chemical annotation in unknown samples, helping us to grasp more complete information in initial data screening.

3.8 Referências

- [1] Currie CR, Scottt JA, Summerbell RC, Malloch D. Fungus-growing ants use antibiotic-producing bacteria to control garden parasites. *Nature*. 1999;398(6729):701–704.

- [2] Currie CR. A community of ants, fungi, and bacteria: a multilateral approach to studying symbiosis. *Annual Review of Microbiology*. 2001;55:357–380.
- [3] Weber NA. The Fungus-culturing Behavior of Ants. *American Zoologist*. 2015;12(3):577–587.
- [4] Currie CR, Mueller UG, Malloch D. The agricultural pathology of ant fungus gardens. *Proceedings of the National Academy of Sciences of the United States of America*. 1999;96(14):7998–8002.
- [5] Currie CR, Poulsen M, Mendenhall J, Boomsma JJ, Billen J.
- [6] Little A, Currie C. Black yeast symbionts compromise the efficiency of antibiotic defenses in fungus-growing ants. *Ecology*. 2008;89:1216–1222.
- [7] Little A, Currie CR. Symbiotic complexity: discovery of a fifth symbiont in the *Atinne* ant-microbe symbiosis. *Biology Letters*. 2007;3:501–504.
- [8] Aksenov AA, Da Silva R, Knight R, Lopes NP, Dorrestein PC. Global chemical analysis of biology by mass spectrometry. *Nature Reviews Chemistry*. 2017;1(7):1–20.
- [9] Heine D, Holmes NA, Worsley SF, Santos ACA, Innocent TM, Scherlach K, et al. Chemical warfare between leafcutter ant symbionts and a co-evolved pathogen. *Nature Communications*. 2018;9(2208):1–11.
- [10] Boya CA, Fernandez-Marin H, Mejia LC, Spadafora C, Dorrestein PC, Gutierrez M. Imaging mass spectrometry and MS/MS molecular networking reveals chemical interactions among cuticular bacteria and pathogenic fungi associated with fungus-growing ants. *Scientific Reports*. 2017;7(1):1–13.
- [11] Oh DC, Poulsen M, Currie CR, Clardy J. Dentigerumycin: a bacterial mediator of an ant-fungus symbiosis. *Nature Chemical Biology*. 2009;5(6):391–393.
- [12] Fukusaki E, Kobayashi A. Plant metabolomics: potential for practical operation. *Journal of Bioscience and Bioengineering*. 2005;100(4):347–354.
- [13] Wang M, Carver J, Phelan V, Sanchez L, Garg N, Peng Y, et al. Sharing and community curation of mass spectrometry data with Global Natural Products Social Molecular Networking. *Nature Biotechnology*. 2016 05;34:828–837.

- [14] Pang Z, Chong J, Li S, Xia J. MetaboAnalystR 3.0: Toward an optimized workflow for Global Metabolomics. *Metabolites*. 2020;10(5):186.
- [15] Ernst M, Kang KB, Caraballo-Rodriguez AM, Nothias LF, Wandy J, Wang M, et al. MolNetEnhancer: Enhanced molecular networks by integrating metabolome mining and annotation tools. 2019;9(7):144–169.
- [16] Angolini CFF, Vendramini PH, Araujo FDS, Araujo WL, Augusti R, Eberlin MN, et al. Direct protocol for ambient mass spectrometry imaging on agar culture. *Analytical Chemistry*. 2015;87:6925–6930.
- [17] Bertrand S, Schumpp O, Bohni N, Bujard A, Azzollini A, Monod M, et al. Detection of metabolite induction in fungal co-cultures on solid media by high-throughput differential ultra-high pressure liquid chromatography-time-of-flight mass spectrometry fingerprinting. *Journal of Chromatography A*. 2013;1292:219–228.
- [18] Bertrand S, Bohni N, Schnee S, Schumpp O, Gindro K, Wolfender JL. Metabolite induction via microorganism co-culture: A potential way to enhance chemical diversity for drug discovery. *Biotechnology Advances*. 2014;32(6):1180 – 1204.
- [19] Rateb M, Hallyburton I, Houssen W, Bull A, Goodfellow M, Santhanam R, et al. Induction of diverse secondary metabolites in *Aspergillus fumigatus* by microbial co-culture. *Royal Society of Chemistry Advances*. 2013;34(3):14444–14450.
- [20] Murakami S, Hayashi N, Inomata T, Kato H, Hitora Y, ST. Induction of secondary metabolite production by fungal co-culture of *Talaromyces pinophilus* and *Paraphaeosphaeria* sp. *Journal of Natural Medicine*. 2020;74(3):545–549.
- [21] Smetanina O, Kalinovsky A, Khudyakova Y, Mikhail P, Dmitrenok P, Fedorov S, et al. Indole alkaloids produced by a marine fungus isolate of *Penicillium janthinellum* Biourge. *Journal of Natural Products*. 2007;70:906–909.
- [22] Dhodary B, Schilg M, Wirth R, Spiteller D. Secondary metabolites from *Escovopsis weberi* and their role in Attacking the garden fungus of leaf-cutting ants. *Chemistry - A European Journal*. 2018;24:4445–4452.
- [23] Harms RL, Martinez DR, Griego VM. Isolation and Characterization of Coproporphyrin Produced by Four Subspecies of *Bacillus thuringiensis*. *Applied and Environmental Microbiology*. 1986;51:481–486.

- [24] Cleary JL, Kolachina S, Wolfe BE, Sanchez LM. Coproporphyrin III Produced by the bacterium *Glutamicibacter arilaitensis* Binds Zinc and Is Upregulated by Fungi in Cheese Rinds. 2018;3(4).

4 Chemical warfare between leaf-cutting ants parasites and black yeasts

Contextualização: Essa sessão discute detalhadamente sobre a comunicação química entre a levedura negra *Phialophora capiguarae* e o parasita do jardim das formigas cortadeiras, *Escovopsis*. Análises por LC-HRMS e imageamento por espectrometria de massas, redes moleculares e análise estatística dos dados obtidos através de cocultivos possibilitaram a realização de uma discussão aprofundada e inédita dessa interação.

4.1 Abstract

Understanding the microbial communication in different environments has been the goal of study in chemical ecology, since microorganisms co-exist in close associations. Leaf-cutting ants are part of a complex symbiosis: the mutualistic fungus with their garden fungus, *Leucoagaricus gongylophorus*, that constitutes the main food source for the ants. Since the garden fungus is threatened by pathogenic fungi from the genus *Escovopsis*. In nature, the ants need to defend their nest from different invaders and pathogens. For this reason, they joined an alliance with symbiotic actinobacteria antibiotics producer that protect the nest of parasites. There are other microbes in the microcosmos of leaf cutting ants, the black yeast (BY) from the genus *Phialophora* that its ecological role is little studied so far. This study shows how to improve the data management from different interactions of leaf-cutting ants symbionts through the use of MS/MS molecular networking and multivariate data analysis (MVDA). Secondary metabolites were annotated in the GNPS libraries, such as shearinines D and E. MS molecular network (MN) data was combined to imaging-MS (IMS) to detect some m/z ratio that was only produced in the co-cultures. The IMS has shown the exact area when the induced metabolites were produced. The studies confirm that a combination of molecular network and metabolomic approaches advance the MS/MS data analysis of secondary metabolites in microbial interactions and collaborate for understanding how the communication works in a complex environment as the leaf-cutting ants garden.

Key-words: Microbial interactions, leaf cutting ants symbionts, *Phialophora*, black yeast, metabolomics, molecular network, shearinines, antibiotic activity.

4.2 Introduction

Attine ants have different kinds of agriculture, such as lower Attine, higher Attine, and leaf-cutting ants. Leaf-cutting ants are a topic for research due to the chemical-ecologic interactions existing between the microbial symbionts [1]. Inside of attine ants nests, there is a complex ant-microbe mutualism: the ants have an ancient obligate mutualism with fungi that cultivate for food, *Leucoagaricus gongylophorus*. However, fungal parasites (genus *Escovopsis*) can be harmful to the garden [2].

Hence, to protect against the parasite, ants have a mutualism with actinobacteria, *Pseudonocardia* and *Streptomyces* genus, that produces important antibiotics to avoid parasites. Recently, a new microbial symbiont associated with leaf cutting ants: black yeast (BY) belonging to *Phialophora* genus was discovered [3]. These different interactions are illustrated in Fig. 4.1. Study related to the isolating of different BYs species in leaf-cutting ants is also reported [4].

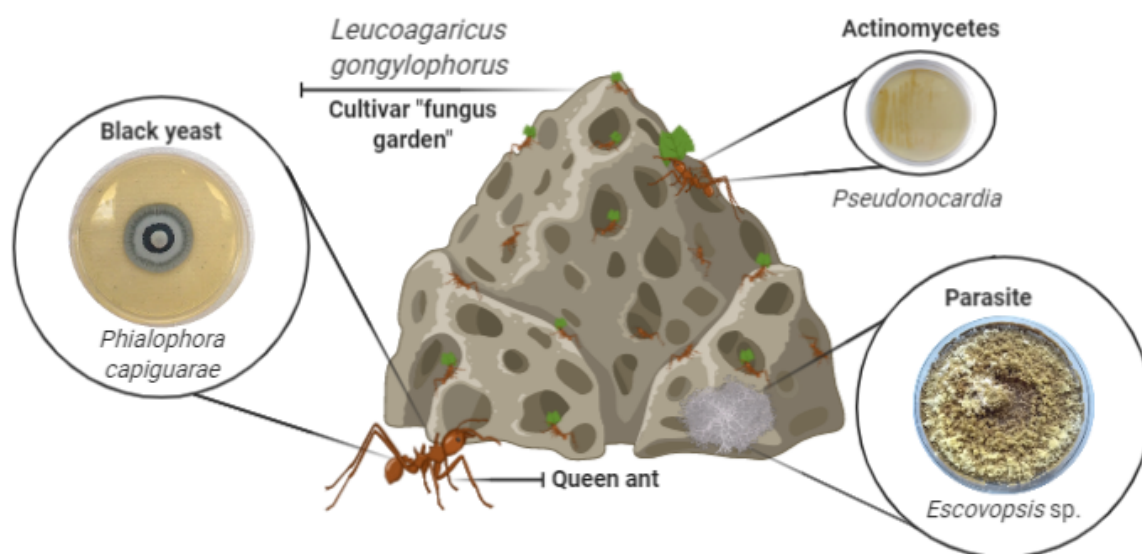


Figura 4.1 – Symbionts microbes interactions of leaf cutting ants: the cultivar *Leucoagaricus gongylophorus*, the actinobacteria that lives in ants cuticle, the parasite, *Escovopsis* sp. and the BYs, isolated from queen ants body, *Phialophora capiguarae*. Main picture was based on photo in NSTA.

However, only a few previous studies tried to understand the BYs relation into the leaf-cutting ants garden and the actinobacterial relationship [3, 5]. Moreover, leaf-cutting ants are important agricultural pests in Latin American mainly in *Pinus* and *Eucalypt-*

tus plantations. The biorational control of them is an important target although their management is still a challenge [4].

Nowadays, the omics tools contribute to facilitate the secondary metabolites discovery from different sources, for microbial metabolites [6]. One of those tools is the Global Natural Products Social molecular networking platform (GNPS) which is an open-access knowledge base for organization and sharing of LC-MS raw data, processed, or identified tandem mass (MS/MS) spectrometry data and a tool for identification and dereplication of primary and secondary metabolites. These comparisons consider the fragmentation patterns of molecules for clustering related-molecules in a spectral network. Molecular Networks can facilitate the data visualization, which maps are constructed based on the alignment of MS/MS spectra with each other. At the same time, MS/MS spectra are searched in GNPS spectral libraries, suggesting annotation compounds [7].

In the microbial co-culture interaction, the metabolomics approach appears to be of great advantage to characterize the metabolic induction. Metabolomics could be defined as a non-selective, universally applicable, comprehensive analytical approach for the identification and quantification of metabolites in a biological system [8].

In this work, LC-HRMS fingerprinting was used to understand the metabolite induction in co-cultures of BY and the parasite *Escovopsis* from leaf-cutting ants garden. The BY and parasite fungus interaction was chosen due to previous co-cultivations statistical analysis of LC-HRMS data (detailed in Chapter 3). Molecular network and multivariate data analysis (MVDA) were applied to the chemical profiles and imaging-MS to highlight compounds that were induced because of the interactions between both microbes.

4.3 Material and methods

4.3.1 Microbial samples

The strains of fungi used in this study were isolated from leaf cutting ants (*Atta* and *Acromyrmex*) and registered in the SISGEN (Sistema Nacional de Gestão do Patrimônio Genético e do Conhecimento Tradicional Associado). BY strain used was strain AP376, classified as *Phialophora capiguarae* isolated from the queen of *A. capiguara* and the parasite strain was LESF016 identified as *Escovopsis* sp. isolated from *A. sexdens rubropilosa* garden. Both strains were isolated in Botucatu-Brazil-SP. Strains were stored in Eppen-

dorf tubes containing yeast and malt extract agar (YEME) at 4°C and maintained using new YEME plates in each 21 days.

4.3.2 Co-culture experiments

For mono-cultures of BY and parasite fungus, a 5 mm agar plug of a microbial pre-culture was inoculated in the center of a 9 cm Petri dish containing 20 mL of yeast malt extract agar media (YEME: 3 g yeast extract, 5 g peptone, 3 g of malt extract, 10 g of D-glucose, 15 g of agar in 1000 mL of dd-water). Similarly, for co-culture two 5 mm agar plugs of each strain were inoculated with 2 cm of distance between the microbial strains of fungi. The Petri dishes were incubated at 25°C.

4.3.3 Crude extraction and sample preparation

The interactions of microbial co-cultures were divided in 3 sections, separating the confrontation zone in section (B), the inoculated microbes were separated in section (A) and (C). The fresh material was transferred into an extraction vessel with 100 mL of ethyl acetate per 50 mg of material. The extractions were performed in a water-bath sonicator (Soni-tech TDR force) at room temperature for 15 min. The sonicated samples were filtered through filter paper and glass cotton. Finally, the extracts were dried under vacuum using a centrifugal evaporator (Büchi, Brazil). Uninoculated plates and mono-cultures were used as blanks and controls, respectively. The dry extracts were dissolved in acetonitrile 100% and filtered through 0.45 μm filters at a concentration of 2 mg \cdot mL⁻¹.

4.3.4 Mass spectral data acquisition

Experiments were performed using a Quadruple-Time of Flight High-Resolution (QToF-HR) ESI (Bruker-Daltonics) mass spectrometer coupled to a LC model UFLC system (Shimadzu), which included an in-line degasser, binary pump, and refrigerated autosampler. A 5 μm C18 column with 250 mm \times 4,6 mm (Phenomenex Luna), maintained at 25°C, was operated using a gradient elution of H₂O and ACN (both with 0.1% formic acid) running at 1.0 mL \cdot min⁻¹. The gradient program was as follows: 5% to 100% ACN over 25 min, 100% ACN for 10 min using 15 μL of injection volume at 40°C. All mass spectra were recorded in the positive-ion mode. MS parameters were a spray voltage of

3.5 kV, a capillary temperature of 220 °C, a dry gas in 9 L · min⁻¹ at 40 psi. The m/z range was 50 to 1500, detecting the signals below $1.0 \cdot 10^3$.

4.3.5 LC-MS data process and analysis

4.3.5.1 Multivariate data analysis

MS raw data .d (Bruker) were converted into .mzXML data using MS Convert software (ProteoWizard). The feature detection was performed between the retention time from 2 to 30 min with MZMine 2.34 (MZmine VTT, Finland) using parameters according to the qTOF-MS detector for data processing. For mass detection, a range of 50 to 1500 Da, during 2 to 35 min and 10^3 noise level was used. Peaks at least wide $1 \cdot 10^3$ and an intensity greater than $6.0 \cdot 10^3$ were selected with a 10 ppm m/z tolerance. Chromatogram deconvolution was performed using the local minimum search algorithm (minimum peak height of $2.1 \cdot 10^3$, peak duration of 0.05 to 5 and baseline level of $2.0 \cdot 10^3$).

Deisotope filtering was applied using the isotopic peaks grouper module with tolerance parameters adjusted to 0.001s and 10 ppm. Feature alignment and gap filling were achieved with a m/z tolerance of 10 ppm and a retention-time (RT) tolerance of 0.1 min. The exported feature lists were exported in .csv file format and organized using Microsoft Excel, and multivariate analyses were performed using Metaboanalyst 4.0 [9]. The processing methods were based on all samples and the data scaling used was mean-centering. Principal component analysis (PCA), partial least squares regression (PLS-DA), hierarchical cluster analysis (HCA) and heat maps applied after unit variance scaling were used for sample discrimination (scores) as well as the generation of biplots and the list of important features (loadings).

4.3.5.2 Classical molecular MS/MS network analysis

A molecular network was created using the online workflow on the GNPS website [7]. The data was filtered by removing all MS/MS fragment ions within ~ 17 Da of the precursor m/z . MS/MS spectra were window filtered by choosing only the top 4 fragment ions in the ± 50 Da window throughout the spectrum. The precursor ion mass tolerance was set to 2.0 Da and a MS/MS fragment ion tolerance of 0.8 Da. A network was then created where edges were filtered to have a cosine score above 0.65 and more than 4 matched peaks. Further, edges between two nodes were kept in the network if and

only if each of the nodes appeared in each other respective top 10 most similar nodes. Finally, the maximum size of a “spectral family” was set to 100, and the lowest scoring edges were removed from molecular families until the “spectral family” size was below this threshold. The spectra in the network were then searched against GNPS spectral libraries. The library spectra were filtered in the same manner as the input data. All matches kept between network spectra and library spectra were required to have a score above 0.64 and at least 4 matched peaks [7]. The molecular network was visualized using Cytoscape 3.7.1 The molecular network was used to compute the propagation with NAP using parameters as follows: 10 first candidates, exact mass searches within 15 ppm, and databases of GNPS, HMDB and MassBank.

4.3.5.3 Feature based molecular MS/MS network analysis

A molecular network was created with the Feature-Based Molecular Networking (FBMN) workflow (Nothias LF et al. bioRxiv 2019) on GNPS website [7, 10]. The mass spectrometry data were first processed with MZMine, according to GNPS Documentation and the results were exported to GNPS for FBMN analysis. The data was filtered by removing all MS/MS fragment ions within ± 17 Da of the precursor m/z . MS/MS spectra were window filtered by choosing only the top 6 fragment ions in the ± 50 Da window throughout the spectrum. The precursor ion mass tolerance was set to 0.01 Da and the MS/MS fragment ion tolerance to 0.025 Da. A molecular network was then created where edges were filtered to have a cosine score above 0.65 and more than 4 matched peaks. Further, edges between two nodes were kept in the network if and only if each of the nodes appeared in each others respective top 10 most similar nodes. Finally, the maximum size of a “spectral family” was set to 100, and the lowest scoring edges were removed from molecular families until the “spectral family” size was below this threshold. The spectra in the network were then searched against GNPS spectral libraries. The library spectra were filtered in the same manner as the input data. All matches kept between network spectra and library spectra were required to have a score above 0.65 and at least 4 matched peaks. (2018)). The molecular networks were visualized using Cytoscape software.

4.3.6 DESI imaging on co-cultivations

The strains were inoculated using water suspension in the agar plates with the microscope slides, photographed and put in a vacuum desiccator for complete agar dehydration

at room temperature [11] MS imaging was performed using a ProSolia DESI source (Model OS-3201) coupled to a Thermo Scientific Q-Exactive Hybrid Quadrupole-Orbitrap Mass Spectrometer. The DESI configuration was set with an emitter height of 2.5 mm, mass spectrometer inlet height of 0.1 mm, inlet to emitter distance of 3.8 mm, 58°C spray angle, 5.0 kV spray voltage, inlet capillary temperature of 320°C, 100 V S-lens, 160 psi ultrapure nitrogen nebulizing gas pressure, and a sprayed solvent of methanol at a $3.0 \mu\text{L} \cdot \text{min}^{-1}$ flow rate. Images were collected from m/z 200 to 1500 with a step sized of $200 \mu\text{m}$, a scan rate of $741 \mu\text{m} \cdot \text{s}^{-1}$, and a pixel size of $200 \mu\text{m} \times 200 \mu\text{m}$. In short, major conditions were as follows: $3 \mu\text{L} \cdot \text{min}^{-1}$ of solvent flow rate, nebulizing gas backpressure of 100 psi, and $2 \text{ mL} \cdot \text{min}^{-1}$ gas flow rate. The DESI-IMS data was converted into imaged files using Firefly data conversion software (version 2.1.05) and viewed using the BioMAP software (version 3.8.04). In BioMAP the data were opened in an m/z 200 to 1000 range and the false-color scaling were adjusted to a fixed value to enable a relative comparison between experiments.

4.3.7 Antimicrobial assays with extracts

The dry extracts were dissolved in methanol at a concentration of $5 \text{ mg} \cdot \text{mL}^{-1}$ for the bioassays. The assays were performed using agar diffusion assays method to reveal if microorganisms interact, or are influenced by each other. For the agar diffusion assays, suspensions of the test organisms were spread on agar plates in small holes into the agar plates. $50 \mu\text{L}$ of the solution was added into the holes. The extract tested against the *Pseudonocardia* W3 were obtained from the Westerdijk Fungal Biodiversity Institute (Utrecht, the Netherlands).

The analysis of the inhibition zone (area) was performed using the software ImageJ to check the bioactivity in three replicates. For the negative control, methanol was used.

4.4 Results and discussion

4.4.1 Co-culture and interaction of black yeast *versus* parasite *Escovopsis* sp.

The communication between the symbiont microbes requires an association between visual confrontation bioassay and spectroscopic information. During the co-cultures experiments, an inhibition of the growth of the parasite fungus, *Escovopsis* was observed,

in all the replicates Petri dishes assays (Fig. 4.2A). Generally, in mono-cultures, the parasite strain grows in a complete dish in five days, but when it is in the co-cultivation system, the parasite was inhibited in 50% of its usual growth. The statistical data comparison of the mycelium grow area of mono and co-cultures are illustrated in Fig.4.2B (Supplementary information).

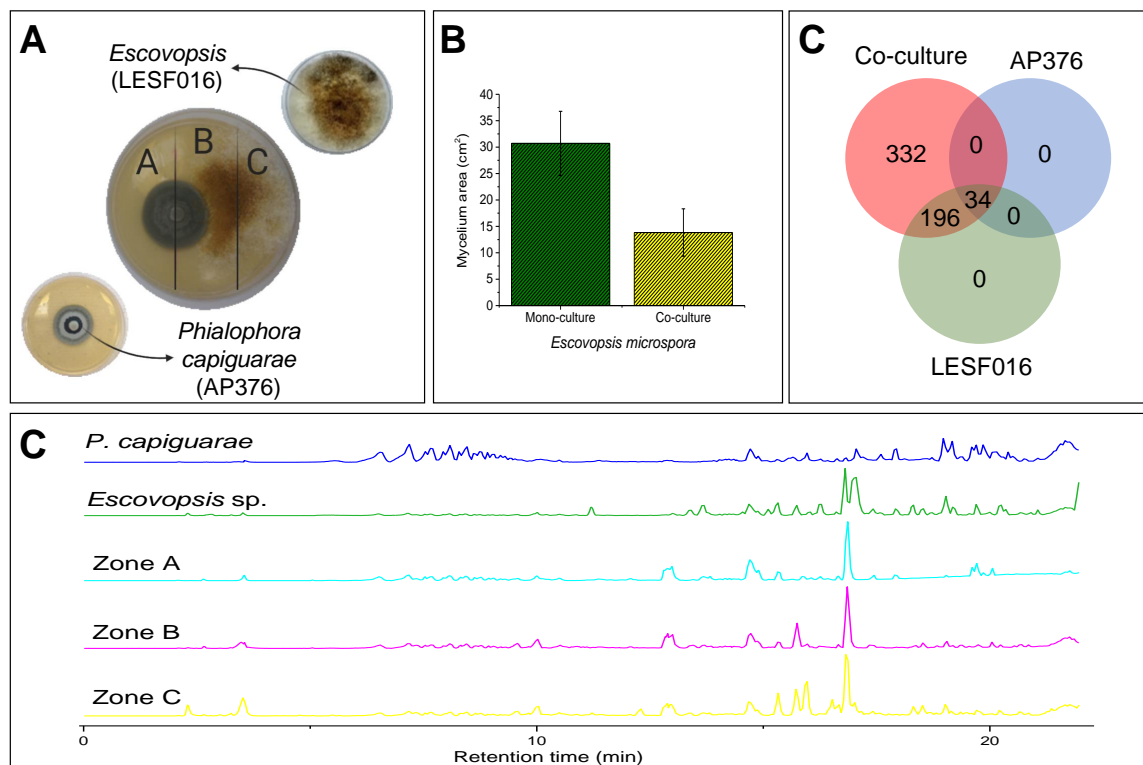


Figura 4.2 – (A) Microbial interactions between BY, *P. capiguarae*, and the parasite *Escovopsis*. (B) the parasite *Escovopsis* (LESF016) mycelium is highlighted the co-culture (yellow) and the mono-culture in front of the BY *P. capiguarae* (green). The mycelium areas were calculated based on the media of three replicates. The BY mycelium does not modified after the co-cultivation. (C) Venn diagram with all the m/z present in mono-cultures and co-culture. (D) LC-HRMS profiling of axenic cultures *P. capiguarae* and *Escovopsis* and the co-cultivation zones A, B and C.

Further characterization of the interactions between the symbiont microbes was performed using LC-HRMS profiling of crude extracts co-cultures. The LC-HRMS profiling with the comparison of the axenic cultures of the BY and the parasite, and the different co-cultivations extracted in different dish zones A, B, and C. All extracts presented a large variety of metabolites due to the high number of chromatographic signals. The visual comparison of LC-HRMS profiles became a challenging task, mainly because of replicates samples comparison and large number of samples (Fig. 4.2C).

The *Escovopsis* sp. inhibition suggests the signaling metabolite production by one of the strains. The same inhibition could also be understood as a spatial limitation, but the same situation does not exist in other symbiont co-cultivations with the parasite (in Chapter 3 in Fig. 3.5). Therefore, the differentiation becomes this particular interaction interesting to be more explored. Moreover, the inhibitory trend is also related to induced antimicrobial compounds in the co-cultures. The induction of different compounds in co-cultivation were observed in different microbial confrontation studies [12, 13]. However, in leaf-cutting ants symbionts, the over-expression of metabolites is more common [14, 15].

4.4.2 Multivariate data analysis in microbial interactions

An optimal comparison between the mono and co-cultures samples was performed based on the LC-HRMS processed data to perform the Multivariate data analysis (MVDA) of the samples proceeding the fungal interaction. The blank data (only solvent injection), the YEME media control, mono-cultures of *P. capiguarae* and *Escovopsis*, co-cultures zones A, B, and C were processed combined using in the same setting parameters. After processing, the data of blanks was subsequently subtracted from the setting to avoid information misinterpretation.

After the previous data treatment, a total of 7,242 features were processed and organized in a .csv table file. A large number of features was detected in an LC-HRMS-based metabolomics analysis due to its high sensitivity of detection. On the other hand, because of the same sensitivity, different challenges arise in this kind of analysis, for example, the high variability of LC-HRMS data in different replicates and metabolite identification challenge [16]. Despite many difficulties, the LC-HRMS based metabolomics is employed in different data analysis approaches in microbiome [17] as well as wild and cultivated plants for instance [18].

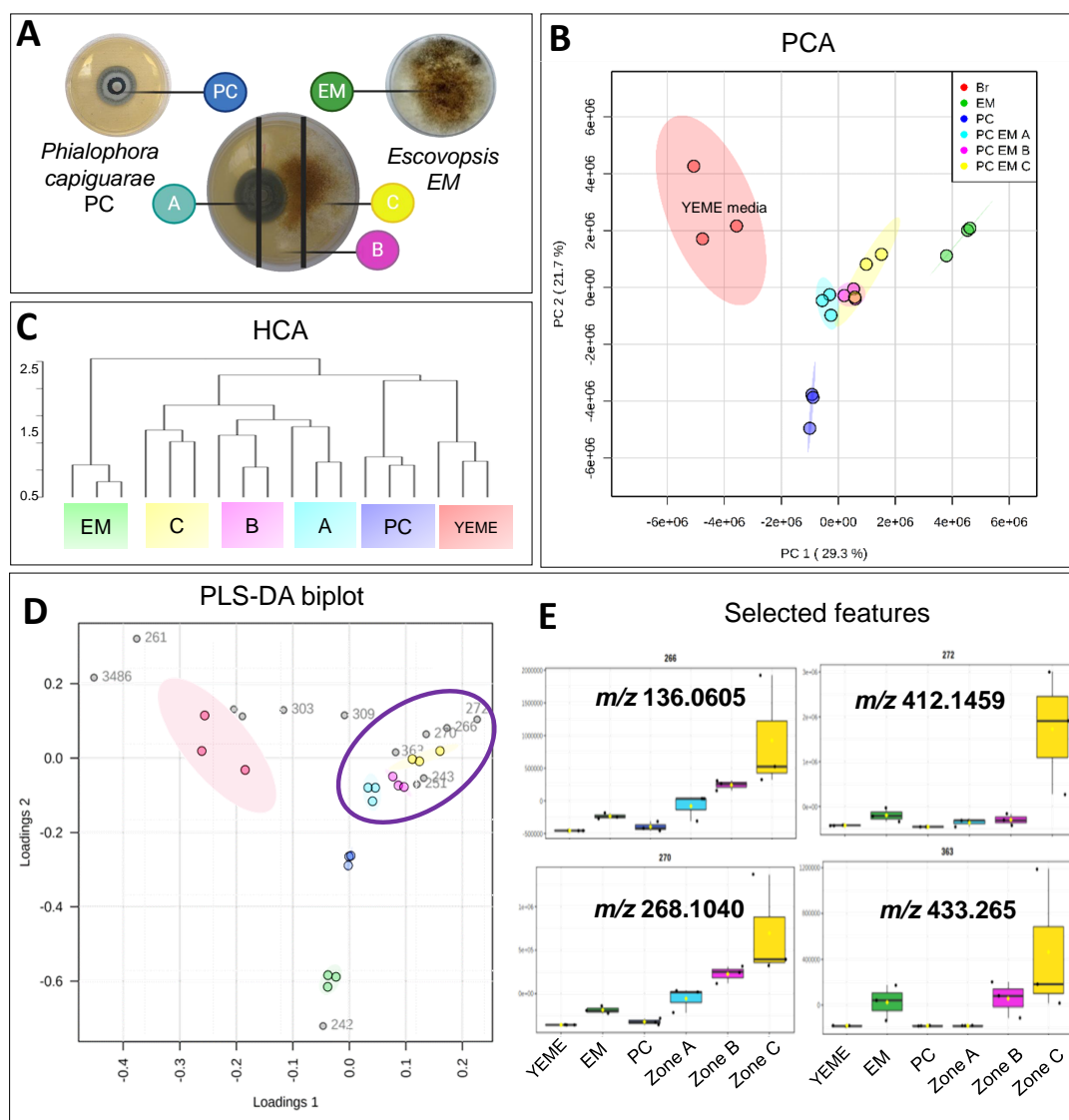


Figura 4.3 – (A) Microbial interactions between BY *P. capiguarae* (in dark blue) and the parasite *Escovopsis* (in dark green) and legend of the colors represents the co-culture part provides from the BY (A) in light blue, the yellow is from the parasite (C) and the intersection zone (B) is shown in pink. (B) Unsupervised MVDA (PCA): scores plot between the selected PCs, the explained variance is 50.4%; (C) Hierarchical cluster analysis (HCA) was constructed pondering *Pearson* distance and the average clustering algorithm. (D) Supervised MVDA (PLS-DA) biplot. The scores plot between the selected PCs the explained variances are 42.1%. (E) Selected features *m/z* 412.1459, 433.2665, 136.0605 and 268.1040 are more expressive present in co-cultures samples. In zone C co-cultures (in yellow) the area is $\geq 10^5$.

Thus, to verify the differences and similarities in co-cultivation between the BY, *P. capiguarae* and the parasite *Escovopsis* the LC-MS profiling was subject to MVDA. High similarity among the co-culture zones were observed in the PCA, HCA, and PLS-DA experiments, whereas a clear separation among mono-cultures was observed (Fig. 4.3B, C, and D). PCA presents an explained variance of 50.4% and PLS-DA, 42.1%. Moreover,

HCA demonstrated a data clustering organization, which co-cultures zones C samples belong to the same cluster. PLS-DA bracketed the co-culture (A, B, and C) samples at the same quadrant (Fig. 4.3D). The statistical model was highly validated, and the accuracy was $> 50\%$, $R^2 > 0.9$ (Supplementary information Fig. C.1). The PLS-DA biplot (loadings and scores) shows which features (m/z) are correlated to the co-cultures samples. The data suggests important features that are only produced in co-cultures, such as m/z 412.1459, 433.265, 136.0605, and 268.1040 (Fig. 4.3D and E).

These data information show the differentiation between mono and co-cultures samples and thereby imply a metabolite induction in confrontation cultures. PLS-DA and HCA plot show the clustering in an outlying area from both mono-cultures. The sample connectivity was verified in a correlation heat-map experiment which allows the visualization among the samples, where A, B, and C samples co-cultures are chemically different from BY and parasite axenic cultures (Fig. C.2). The clustering organization among the cultivations in PCA and PLS-Da means that co-cultures are chemically different from their axenic cultures. Although this interpretation could be evident, the same situation is not often observed in the literature in most of the reported co-cultures experiments. Bertrand and coworkers examined 657 co-culture experiments and continued the studies with only 21% of the experiments due to the morphological interactions of the co-cultures [19].

The MVDA results indicate both microbes produce different metabolites when they are cultivated in co-cultures whereas the presence of the other fungus affects the fungal metabolic expression in the same physical space. Co-cultivation experiments show to be a good strategy to increase the chemo-diversity throughout the activation of biosynthetic genes [19, 20]. Even though the co-culture approach is a useful tool to induce cryptic metabolites, not all fungal strains respond as a metabolite answer to chemical-epigenetic modifiers [21].

For this reason, this notable difference in the co-culture system is interesting to make a further investigation of the interaction. In the face of these results, we pursued the study to understand which metabolites were induced in co-cultures based on statistical analysis using important features identified by PLS-DA and other LC-HRMS collected information.

4.4.3 Classical molecular networking of black yeast and parasite interactions

Molecular networking facilitates clarification of the data organization in metabolites' complete visual map. The complete built networking presented 1846 different nodes and 884 of them were connected in a networking. The general data showed a high diversity of primary and secondary metabolites produced at the interaction between *P. capiguarae* and *Escovopsis*. The co-cultures regarding A, B and C zones samples were more representative in the overview of networking.

A high number of nodes (spectral MS/MS information) was observed in the global networking visualization. Most nodes are related to the co-cultures which confirm our metabolite induction in the co-cultures hypothesis (Fig 4.4A). Besides, a known "spectral family" formed by shearinines D-F and 22,23-dehydro-shearinine A, with samples coming from the parasite *Escovopsis* and co-cultivation samples were annotated using the spectral library in GNPS-platform (Fig 4.4B).

We also classified different metabolites classes in MolNetEnhancer analysis, such as carboxylic acids and derivatives, benzothiazoles, fatty acyls, flavonoids, indoles and derivatives, steroids, and naphthopyrans (Fig. C.3). The co-cultivation chemical classes diversity emphasize the large variety of compound can be induced in fungal co-cultures. Even with the non-identified compounds, it is possible to classify the class of metabolites based on the fragmentation pattern [22]. In general, this kind of analysis could be helpful for further isolation procedures.

In most of the nodes, MS/MS spectra were not annotated mainly due to limitation of the GNPS-library, or they are metabolites not described yet (Fig. 4.4). We compared the MS/MS fragmentation to MS/MS in the GNPS library and the similarity presented the cosine ≥ 0.67 , with more than ten shared peaks. The mirror match of three compounds, Shearinine D (Fig. C.4), shearinine F (Fig. C.5) and, 22,23-dehydro-shearinine A (Fig. C.6), are represented in Supplementary information.

So far, different chemical diversity studies with the fungus-growing ants' parasite *Escovopsis* sp. described shearinines, or related compounds. In the beginning, only the characterization of these natural products was reported [14], then the activity of the compounds was tested against the mutualist fungus [23]. Afterward, the antimicrobial activity against the actinobacteria *Pseudonocardia* sp. was also confirmed and the influence of shearinines in the ants' mortality was observed in previous work [15]. For this reason, we assumed that the non-annotated compound can be related to novel natural

products analogous to shearinines.

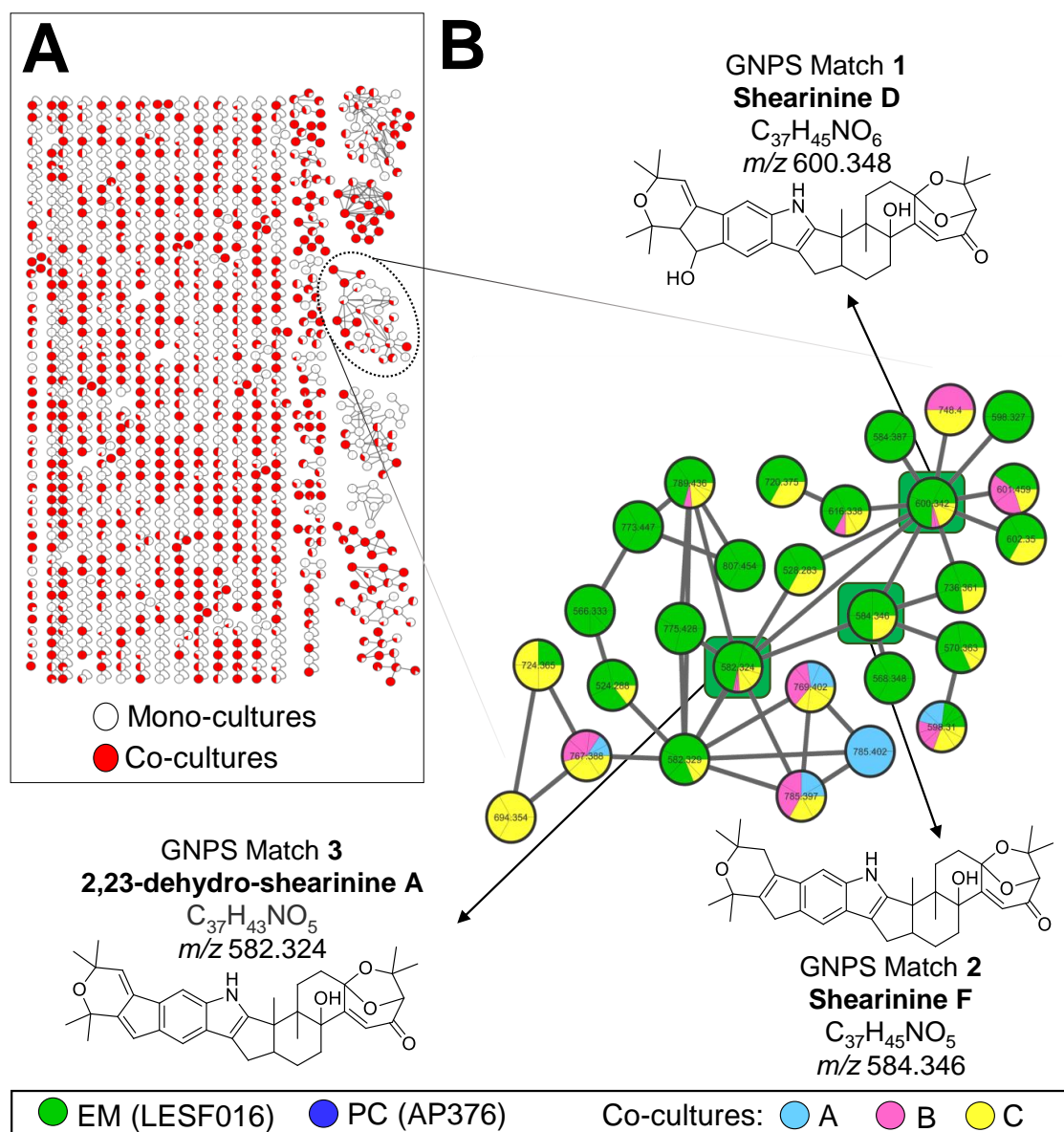


Figura 4.4 – (A) Molecular networking of microbial interactions between BY and the parasite and legend of the colors in details: red nodes are related to co-cultures samples and white nodes to mono-cultures. (B) Shearinines spectral family presented three annotated compounds: 1) Shearinine D, 2) Shearinine F and 3) 22,23-dehydro-shearinine A.

Shearinines are indole triterpenes produced by different fungus: shearinines A, B, C were found for the first time in *Eupenicillium shearii* [24] and shearinine D to K were isolated from *Penicillium* sp. [25], both from *Penicillium* genus and with potential antimicrobial activity. The chemical annotation of these shearinines was based on m/z observed, molecular formula and error in ppm, MS/MS fragmentation and mirror match. This kind of annotation is related as a level 2 of annotation according to the Metabolomics

Standarts Initiative (MSI) [26, 27].

Molecular networking analysis collaborated in understanding the high chemical diversity in co-cultures between the BY and the parasite throughout correlation of the co-cultures induced m/z with the annotated shearinines-type metabolites at the same spectral family. The confrontation assays with both fungal strains induced the production of the metabolites related to shearinines and the approach is a relevant tool to understand the communication in microbial environments. Moreover, the networking data supported the MVDA information, in which a separation among the parasite and co-culture samples was observed. Although the annotation tools assisted the metabolites organization, the m/z linked to the co-cultures samples were not sorted in the current approach.

4.4.4 DESI-IMS of spectral families of the microbial interaction

The visualization created by molecular networking analysis led us to search for specific m/z in DESI MS-imaging data tools. We investigated the hits to identify which m/z are also present in confrontation zones using MS-imaging. Two clusters were selected for different reasons. The first one (A) was elected due to most nodes in the “spectral family” be related to the co-cultures samples, and the second one (B) was chosen because of their similarity to shearinines “spectral family” (Fig. 4.5). The nodes present in the same family means the high fragmentation similarity, which is helpful to understand the chemical information of those m/z highlighted.

All the nodes from A and B molecular families were searched in IMS data and six of them were also found in the imaging of interaction zones. “spectral family” (A) confirmed three different nodes in imaging-MS: m/z 440, 411 and 474. We identified the m/z 440 around the BY strain contradicting the networking information, wherein m/z 411 was noticed in *Escovopsis* area and in the interaction area between both fungi. And lastly, m/z 474 was traced mostly around the BY but also in the whole intersection area, what is not in compliance with networking organization (Fig. 4.5A).

The LC-HRMS data combined with imaging-MS suggest the metabolic induction of those unknown compounds. Even with no annotation in GNPS library, we deduced class similarity according to the MS/MS fragmentation. Further studies are necessary to understand the classification of these induced compounds.

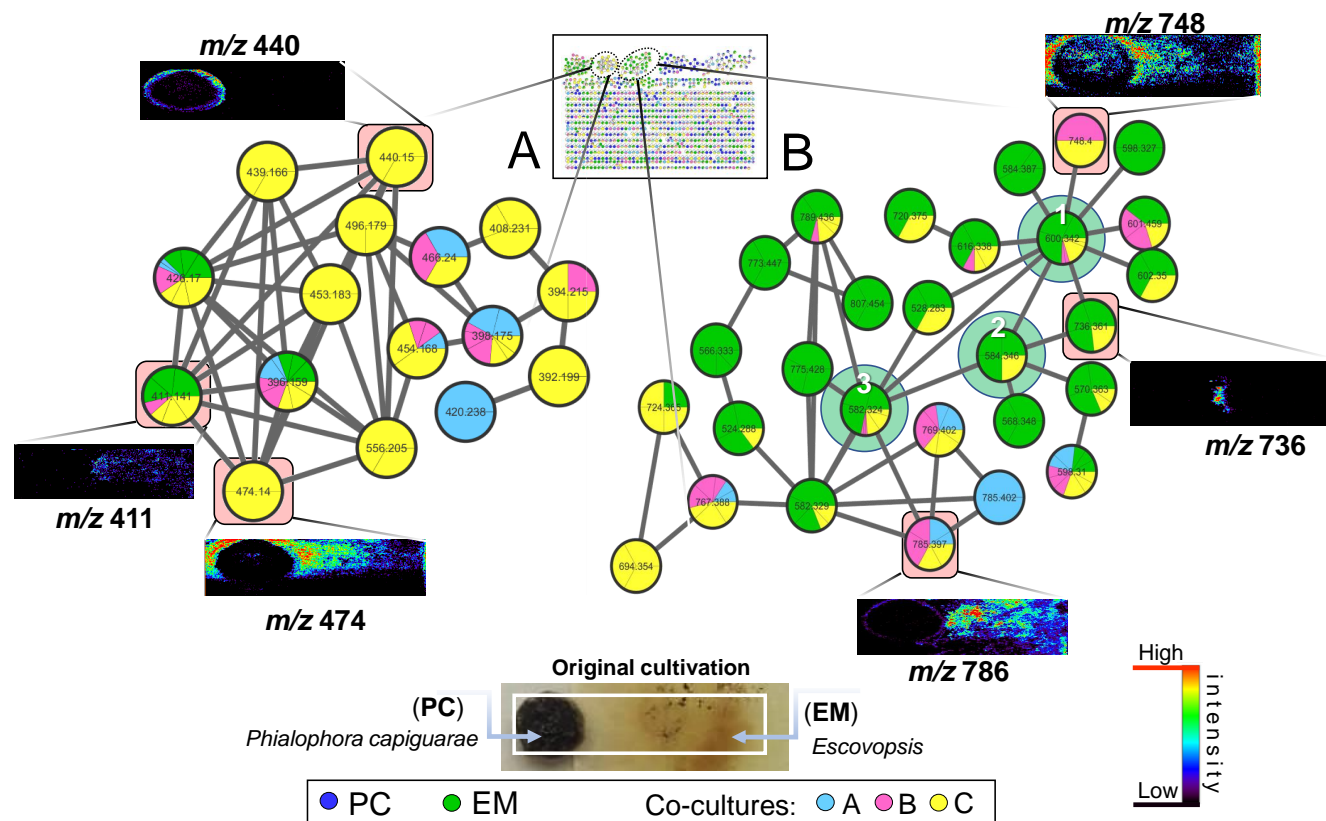


Figura 4.5 – (A) Molecular family generated mainly by spectra from co-cultures A, B and C zones samples. Found m/z in imaging-MS are highlighted: 440, 411 and 474. (B) Shearinine "molecular family" was selected to search the ions in the imaging-MS. The found nodes are highlighted m/z 748, 786, and 736. The numbers 1, 2 and 3 are related to the annotated chemical compounds 1) Shearinine D, 2) Shearinine F, and 3) 22,23-dehydro-shearinine A. The imaging-MS shows the spatial distribution of a specific m/z over the co-cultivation surface. The images are plotted on the same color scale from 0 (dark purple) to 2 10⁵ (red). Nodes colors in the molecular networking are regarding to the BY, *P. capiguarae* in dark blue, the parasite fungus, *Escovopsis*, in dark green, and in light blue, pink and yellow are originating from co-cultures zone, A, B, and C, respectively.

We also searched the nodes belonging to “shearinines spectral families” in imaging-MS data. Most of the nodes are related to *Escovopsis* mono-culture samples and in co-cultures. The proof was confirmed in imaging-MS experiments, in which it is possible to see the exact zone where the ion was produced. This spectral family showed some nodes only produced in co-cultures samples and non-annotated compounds. For instance, the ions at m/z 748, m/z 786 and, m/z 736 (Fig. 4.5B).

Some ions are highlighted due to their presence in co-cultures samples: m/z 748 was detected closer to the BY and scattering to parasite direction, the ion m/z 748 has 148 Da mass difference of Compound 1 (Shearinine D); m/z 736 presented high intensity in a small confrontation area, this ion has 152 mass difference of Compound 2 (Shearinine F) and m/z 786 was observed mainly in the parasite area and high intensity closer to the BY, the ion 786 has 203 mass difference of Compound 3 (22,23-dehydro-shearinine A). Hence, we organized the data for a better understanding of this possibility. The addition of specific groups of atoms to known compounds results in non-annotated metabolites. The fragmentation patterns are still under analysis.

4.4.5 Network annotation propagation of induced chemical compound in co-cultures

The presence of ions in imaging-MS proves our hypothesis that parasite or BY induces those compounds in confrontation situations affected by the co-cultures experiments. Different from the other analytical tools, the IMS shows in detail the interaction area where the ion is produced. Based on these images, we implied metabolites quite similar to shearinines are produced when those both microbes are cultivated together, and the m/z 748 and 786 are only induced in co-culture samples. However, the chemical compound proposal is a challenging task based on only in the MS-fragmentation. An *in silico* suggestion was made using Network Annotation Propagation (NAP).

The fragmentation studies were performed using the Network Annotation Propagation (NAP), in the GNPS platform. The “*in silico*” fragmentation suggested some possible structures related to the shearinines. The proposal is according to the MS/MS pattern and the structures are linked to the most similar structure. The annotated chemical compound, shearinine D and F, 22,23-dehydro-shearinine A improves the NAP suggestions (Fig. 4.6).

In GNPS platform, the NAP tools are still under improvements, but the initial results showed that NAP gives us a ranking of possible candidate structure generated by an *in silico* tool. The candidates of NAP Consensus, Fusion, and MetFrag scores improve the rank of the correct structure, but further fragmentation studies are still needed [28].

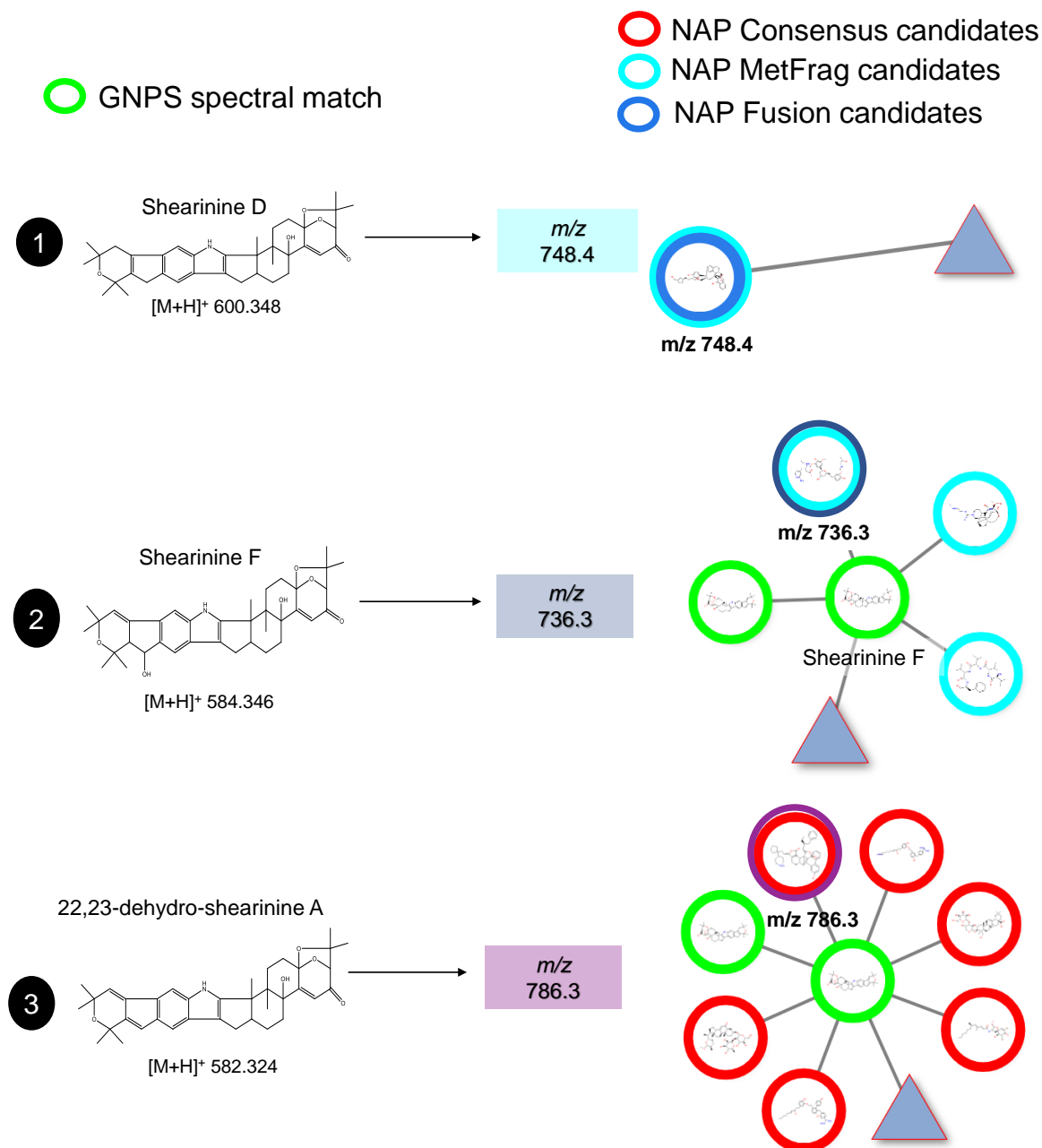


Figura 4.6 – Ions detect in imaging-MS related to shearinine compounds: (1) m/z 748 is correlated to the shearinine D. (2) m/z 736 to the shearinine F (3) 22, 23 dehydro-shearinine A is connected to m/z 786.

The suggested compounds are unusual in fungal natural products. The structure of m/z 736, 786 and 748 were important ions detected in the co-cultures between the black

yeast and parasite fungus (PC-EM). The NAP is an important tool to help us to suggest the class of the chemical compounds but fragmentation studies were still needed.

4.4.6 Fragmentation studies of shearinines-analogous compounds

NAP-annotation does not suggest good or reasonable compounds. The proposes based on the fragmentation were developed to indicate some hits about the compounds we have in culture samples. Based on the fragmentation pattern the shearinines-analogous was a proposal, using the m/z and the main fragments of the spectra (Fig. 4.7).

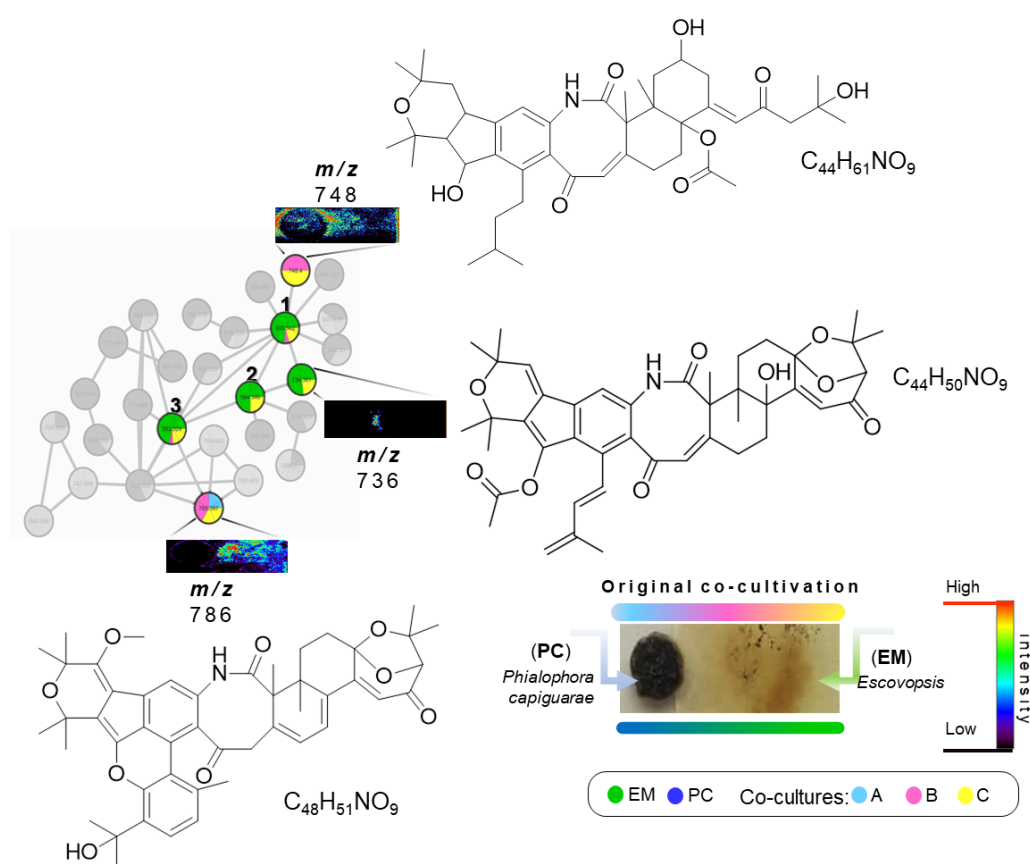


Figura 4.7 – Shearinines-analogous proposals of m/z 736, 786 and 748 and their relation to the co-culture IMS.

The proposal structures were based on the fragmentation studies and neutral losses, according also to the genomics possibilities of *Escovopsis* and *Phialophora* [29, 30]. The proposal fragmentation of the unknown compounds are detailed in SI Fig. C.7, C.8 and C.9.

4.4.7 Antimicrobial assays against actinobacterias

We investigated the antimicrobial activity of the extracts produced in the co-culture between *P. capiguarae* and *Escovopsis* in agar diffusion assays against *Pseudonocardia* sp. The incubation was monitored for two weeks to verify the evolution of cultivation. In the five first days of incubation, the sample regarding the C-zone of co-culture presented a high inhibition zone of 4.5 cm², 40% more than B-zone, and 90% more than A-zone (Fig. 4.8A and B). On the other hand, after 15 days of incubation, the final situation switched: the highest inhibition zone in *Pseudonocardia* sp. plates was regarding B-zone of co-cultures with an inhibition zone of 1.2 cm², 40% more than C-zone area inhibition (Fig. 4.8 C and D).

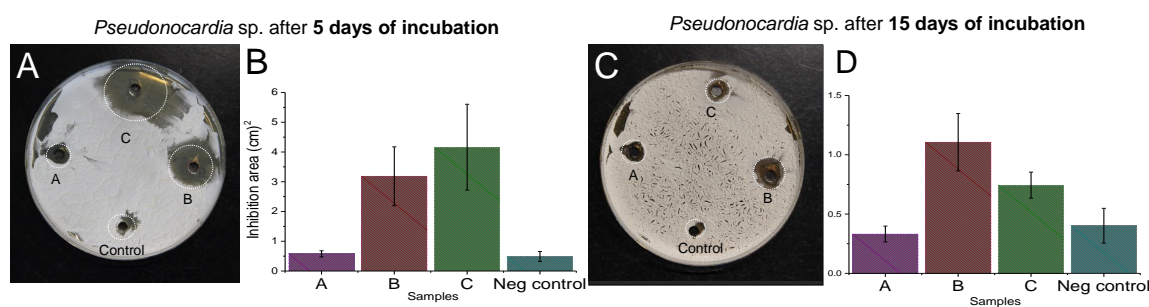


Figura 4.8 – Agar diffusion assay with co-cultivation extracts A-zone, B-zone, C-zone and negative control: (A) the bioassay with *Pseudonocardia* sp. after 5 days of incubation. (B) Statistical analysis of the inhibition zones. (C) the same bioassay after 15 days of incubation. (D) Statistical analysis of the inhibition zones. The comparison was performed using as negative control MeOH. The mono-cultures were also tested and the *Escovopsis* extract showed a similar inhibition than C zone and *P. capiguarae* has not showed bioactivity.

Those results indicated that the induced metabolites involved in the fungal confrontation have substantial bioactivity. The C-zone sample lost its activity, comparing to B-zone. The reason of the bioactivity decreased is related to three possibilities: i) an actinobacteria resistance in front of the compound present in the extract, ii) bacterial metabolization of the chemical compound, or iii) the bioactive compound can present a short half-life, being naturally degraded [31]. In a previous study, shearinine D already proved its activity against both tested *Pseudonocardia* strains [15]. We believe this activity is found in some compounds present in the extract related to the shearinines-analogous compounds due to the previously reported activity for this compound class.

4.5 Outlook

A combination of metabolomic tools and molecular network for MS/MS data approaches gave access to a shorter route to explore the metabolic diversity in microbial interactions of leaf cutting ants symbionts, and this study can help to understand the communication in this complex environment. We verified the co-cultures between the BY and parasite were different from the mono-cultures, and probably compounds were being induced in the interaction. Molecular networking helped us to clarify the class of compounds the samples had, such as the terpene-indole alkaloid shearinines produced by *Escovopsis*. We connected the LC-MS data to imaging-MS to search metabolites that are certainly induced in the confrontation cultures. Those MS/MS spectra were helpful to understand which kind of compounds they could be.

Co-culture between the BY, *P. capiguarae*, and the parasite *Escovopsis* contribute to conclude the production of metabolites that are not produced in mono-cultures. The anti-microbial activity against *Pseudonocardia* sp. can be related to those unknown compounds and contribute to damage the garden development, once they affect the actinobacteria antibiotics production and harm the whole nest.

In summary, the leaf-cutting ants microbial communication plays with several organisms, and co-culture works as an ecological approach which induce metabolic pathways silenced in common mono-cultures experiments. In this current study, the communication between BY and parasite was studied in detail for the first time and helped to understand how this fungal interaction induce compound that can harm whole garden.

4.6 Referências

- [1] Schultz TR, Brady SG. Major evolutionary transitions in ant agriculture. Proceedings of the National Academy of Sciences. 2008;105(14):5435–5440.
- [2] Currie CR, Scottt JA, Summerbell RC, Malloch D. Fungus-growing ants use antibiotic-producing bacteria to control garden parasites. Nature. 1999;398(6729):701–704.
- [3] Little A, Currie CR. Symbiotic complexity: discovery of a fifth symbiont in the Atinne ant-microbe symbiosis. Biology Letters. 2007;3:501–504.

- [4] Della Lucia TM, Gandra LC, Guedes RN. Managing leaf-cutting ants: peculiarities, trends and challenges. *Pest Management Science*. 2014;70(1):14–23.
- [5] Little A, Currie C. Black yeast symbionts compromise the efficiency of antibiotic defenses in fungus-growing ants. *Ecology*. 2008;89:1216–1222.
- [6] Chandra Mohana N, Yashavantha Rao HC, Rakshith D, Mithun PR, Nuthan BR, Sathish S. Omics based approach for biodiscovery of microbial natural products in antibiotic resistance era. *Journal of Genetic Engineering and Biotechnology*. 2018;16(1):1–8.
- [7] Wang M, Carver J, Phelan V, Sanchez L, Garg N, Peng Y, et al. Sharing and community curation of mass spectrometry data with Global Natural Products Social Molecular Networking. *Nature Biotechnology*. 2016 05;34:828–837.
- [8] Wolfender JL, Marti G, Thomas A, Bertrand S. Current approaches and challenges for the metabolite profiling of complex natural extracts. *Journal of Chromatography A*. 2015;1382:136 – 164.
- [9] Pang Z, Chong J, Li S, Xia J. MetaboAnalystR 3.0: Toward an optimized workflow for Global Metabolomics. *Metabolites*. 2020;10(5):186.
- [10] Nothias LF, Petras D, Schmid R, Duhrkop K, Rainer J, Sarvepalli A, et al. Feature-based molecular networking in the GNPS analysis environment. *Nature Methods*. 2020;17(9):905–908.
- [11] Angolini CFF, Vendramini PH, Araujo FDS, Araujo WL, Augusti R, Eberlin MN, et al. Direct protocol for ambient mass spectrometry imaging on agar culture. *Analytical Chemistry*. 2015;87:6925–6930.
- [12] Netzker T, Flak M, Krespach MK, Stroe MC, Weber J, Schroeckh V, et al. Microbial interactions trigger the production of antibiotics. *Current Opinion in Microbiology*. 2018;45:117 – 123.
- [13] Costa J, Wassano C, Fill T. Antifungal potential of secondary metabolites involved in the interaction between citrus pathogens. *Scientific Reports*. 2019;9(18647).
- [14] Boya CA, Fernandez-Marin H, Mejia LC, Spadafora C, Dorrestein PC, Gutierrez M. Imaging mass spectrometry and MS/MS molecular networking reveals chemical

- interactions among cuticular bacteria and pathogenic fungi associated with fungus-growing ants. *Scientific Reports*. 2017;7(1):1–13.
- [15] Heine D, Holmes NA, Worsley SF, Santos ACA, Innocent TM, Scherlach K, et al. Chemical warfare between leafcutter ant symbionts and a co-evolved pathogen. *Nature Communications*. 2018;9(2208):1–11.
- [16] Zhou B, Xiao JF, Tuli L, Ransom HW. LC-MS-based metabolomics. *Molecular BioSystems*. 2012;8:470–481.
- [17] The microbiome and metabolome of Napier grass silages prepared with screened lactic acid bacteria during ensiling and aerobic exposure. *Animal Feed Science and Technology*. 2020;269:114673.
- [18] Albrecht CF, Stander MA, Grobbelaar MC, Colling J, Kossmann J, Hills PN, et al. LCMS-based metabolomics assists with quality assessment and traceability of wild and cultivated plants of *Sutherlandia frutescens* (Fabaceae). *South African Journal of Botany*. 2012;82:33 – 45.
- [19] Bertrand S, Schumpp O, Bohni N, Bujard A, Azzollini A, Monod M, et al. Detection of metabolite induction in fungal co-cultures on solid media by high-throughput differential ultra-high pressure liquid chromatography-time-of-flight mass spectrometry fingerprinting. *Journal of Chromatography A*. 2013;1292:219–228.
- [20] Yang YL, Xu Y, Straight P, Dorrestein PC. Translating metabolic exchange with imaging mass spectrometry. *Nature Chemical Biology*. 2009;5:885–887.
- [21] Chiang YM, Lee KH, Sanchez JF, Keller NP, Wang CCC. Unlocking fungal cryptic natural products. *Natural Product Communications*. 2009;4(11):1505–1510.
- [22] Ernst M, Kang KB, Caraballo-Rodriguez AM, Nothias LF, Wandy J, Wang M, et al. MolNetEnhancer: Enhanced molecular networks by integrating metabolome mining and annotation tools. 2019;9(7):144–169.
- [23] Dhodary B, Schilg M, Wirth R, Spiteller D. Secondary metabolites from *Escovopsis weberi* and their role in Attacking the garden fungus of leaf-cutting ants. *Chemistry - A European Journal*. 2018;24:4445–4452.

- [24] Antiinsectan alkaloids: Shearinines A-C and a new paxilline derivative from the ascostromata of *Eupenicillium shearii*. *Tetrahedron*. 1995;51(14):3959 – 3968.
- [25] Xu M, Gessner G, Groth I, Lange C, Christner A, Bruhn T, et al. Shearinines D-K, new indole triterpenoids from an endophytic *Penicillium* sp. with blocking activity on large-conductance calcium-activated potassium channels. *Tetrahedron*. 2007;63(2):435–444.
- [26] Schymanski E, Jeon J, Gulde R, Fenner K, Ruff M, Singer H, et al. Identifying Small Molecules via High Resolution Mass Spectrometry: Communicating Confidence. *Environmental science technology*. 2014 01;48.
- [27] Sumner L, Amberg A, Barrett D, Beale M, Beger R, Daykin C, et al. Proposed minimum reporting standards for chemical analysis: Chemical Analysis Working Group (CAWG) Metabolomics Standards Initiative (MSI). *Metabolomics : Official journal of the Metabolomic Society*. 2007 09;3:211–221.
- [28] da Silva RR, Wang M, Nothias LF, van der Hooft JJJ, Caraballo-Rodríguez AM, Fox E, et al. Propagating annotations of molecular networks using *in silico* fragmentation. *PLoS Computational Biology*. 2018;14(4):1–26.
- [29] de Man TJB, Stajich JE, Kubicek CP, Teiling C, Chenthamara K, Atanasova L, et al. Small genome of the fungus *Escovopsis weberi*, a specialized disease agent of ant agriculture. *Proceedings of the National Academy of Sciences*. 2016;113(13):3567–3572.
- [30] Moreno L, Stielow B, Vries M, Almir Weiss V, Vicente V, Hoog S. Draft Genome Sequence of the Ant-Associated Fungus *Phialophora attae* (CBS 131958). *Genome announcements*. 2015 11;3.
- [31] Nodwell JR. Novel links between antibiotic resistance and antibiotic production. *Journal of Bacteriology*. 2007;189(10):3683–3685.

5 Black yeast *Phialophora* genus ecological function associated with leaf-cutting ants

Contextualização: Uma abordagem dos estudos sobre a função ecológica no ninho das formigas cortadeiras dos metabólitos produzidos pelos fungos negros será o foco desse capítulo, assim como a busca por melhores condições nos cultivos e isolamento de metabólitos secundários guiado por bioensaios frente à actinobacteria *Pseudonocardia* sp.

5.1 Abstract

Leaf-cutting ants live in mutualistic symbiosis with their garden fungus *Leucoagaricus gongylophorus* that constitutes their main food source. Since the garden fungus is threatened by the pathogenic fungus *Escovopsis weberi*, the ants need to defend their nest. For this, they joined alliance with symbiotic actinobacterias from *Pseudonocardia* and *Streptomyces* genus. Black yeasts, such as *Phialophora* genus, have been reported as a possible fifth symbiont, competing with the actinobacteria. However, their chemo-ecological role has been underexploited. Therefore, the phylogenetic analysis was performed to confirm the species and genus of the microorganism under study. In addition, the genomics information was useful to compare the gene clusters and the potential metabolites that can be produced. To isolate bioactive secondary metabolites from *P. capiguarae*, the growth conditions were optimized. Different media and different growth time were used in the screening studies. The compound F5-30 was isolated, and it presented a smooth inhibition against *Pseudonocardia* symbionts using bioassay-guided isolation. The data suggests the compound is like aliphatic ester compounds. This bioactive compound from black yeasts is related for the first time in this study. Our studies contribute to the interaction studies among black yeasts symbionts in the leaf-cutting micro-environment. However, further studies are necessary to conclude the chemical-ecology hypothesis of the isolated compound.

Key-words: Bioassay-guided isolation, black yeast, leaf-cutting ants, microbial interactions, *Pseudonocardia* genus, *Phialophora* genus, secondary metabolites.

5.2 Introduction

Leaf-cutting ants live in a mutualistic symbiosis with the fungus *Leucoagaricus gongylophorus* which uses fresh plant material and lead to significant impacts on human activity as such as agriculture [1]. The Attini ants have developed mechanisms to defend their gardens. Nevertheless, the defense, specialized pathogenic fungus *Escovopsis* sp. can attack the garden and destroy the whole colony of leaf-cutting ants [2, 3]. The Figure 5.1 presents a schematic representation of the experimental part within black yeast symbionts.

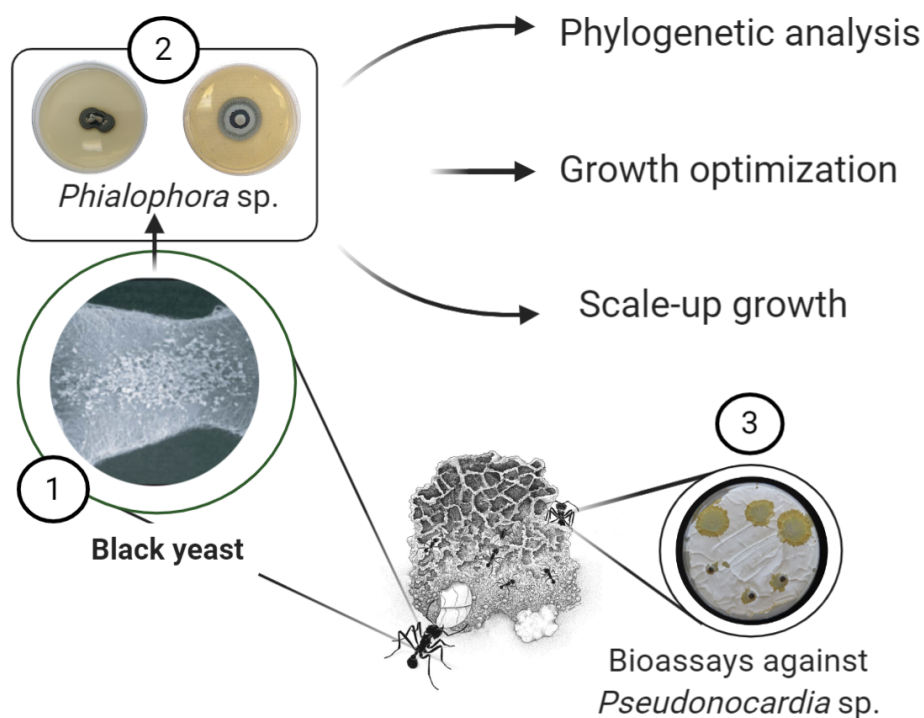


Figura 5.1 – Schematic representation of the experimental part within black yeast symbionts: (1) Black yeasts isolated of leaf-cutting ants cuticle and the electronic microscopy of ants body are represented in the Figure [4]. (2) The black yeast in Petri dishes, *Phialophora* genus, *P. attae* (left) and *P. capiguarae* (right). (3) the bioassays of *P. capiguarae* extract against the actinobacteria *Pseudonocardia* sp. is also showed.

The protection in leaf-cutting ants garden is supported by the actinobacteria symbiosis, from the genus *Pseudonocardia* and *Streptomyces*, which produce potent antimicrobial compounds that protects the nest of other pathogens [5, 6]. Invasive microbes can colonize the nest of leaf cutter ants, such as *Escovopsis* sp., *Fusarium* sp., *Cladosporium* sp. and *Trichoderma* sp., when there is an environmental unbalance in the garden [7, 8] and this can lead to the workers death, which suggests low protection by actinobacteria [9].

The black yeast-symbiosis in the gardens were described for the first time in 2007 [10], and they are closely related to the genus *Phialophora*. In the nature, black yeasts (or similar genus) live as endophytes in plants [11]. Thus, ants may have acquired the black yeast by manuring their gardens with vegetation containing *Phialophora* endophytes [12]. Black yeasts are also found in soil, water and wood and have this name because of the occurrence of melanin deposits in their cell walls [13]. Some black yeasts species can still infect humans and other animals such as *Exophiala dermatitis* that causes pulmonary disease [14, 15]. The black yeasts have the potential to directly and indirectly affect each member of the symbiosis.

Most of black yeasts have been found in the same microenvironment than the actinobacteria: in the cuticle structures of worker ants [8]. Previous studies have demonstrated that black yeast have a direct impact on *Pseudonocardia* and suggests that has potential to indirectly impact the health of ants by disrupting their ability to inhibit the parasite *Escovopsis* sp. via their antibiotic-producing [12]. However, the chemical details of black yeasts-interactions remain severely unknown.

Few previous studies presented the interaction among the leaf-cutting ants symbionts and the black yeasts [10, 12]. The evidences indicated that the black yeast is a one of the leaf-cutting ants symbionts for different reasons i) they are easily found in leaf-cutting ants colonies in specialized location on the ants cuticle, ii) the most of black yeast species represents the same monophyletic group and, iii) the black yeasts can originated and be maintained in the leaf-cutting ants garden over the time [10].

This study proposes to extend the knowledge on the interaction between black yeasts and leaf-cutting ants symbionts. Different aspects were verified in this study i) the phylogenetic analysis of *P. capiguarae* strain, ii) its biological activity in the ants environment in front to other microbes, and iii) the bio-guided isolation and identification of the metabolite produced by the black yeast. Here, we correlated the microbial interactions of black yeasts isolated from leaf-cutting ants by studying the chemical profile using LC-MS and bioassays-guided isolation against symbiont microbes.

5.3 Experimental part

5.3.1 Biological material

- Mutualist fungus: *Leucoagaricus gongylophorus* was isolated from an *A. octospinosus* nest maintained at University of Kaiserslautern by Dr. Rainer Wirth and verified by 18S rDNA sequencing.
- Parasite fungus: *Escovopsis weberi* CBS 110660 was obtained from the Westerdijk Fungal Biodiversity Institute (Utrecht, the Netherlands).
- Black yeasts: *Phialophora attae* (AP399 - PA) and *P. capiguarae* (AP376 - PC) isolated from *Atta capiguara* queen ants (Botucatu, Brazil).
- Actinobacteria: *Streptomyces* 28.2 and *Pseudonocardia* W3 were obtained from the Westerdijk Fungal Biodiversity Institute (Utrecht, the Netherlands).

5.3.2 Phylogenetic analysis of black yeast strains

5.3.2.1 Genomics DNA from black yeasts from a agar culture

Primers used in the polymerase chain reaction (PCR) experiments were the ITS 1F code: H186 14 1491 1/4 (5-CTTGGTCATT TAGAGGGAGTA-3) and LR3 code: H183 14 1491 2/4 (5-CCGTGTTT CAAGACGGG-3). PCR products were cloned into the vector pJET 1.2 and sequenced. The sequences were analyzed by *Eurofins Genomics*.

5.3.2.2 DNA extraction of the strain

After 2 weeks of incubation at 28 °C, the fungal mycelium was scrapped off into sterile tubes and resuspended using EDTA, proteinase K and SDS (10%). The strain was incubated at 55 °C for 3 h. NaCl solution (5M) and cold-chloroform were added to precipitate the proteins. After centrifugation, the upper phase with genomics DNA was separated and cleaned with ethanol twice. The pellet was resuspended with ethanol (ice-cold 70%) and solubilized using sterile water (ddH₂O).

5.3.2.3 PCR condition - 18S rDNA

The master mix was prepared with 10 μ L 5xPhusion GC Buffer, 7.5 μ L dNTPS, 1 μ L of each one primers *Eurofins* genomics ITS-1F (H186 14 1491 1/4) and LR3 (H183 14

1491 2/4) and 1 μL of Phusion polymerase. After that, a mixed was made using 46 μL of ddH₂O, 6 μL of MgCl 50mM, 3 μL of DMSO, 4 μL of gDNA and 41 μL of master mix. The PCR was performed using PEQ STAR with a gradient of temperature 98 °C to 72 °C for 1 h, followed by agarose gel electrophoresis of the amplified DNA. *P. capiguarae* DNA extraction from agarose gel was performed using *PeqLab* kit.

5.3.2.4 Transformation with cloning vector pJET 1.2

Ten best strains of *Escherichia coli* in Luria-Bertani (LB) solid media and in LB liquid media (10g of peptone, 5g of yeast extract, 5g of sodium chloride and 15g of agar in 1000 mL of ddH₂O) with antibiotic ampicillin (100 mg · mL⁻¹ of media) incubated for 18 hours at 37 °C. The plasmide was extracted using *PeqLab* kit. The restriction digest was performed for 3 h using BgII or NotI enzymes and electrophoresis verification.

5.3.2.5 Sequencing of DNA (18S)

For sequencing the 18SrDNA insert, the T7 primer and xy were used Standard Primer. The genome was sequencing by *Eurofins Genomics*. Obtained sequences were edited in SnapGene and analyze during BLAST-n.

5.3.3 Initial screening of black yeasts isolates for biological activity

5.3.3.1 Optimization of the growth conditions of *Phialophora* black yeasts

The strains *P. attae* and *P. capiguare* were cultivated in three different solid media to activate metabolic pathways [16]: Yeast and malt medium agar (YEME): 3g yeast extract, 5g peptone, 3g malt extract, 10g D-glucose, 15g agar in 1000 mL of dd-water, Potato Dextrose Agar (PDA): 39 g in 1000 mL dd-water, and Soya Flour Manitol (SFM): 20 g soya flour, 20g manitol, 15g agar in 1000 mL of dd-water. After incubation by 7, 14 and 21 days at 28 °C. The material was transferred into an extraction vessel with 100 mL of ethyl acetate per 5 agar plates. The plates were triturated using ultra-turrax (Ultra-Turrax T25 IKA WERKE, Altana Pharma AG) at room temperature for 5 min, then extractions were performed in a water-bath sonicator (Elma Sonicator) for 15 min. Blanks with no fungal were extracted in the same way. The sonicated samples were filtered through glass cotton and filter paper. Finally, the extracts were dried under pressure using a rotaevaporator at 40 °C.

5.3.3.2 LC-MS analysis

The dry extracts were dissolved in methanol at a concentration of $2 \text{ mg} \cdot \text{mL}^{-1}$ for LC-MS analysis. Experiments were performed using (1) Low resolution MS: LTQ ion trap mass spectrometer coupled to an Agilent HPLC model system (Agilent) and (2) High resolution: Exactive Orbitrap Thermo Fisher mass spectrometer coupled to a Waters UPLC, which both included an in-line degasser, binary pump, and refrigerated autosampler. In (1), a $5 \mu\text{m}$ C18 column with $250 \text{ mm} \times 4,6\text{mm}$ (*Macherey-Nagel*), maintained at 25°C , was operated using a gradient elution of H_2O and ACN (both with 0.1% acetic acid) running at $0.2 \text{ mL} \cdot \text{min}^{-1}$. The gradient program was as follows: 10% to 100% ACN over 18 min, 100% ACN for 12 min using $5 \mu\text{L}$ of injection volume at 40°C . All of the mass spectra were recorded in the positive-ion mode. MS parameters were a spray voltage of 3.5 kV, a capillary temperature of 220°C . The m/z range was 100 to 2000 Da. The data were analyzed using Software X-calibur (Thermo) and the chromatogramas were edited using Origin Lab 9.

5.3.3.3 Bioassays with extracts

The dry extracts were dissolved in methanol at concentration of $5 \text{ mg} \cdot \text{mL}^{-1}$ for the bioassays. The assays were performed using agar diffusion method to reveal if microorganisms interact or are influenced by each other. For the agar diffusion assays, suspensions of the test organisms (1 mg of microbial cells in 1 mL of water) were spread on agar plates, small holes with $25 \mu\text{m}$ were chopped into the agar plates into which the test solutions and fractions were applied in $5 \text{ mg} \cdot \text{mL}^{-1}$. The extract was tested against the following microbes: *Escovopsis weberi*; *Leucoagaricus gongylophorus*; *Streptomyces* 28.2, *Streptomyces* 28.1, *Pseudonocardia* ants W3, *Pseudonocardia* ants 2, *Blattschneiderameise* 10, *Blattschneiderameise* 26.3 and *Pseudomonas aureofaciens*. The strains were incubated at 28°C for three weeks and verified every day to check some inhibition zone. The inhibition zone was verified by visual analysis to check the bioactive extracts.

5.3.4 Cultivation of black yeasts and isolation of bioactive metabolites

5.3.4.1 Scale-up growth, silica column and data analysis

After all the bioactivity tests, the bioactive experiment was selected and cultivated in scale-up. *P. capiguarae* cultivated in SFM medium plates was cultivated for 21 days at 28°C

°C. Four different kind of extractions were tested 1) Ethyl acetate; 2) Ethyl acetate with HCl; 3) Ethyl acetate with NaOH, and 4) Ethyl acetate: Dichloromethane: Methanol (1:2:3). The plates were extracted with ethyl acetate and centrifuged with MeOH as a clean-up procedure. The ethyl-acetate extract was dried under vacuum and fractionated using silica column and eluted with 100 mL of petroleum ether and ethyl acetate solvents in different ration (10:1; 6:1; 3:1; 1:1; 1:3; 1:6 and 100% of ethyl acetate) and were concentrated to dryness. All fractions were submitted to bioassays against *Streptomyces* sp. and *Pseudonocardia* sp. W3 and analyzed by LC-MS, or GC-MS. The fifth fraction from crude extract (F5) was further purified by semi-preparative HPLC. The dry extracts were dissolved in methanol at concentration of $2 \text{ mg} \cdot \text{mL}^{-1}$ for LC-MS analysis and in ethyl acetate at concentration of $2 \text{ mg} \cdot \text{mL}^{-1}$ for GC-MS.

5.3.4.2 Bioactive compounds isolation

The compounds were isolated using HPLC semi-preparative. Experiments were performed using HPLC-UV (Agilent) with fraction-collector. A $5 \mu\text{m}$ C18 column with (Macherey-Nagel), maintained at $25 \text{ }^\circ\text{C}$, was operated using a gradient elution of H_2O and ACN (both with 0.1% acetic acid) running at $0.8 \text{ mL} \cdot \text{min}^{-1}$. The gradient HPLC program was as follows: 10% to 100% ACN over 18 min, 100% ACN for 12 min, using $30 \mu\text{L}$ of injection volume at room temperature. The samples were collected in each 1 min, resulting in 34 samples in total.

5.3.4.3 NMR Spectroscopy

^1H NMR, ^{13}C NMR and 2D experiments were performed on a Bruker Avance III 600 (^1H 600.13 MHz and ^{13}C 150.9 MHz). Deuterated methanol (MeOD) was used as solvent and internal reference. Chemical shifts (δ) were expressed in (ppm) and the coupling constants (J) in Hertz (Hz). 3 mm NMR sample tubes were placed inside of 5 mm NMR tubes with $180 \mu\text{L}$ of MeOD. Spectrum calibration was performed using the deuterated solvent as internal reference cite (MeOD: 4.87 ppm (singlete) for ^1H NMR and 49 ppm (multiplete) for ^{13}C NMR).

5.3.4.4 Bioassays against actinobacteria

The isolated compounds were dissolved in methanol at a concentration of $5 \text{ mg} \cdot \text{mL}^{-1}$ for the bioassays. The assays were performed using agar diffusion methods. For the agar

diffusion assays, suspensions of the test organisms were spread on agar plates, small holes were cut into the agar plates into which the test solutions/fractions will be applied in $5 \text{ mg} \cdot \text{mL}^{-1}$ in $10 \text{ } \mu\text{L}$. All the extracts and the fractions were tested against *Pseudonocardia* sp. The negative control was performed using the same solvent used to solubilize the sample, methanol, or ether. The area of inhibition zone was calculated using the *Image J* software and the graphics were performed using *Origin* software.

5.3.5 DESI imaging analysis on co-cultivations

The strains were inoculated using water suspension in the agar plates with the microscope slides, photographed and put in a vacuum desiccator for complete agar dehydration at room temperature [17]. MS imaging was performed using a ProSolia DESI source (Model OS-3201) coupled to a Thermo Scientific Q Exactive Hybrid Quadrupole-Orbitrap Mass Spectrometer. The DESI configuration was set with an emitter height of 2.5 mm, mass spectrometer inlet height of 0.1 mm, inlet to emitter distance of 3.8 mm, $58 \text{ } ^\circ\text{C}$ spray angle, 5.0 kV spray voltage, inlet capillary temperature of $320 \text{ } ^\circ\text{C}$, 100 V S-lens, 160 psi ultrapure nitrogen nebulizing gas pressure, and a sprayed solvent of methanol at a $3.0 \text{ } \mu\text{L} \cdot \text{min}^{-1}$ flow rate. Images were collected from m/z 200 to 1500 with a step sized of 200 m, a scan rate of $741 \text{ } \mu\text{m} \cdot \text{s}^{-1}$, and a pixel size of $200 \text{ } \mu\text{m} \times 200 \text{ } \mu\text{m}$. In short, major conditions were as follows: $3 \text{ } \mu\text{L} \cdot \text{min}^{-1}$ of solvent flow rate, nebulizing gas backpressure of 100 psi and $2 \text{ mL} \cdot \text{min}^{-1}$ gas flow rate. The DESI-IMS data was converted into imaged files using Firefly data conversion software (version 2.1.05) and viewed using the BioMAP software (version 3.8.04). In BioMAP the data were opened in an m/z 200 to 1000 range, and the false-color scaling were adjusted to a fixed value to enable a relative comparison between experiments.

5.4 Results and discussion

5.4.1 Black yeast *P. capiguarae* phylogenetic comparison

Phylogenetic studies of AP376 showed the successful 18S rDNA of the strain, with a DNA size with 1000-1500 bp (right size according to the used primers ITS1F and LR3). The restriction digest worked after 3h of incubation at $37 \text{ } ^\circ\text{C}$. The size around 1000 to

1500 bp was related to the fungus strain. After the restriction digest, the agar-gel was extracted and separated in electrophoresis (Fig. 5.2).

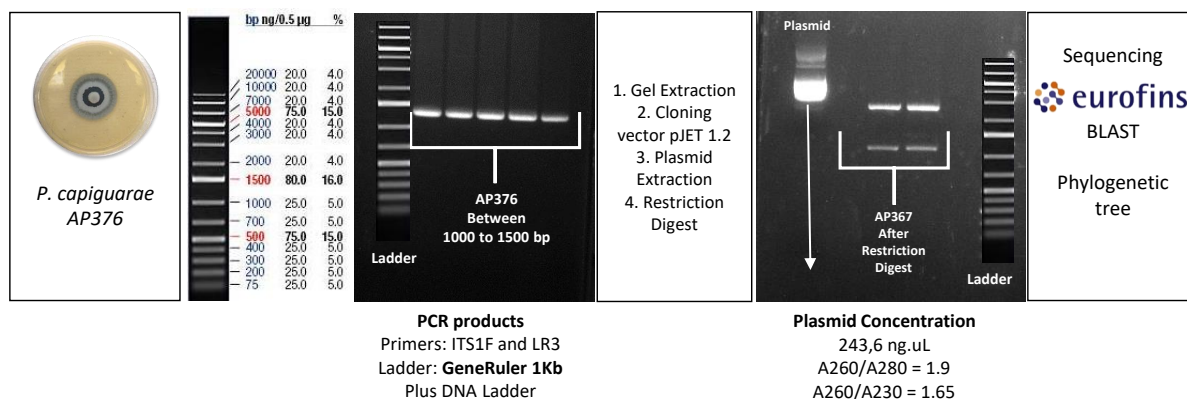


Figura 5.2 – Phylogenetic study of *P. capiguarae*: electrophoresis of PCR amplification with 1000-1500 bp size and plasmide extraction with a concentration of 243.6 $\text{ng} \cdot \mu\text{L}^{-1}$, and a high level of purity A260/A280 of 1.9 and A260/A230 of 1.65.

The material was sent to *Eurofins* and the 18S rRNA sequence was analyzed in available online data analysis GenBank. The comparison with the data bank showed that the strain is similar to *P. capiguarae* and *Cyphellophora oxyspora*. However, both strains have no chemical studies so far. Previous studies have shown how these strains are phylogenetically similar as is shown in the Figure 5.3 [11]. Although they are isolated of different environments *P. capiguarae* isolated from leaf-cutting ants and *C. oxyspora* isolated from plants, the strains are phylogenetically similar.

The AntiSmash website [18] helps to identify the possible compounds produced by the strains. The black yeast *P. attae* has a quite simple biosynthetic gene cluster with thirteen regions (4 PKS-like, 1 NRPS, 4 NRPS-like and 4 terpene) and only two similar clusters with 100% of similarity showing melanin (characterized by melanized strains) and clavatic acid (a triterpenoid inhibitors of farnesyl-protein transferase). Recent studies observed the biological activities of melanin pigment extracted from insect *Bombyx mori* gut-associated yeast *Cryptococcus rajasthanensis*, among the activities there are antimicrobial, antioxidant, anti-inflammatory and anticancer properties [19].

Previous secondary metabolite gene cluster studies in some species of black yeasts have been done [11] and are shown in Table 5.1 for *Phialophora*. genus: *P. attae* and *P. europaea*. These strains usually have biosynthetic gene clusters of terpene, polyketide, non-ribosomal peptide synthases, showing different possibilities from these microbes for producing natural products. However, any biosynthetic gene cluster information to *P.*

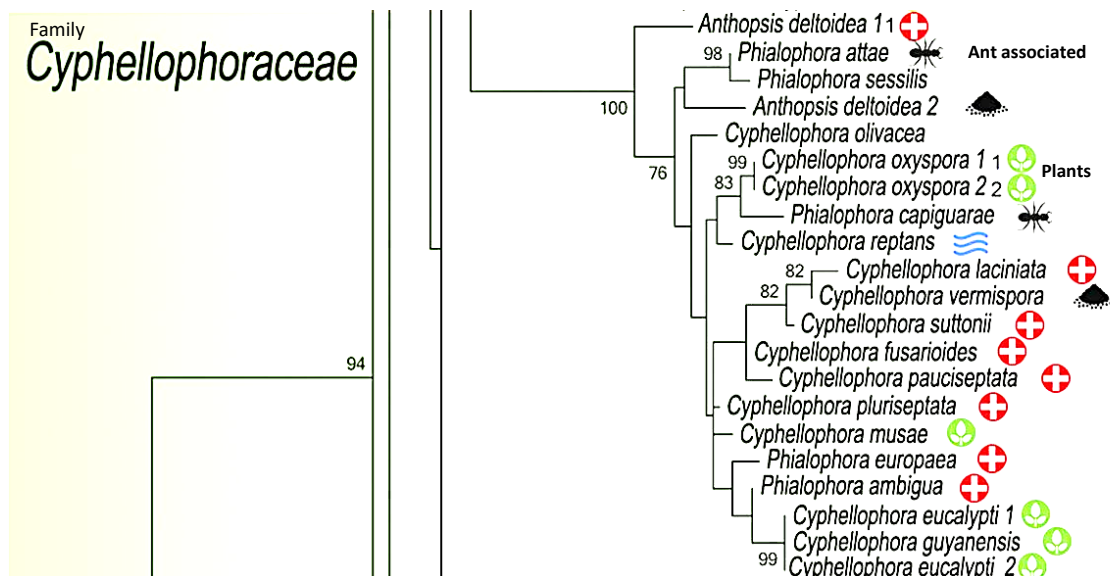


Figura 5.3 – Black yeasts phylogenetic comparison: phylogenetic analysis of members of *Chaetothyriales* (Class Eurotiomycetes), more details in the *Cyphellophoraceae* family [11]. Different species of black yeasts can be found in different environments: plant endophytes, soil microbiome, wood, water, or ant-associated. *P. attae* and *P. capiguarae* were both found in ant-association and they are quite phylogenetically similar to *Cyphellophora* genus.

capiguarae has been found in NCBI data bank, which was one reason to keep further the studies with this strain.

Tabela 5.1 – Summary of black yeast *P. attae* and *P. europaea* secondary metabolite gene classes [11].

Species	Terpene	III PKS	I PKS	NRPS	Terpene/indole/ I PKS
<i>P. attae</i>	4	1	3	1	0
<i>P. europaea</i>	4	0	2	2	0

Despite these two strains are phylogenetically similar and isolated from leaf-cutting ants, they showed distinct behavior according to their chemical and biological studies. The details of Antismash analysis present the Biosynthetic gene clusters (BGC) (Fig. D.1). *P. attae* had the sequence genome in NCBI website. The comparison by similarity (Antismash) presented two identified compounds: (1) clavarinic acid, a terpene that has been characterized from *Clavariadelphus truncatus*. Clavarinic acid inhibited the human farnesyl-protein transferase (FPTase) [20] that is essential for oncogenic activity in oncogene-mediated tumors. The other compound is the (2) melanin, a polyketide type 1, pigment responsible for the color of the black yeasts. Melanin is essential in the virulence of plant and human pathogenic fungi [21] and it was identified in *Aspergillus fumigatus*

[22] and *Colletotrichum lagenarium* [23]. The chemical structure of both suggested compounds based on the gene cluster analysis can be verified in Figure 5.4. Unfortunately, the experiments with the strain *P. attae* (AP399) were not satisfactory to proceed the experiments due to the PCR products were not of the correct base size (1000-1500 bp).

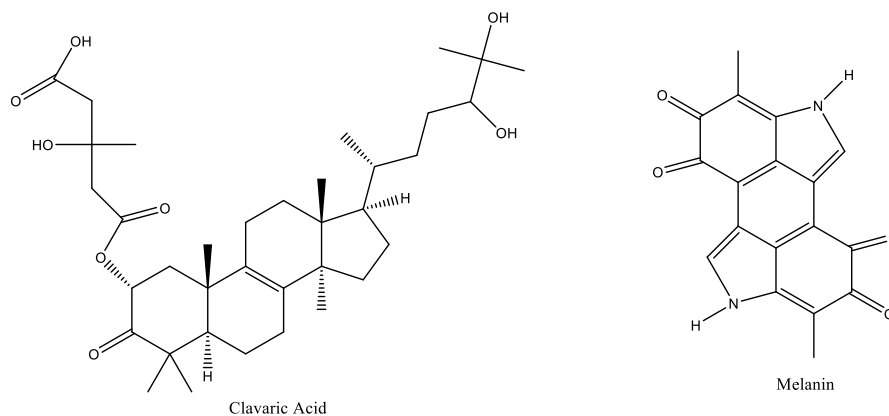


Figura 5.4 – Chemical structure of clavarinic acid (terpene) and melanin (PKS-type 1) found in the AntiSMASH analysis of *P. attae* BGC with 100% of similarity.

5.4.2 Chemical profiling comparison of the black yeasts: LC profile and bioassays

5.4.2.1 Growth optimization of black yeasts: LC-profiling and bioactivity analysis

“One strain many compounds” (OSMAC) approach with medium variation approach [24] is an important technique when the main goal is to see biologic activity of microbial strains. The LC-MS profiles were compared among three distinct media and the extracts were bioassayed against *Streptomyces* sp. The profiling varied according to three-point times at 7, 14 and 21 days of incubation.

P. capiguarae OSMAC experiments showed a huge variation in PDA agar plates, with 7 to 14 and 21 days. Comparing the chemical profiling, most of the peaks disappeared after two weeks in PDA media. In YEME plates, the fungus did not show a large variation after two weeks comparing to 7 days, which it can be explained by a possible degradation, but so many signals appeared after 21 days. In SFM plates the LC-profiling changed softly after 14 days and new peaks raised after three weeks of incubation. *P. capiguarae*

presented some variation in the chemical profile appearance in different media and time of incubation (Fig. 5.5).

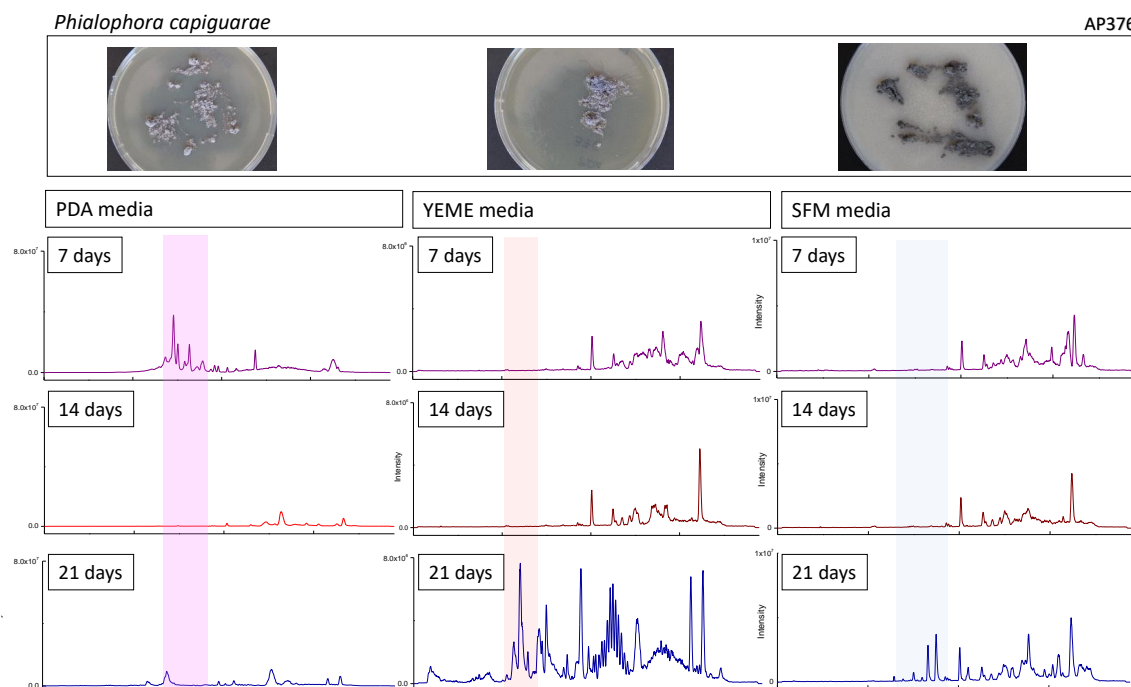


Figura 5.5 – *P. capiguarae* (PC) strain LC profiling cultivated in different media PDA, YEME and SFM at three different times (7, 14 and 21 days). The highlighted sections show the outstanding chromatographic peaks in the *P. capiguarae* cultivations.

P. attae also presented some differences in the chemical profile (Fig. 5.6). AP399 showed a variation in PDA agar plates, comparing 14 to 21 days. Most of the peaks disappeared after 14 days of growth in YEME media. The same situation was observed in SFM agar plates, in which the most peaks disappeared in two weeks and other new peaks have appeared in the LC profile after 21 days of incubation.

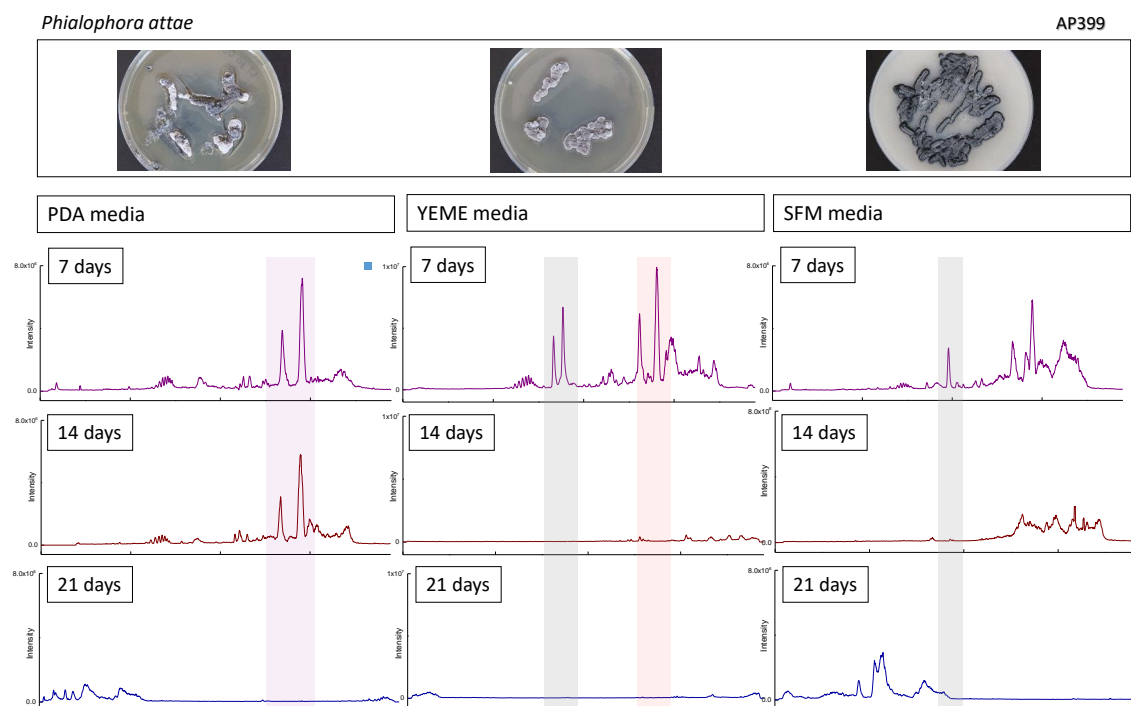


Figure 5.6 – *P. attae* AP399 strain LC profiling cultivated in different media PDA, YEME and SFM at three different times (7, 14 and 21 days). The highlighted sections show the outstanding chromatographic peaks in the *P. attae* cultivations.

Different media cultivation or “OSMAC approach” has been efficient to differentiate the black yeasts chemical profiling, as well as the extracts bioactivity. All the 18 extracts were bioassayed against *Streptomyces* sp. Only *P. capiguarae* in SFM medium cultivated for 21 days presented bioactivity. The following experiments were performed with the active setting cultivation.

5.4.2.2 Different extraction procedures

The AP376 strain was cultivated for 21 days in SFM plates. Then, the same setting cultivation was repeated three more times to confirm the inhibition reproducibility. Subsequently, three other different solvent extraction types were tested against *Streptomyces* sp. and analyzed by LC-MS: i) the usual ethyl acetate extraction; ii) Acid extraction: ethyl acetate extraction with hydrochloric acid (HCl) with $\text{pH} \leq 3$; iii) Basic extraction: ethyl acetate extraction with hydroxide of sodium (NaOH) with $\text{pH} \geq 9$ and iv) extraction with mixed solvents ethyl acetate: dichloromethane: methanol (1:2:3). The highest bioactivity was observed in (2) and (3) extraction. Therefore, the following experiments were

done using the acid extraction (ii) to lead the next experiments in barely one extraction (Fig. D.2).

However, the activity against *Streptomyces* sp. 28.2 disappeared after the third day of incubation. The crude extract was tested against other strains and showed permanent activity against *Pseudonocardia* W3. Therefore, the upcoming experiments and bioassays were performed against *Pseudonocardia* sp. and not against *Streptomyces* sp. anymore. This choice was also related to the previous studies [10] that it showed the relation between the black yeasts and *Pseudonocardia* sp, since this genus of actinobacteria on ants tegument is potentially easier to be found than *Streptomyces* sp (Fig. D.3).

5.4.3 Bioactive compound isolation of black yeast

5.4.3.1 Silica column chromatography

The crude extract was purified in the first step using silica column, to clean and purify the sample. The sample was divided in seven fractions with different polarities. The LC and GC profile of seven (F1 - F7) fractions can be viewed in the Figure 5.7. The fractions 1, 2, 5 and 6 have showed some inhibition in *Pseudonocardia* bioassays, but fractions 1, 2 and 6 have not shown the same activity when the experiment was repeated.

The reproducibility was observed only in the fraction 5, and a reasonable inhibition zone is shown in the statistical analysis, showing an inhibition of ≈ 1.0 cm of diameter (Fig. 5.7). The three first fractions (1, 2 and 3) were completely apolar, presenting aliphatic appearance when they were dried in the vials. For these reasons, the first three fractions were analyzed using GC-MS. According to the library some compounds were identify hexadecanoic acid, 9,12-octadecadienoic acid, 9-octadecenoic acid and methyl stearate. Actually, these volatile compounds are originated from the culture medium and they are not important for the bioactivity. The more polar fractions (4, 5, 6 and 7) were analyzed by LC-MS in reverse phase because they were completely soluble in MeOH and water (Fig. 5.7). According to the Figure 5.7C and D.4B, it is possible to see a smooth inhibition of *Pseudonocardia* sp. by fraction 5 and 7 ($5 \text{ mg} \cdot \text{mL}^{-1}$).

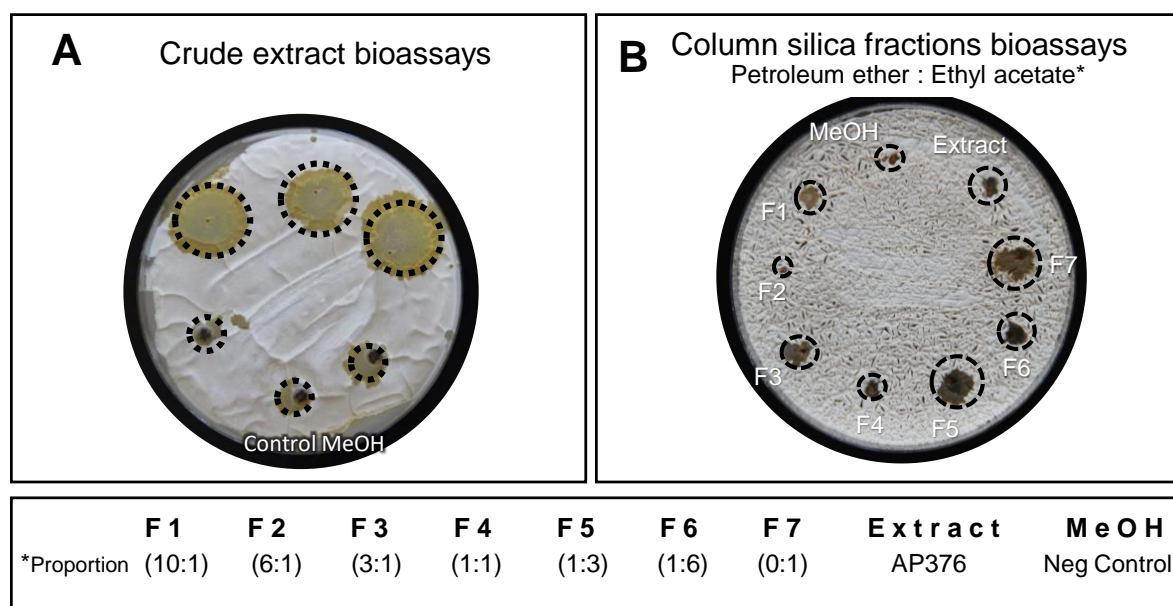


Figura 5.7 – A) Bioassays against *Pseudonocardia* sp. using the crude extract (above) and the negative control (MeOH); B) Bioassays against *Pseudonocardia* sp. using the different fractions 1 to 7. All the bioassays were made in three replicates in different agar plates. The proportion with petroleum ether and ethyl acetate is shown below F1 to F7 according to the proportion of petroleum ether and ethyl acetate.

The fraction 5 and 7 presented a good inhibition zone against the bacteria. Thus, this bioassay showed a high area inhibition of F5 ($\approx 0.2\text{cm}^2$) and F7 ($\approx 0.4\text{cm}^2$) against the actinomycetes *Pseudonocardia* sp. Although fraction 7 also has showed a smoothly inhibition, only the fraction 5 had enough material to proceed to further separation steps (Fig. D.4 - Supplementary information).

5.4.3.2 Bioactive metabolite: isolation and elucidation

The fraction 5 was analyzed by HPLC-DAD with fraction collector. The samples were collected for 38 minutes and the sub-fractions were submitted in bioassays against *Pseudonocardia* W3. Ten different collect samples were submitted to biological assays. The inhibition area was predicted using Image J and compared among the other. Three fractions A2 (II), B30 (VII) and B32 (IX) have showed meaningful activity against *Pseudonocardia* sp (Fig. D.5).

The amount was enough to proceed to the bioassays studies and the F5-B30 activity was verified and reproduced (Fig. D.6 - Supplementary information). The sub-fractions were analyzed by 1D and 2D NMR (^1H , ^{13}C , COSY, HMBC, HSQC) and MS to collaborate in determining the chemical structure (Fig. D.8).

Compound F5-B30: The compound F5-30 was isolated of *P. capiguarae* (SFM plates incubated after 28 days) and presented activity against *Pseudonocardia* W3 sp. Approximately 5 mg of the pure compound in a pound white was obtained. The graphic information of structure elucidation can be visualized in the Figure D.7 and the NMR information are showed in Table 5.2 and the 1D and 2D NMR spectra are in Supplementary information (Fig. D.8).

Tabela 5.2 – NMR Spectroscopic Data for compound F5-B30 in MeOD. ^1H (600 MHz) and ^{13}C (150 MHz) NMR spectroscopic data for F5-B30 in Methanol- d_4 at 298 K. The δ is in ppm and J in Hz. All the NMR spectra is in Supplementary information D. The NMR ^{13}C shows the duplicate signals, which indicates that molecule is a dimer. *The chemical shifts can be switched due to the proximity among them. Abbreviations: d = doublet, dd = doublet of doublets, t = triplet, m = multiplet.

C/H	Type	HSQC ^1H (ppm)	^{13}C (ppm)		H-H COSY	HMBC
1	COOR		175.49	175.53		(1.62, 2,35)
2	CH ₂	2.35 t (6.9 Hz)	34.93	34.94	1.62	175.5, 26.0 e 30.6
3	CH ₂	1.62 (m)	25.99	26.00	1.33 e 2.35	
4*	CH ₂	1.29-1.33 m	30.61	30.61	1,29-1,33	
5*	CH ₂	1.29-1.33 m	30.73	30.77	1,29-1.33	
6*	CH ₂	1.29-1.33 m	30.79	30.79	1.29-1.33	
7*	CH ₂	1.29-1.33 m	30.80	30.84	1.29-1.33	
8	CH ₂	2.03 m	28.12	28.15	1.33 e 5.35	130.8 e 30,8
9	CH=C	5.35 m	130.79	130.79	2.03	28.1
10	C=C	1.29-1.33 m	139.0	139.0		(1.29 e 1.33)
11*	CH ₂	1.29-1.33 m	30.31	30.34	1,29-1,33	139.9 e 130,8
12*	CH ₂	1.29-1.33 m	30.43	30.46	1,29-1,33	
13*	CH ₂	1.29-1.33 m	30.19	30.20	1,29-1,33	
14*	CH ₂	1.33 m	33.07	33.09	1.33 e 1.29	
15	CH ₂	1.29 m	23.75	23.75	0.90 e 1.33	14.6 e 33.1 e 30.20
16	CH ₃	0.90, d (6.8)	14.45	14.46	1.29	23.7 e 33.1
1'	CH ₂	4.07, dd	66.47	66.47	3.82 e 4.15	175.5, 71.1 e 64.1
		4.15, dd			3.82 e 4.07	175.5, 71,1 e 64.1
2'	CH	3.82, m	71.14	71.14	3.55; 4.07; 4.15	66.5 e 64.1
3'	CH ₂	3.55 m	64.05	64.05	3.82	71.1 e 66,5

The structural elucidation of this compound is related to a type of aliphatic ester derivatives or phomesters, described newly [25] according to the chemical shifts at NMR spectrum appearance in the Table 5.2, and mainly for the 2D NMR experiments, HSQC and HMBC (Fig D.11 - D.12). The compound has a long aliphatic part, probably connected in its dimer, and it will be the first time where this kind of compound can be

active against an actinobacteria. Recently, a similar new secondary metabolite from a co-culture between the endophytic fungus *Phoma* sp. with *Armillaria* sp. was identified, but no significant cytotoxicity or antimicrobial activities were detected [25].

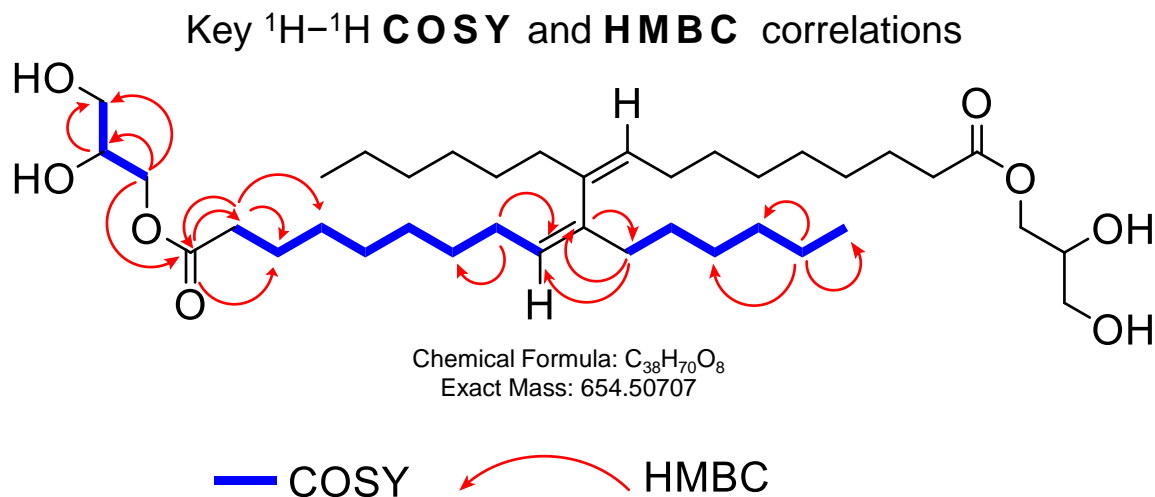


Figura 5.8 – Suggested F5-30 compound related to the phomester [25] isolated from the black yeast *P. capiguarae*. The numbers are related to the Table 5.2 and the COSY and HMBC correlations as well.

The co-cultivation between *P. capiguarae* and *Pseudonocardia* sp. (PC-Bac) and *P. capiguarae* and *Escovopsis* (PC-EM) presented the m/z 393 in confrontation assay through the DESI-imaging-MS analysis (Fig. D.7 D). Furthermore, the ion m/z 393 was visualized mainly in the intersection zone between the strains. This fact suggests that the compound F5-30 is stimulated by the black yeast in specific situations (SFM media) and the confrontation against the symbionts. The MS/MS spectra is show in Fig. D.7.

The propose compound is with a fusion of the two identical fatty acids connected by a double bound. The 2D NMR data of COSY and HMBC are shown in Fig. 5.9. The same correlations are visualized in both fatty acids chain, due to the duplicate signals in ^{13}C NMR spectra (Fig. D.9). Deeper NMR experiments are necessary to confirm the both aliphatic chain and also the correct position. A fragmentation propose is explained for the m/z 393 and can be visualized in Fig. 5.9.

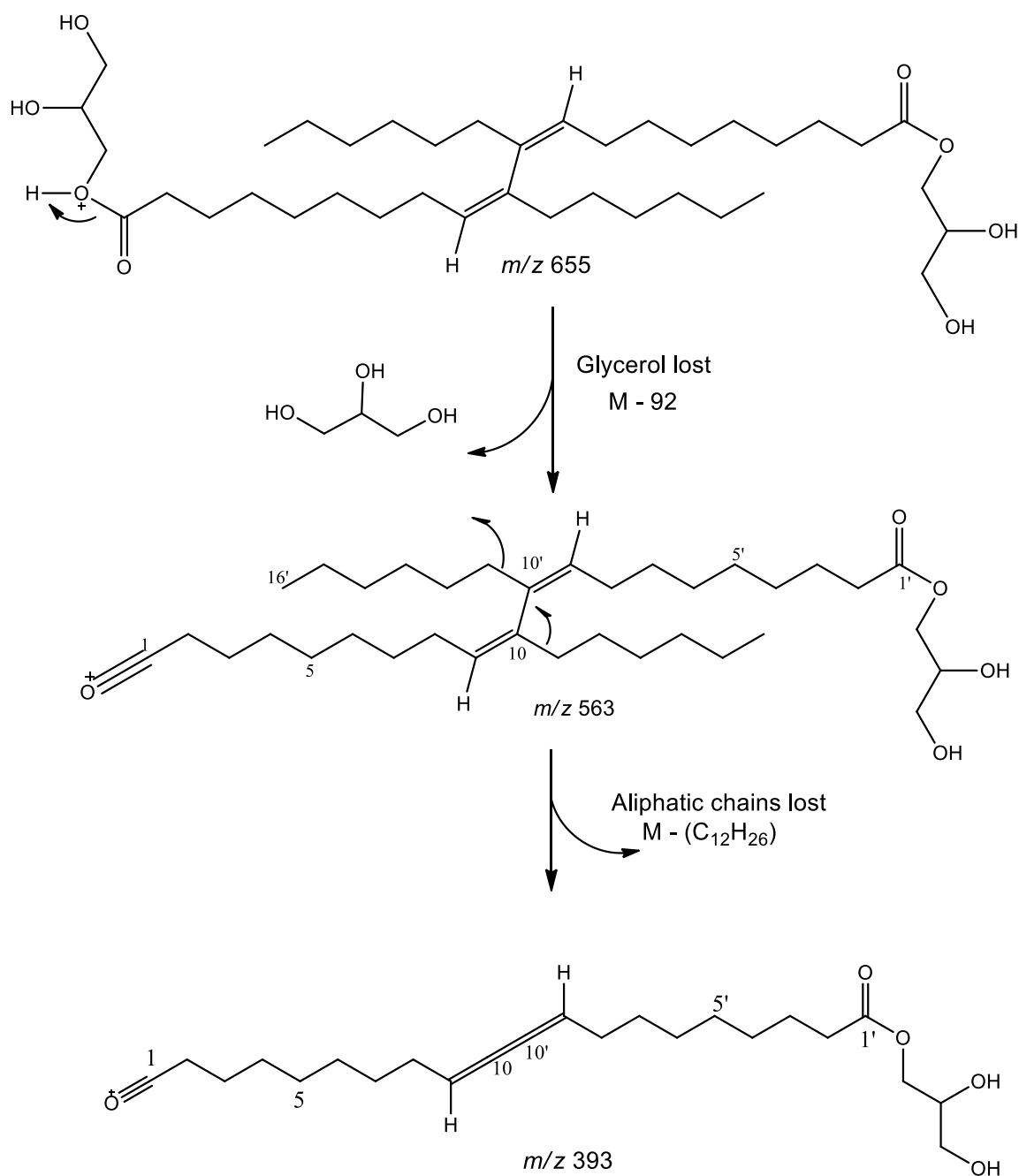


Figura 5.9 – Fragmentation propose for the isolated compound related from the black yeast *P. capiguarae*.

5.5 Outlook

Our results contributed with the symbiosis studies as potential complex networks of microbial interactions. Here, we showed the *in vitro* bioactivity of the black yeast *P. capiguarae* against the actinobacteria *Pseudonocardia* sp., both isolated from the ants turguments. Our study has searched for interactions within the fungus growing ant and

microbe symbiosis and reveals for the first time a chemical compound produced by black yeast symbionts *P. capiguarae* and how it affects the mutualism relation among ants-actinobacteria-black yeast inside of the gardens. The following steps of this work will be the complete compound elucidation and further studies in the leaf-cutting ants garden such the *in vivo* bioassays. These experiments will collaborate with the understanding about the chemical function of black yeasts metabolites and their function in the nests.

5.6 Referências

- [1] Mehdiabadi NJ, Schultz T. Natural history and phylogeny of the fungus-farming ants (Hymenoptera: Formicidae: Myrmicinae: Attini). *Myrmecological News*. 2010;13:37–55.
- [2] Currie C, Mueller U, Malloch D. The agricultural pathology of ant fungus gardens. *Proceedings of the National Academy of Sciences*. 1999;96:7998–8002.
- [3] Dhodary B, Schilg M, Wirth R, Spiteller D. Secondary metabolites from *Escovopsis weberi* and their role in attacking the garden fungus of leaf-cutting ants. *Chemistry: A European Journal*. 2018;24:4445–4452.
- [4] Currie CR, Scottt JA, Summerbell RC, Malloch D. Fungus-growing ants use antibiotic-producing bacteria to control garden parasites. *Nature*. 1999;398(6729):701–704.
- [5] Chevrette M, Carlson C, Ortega H, Thomas C, Ananiev G, Barns K, et al. The antimicrobial potential of *Streptomyces* from insect microbiomes. *Nature Communications*. 2019 01;10.
- [6] Haeder S, Wirth R, Herz H, , Spiteller D. Candicidin-producing *Streptomyces* support leaf-cutting ants to protect their fungus garden against the pathogenic fungus *Escovopsis*. *Proceedings of the National Academy of Sciences*. 2009;106(12):4742–4746.
- [7] Rodrigues A, Pagnocca CF, Bueno OC, Bueno, Pfenning LH, Bacci M. Assessment of microfungi in fungus gardens free of the leaf-cutting ant *Atta sexdens rubropilosa* (Hymenoptera: Formicidae). *Sociobiology*. 2005;46:329–334.

- [8] Attili-Angelis D, Duarte A, Pagnocca F, Nagamoto N, Vries M, Stielow B, et al. Novel *Phialophora* species from leaf-cutting ants (tribe Attini). *Fungal Diversity*. 2014;65:65–75.
- [9] Heine D, Holmes NA, Worsley SF, Santos ACA, Innocent TM, Scherlach K, et al. Chemical warfare between leafcutter ant symbionts and a co-evolved pathogen. *Nature Communications*. 2018;9:2208.
- [10] Little A, Currie CR. Symbiotic complexity: discovery of a fifth symbiont in the Atinne ant-microbe symbiosis. *Biology Letters*. 2007;3:501–504.
- [11] Teixeira M, Moreno L, Stielow B, Muszewska A, Hainaut M, Gonzaga L, et al. Exploring the genomic diversity of black yeasts and relatives (Chaetothyriales, Ascomycota). *Studies in Mycology*. 2017 01;86:1–28.
- [12] Little A, Currie C. Black yeast symbionts compromise the efficiency of antibiotic defenses in fungus-growing ants. *Ecology*. 2008;89:1216–1222.
- [13] Hofer U. The cost of antimicrobial resistance. *Nature Reviews Microbiology*. 2019;17.
- [14] Gu J, Xu J, Su Q, Chen Y. *Exophiala dermatitis* and exacerbation of chronic obstructive pulmonary disease. *QJM: An International Journal of Medicine*. 2019;112(11):869–871.
- [15] Ulson CM. Contribuição para o estudo das chamadas leveduras pretas. Teses Universidade de São Paulo. 1959;(167p).
- [16] Wei H, Lin Z, Li D, Gu Q, Zhu T. [OSMAC (one strain many compounds) approach in the research of microbial metabolites—a review]. *Acta microbiologica Sinica*. 2010;50(6).
- [17] Angolini CFF, Vendramini PH, Araujo FDS, Araujo WL, Augusti R, Eberlin MN, et al. Direct protocol for ambient mass spectrometry imaging on agar culture. *Analytical Chemistry*. 2015;87:6925–6930.
- [18] Blin K, Shaw S, Steinke K, Villebro R, Ziemert N, Lee SY, et al. antiSMASH 5.0: updates to the secondary metabolite genome mining pipeline. *Nucleic Acids Research*. 2019;47(W1):W81–W87.

- [19] Barretto D, Kumar S. Biological activities of melanin pigment extracted from *Bombyx mori* gut associated yeast *Cryptococcus rajasthanensis* KY627764. *World Journal of Microbiology and Biotechnology*. 2020;36:1–8.
- [20] Russell B. Clavarinic Acid and Steroidal Analogues as Ras- and FPP-Directed Inhibitors of Human Farnesyl-Protein Transferase. *Journal Medical Chemistry*. 1998;41, 23:4492–4501.
- [21] Bell AA, Wheeler MH. Biosynthesis and function of fungal melanin. *Annual Review Phytopathology*. 1986;24:411–451.
- [22] Brakhage AA, Langfelder K, Wanner G, Schmidt A, Jahn B. Pigment biosynthesis and virulence. *Contribution to Microbiology*. 1999;2:205–215.
- [23] Solano F. Melanins: Skin Pigments and Much More Types, Structural Models, Biological Functions, and Formation Routes. *New Journal of Science*. 2014;2014:1–28.
- [24] Bod H, Bethe B, Hofs R, Zeeck A. Big effects from small changes: possible ways to explore nature's chemical diversity. *Chembiochemistry*. 2002;3:619–627.
- [25] Li HT, Zhou H, Duan RT, Li HY, Tang LH, Yang XQ, et al. Inducing secondary metabolite production by co-culture of the endophytic fungus *Phoma* sp. and the symbiotic fungus *Armillaria* sp. *Journal of Natural Products*. 2019;82(4):1009–1013.

6 Considerações e Perspectivas

Os estudos relacionados à simbiose de leveduras e fungos negros das formigas cortadeiras são ainda escassos e sua relação química e ecológica ainda é desconhecida. Desde sua descoberta, a relação dos fungos negros com as formigas da tribo Attini despertou a curiosidade de pesquisadores de diversas áreas a fim de compreender como a comunicação dessa microbiota acontece.

O ninho das formigas cortadeiras abriga uma diversidade de microrganismos, além do fungo mutualista e de parasitas, encontram-se ainda nas cutículas dos insetos as actinobactérias e leveduras negras. Diferentes interações de cocultivos entre esses microrganismos puderam ser investigadas a partir de análises de LC-MS. A combinação das análises multivariadas, com os mapas moleculares e imageamento por espectrometria de massas mostraram uma variedade e indução metabólica nos cocultivos, facilitando a organização, visualização dos dados e anotações de metabólitos produzidos nas interações.

Os estudos prévios e as abordagens de análises utilizadas evidenciaram como promissor o cocultivo entre fungo negro *P. capiguarae* e do parasita *Escovopsis*. Nós utilizamos estudos metabolômicos do cocultivo para evidenciar a indução de metabólitos e relacionar com atividade antimicrobiana contra a actinobactéria *Pseudonocardia*.

A inibição do crescimento de actinobactérias pelos fungos negros foi apresentada em trabalhos anteriores, porém pouco explorada. Nesse trabalho, nós buscamos entender o potencial metabólico da levedura negra através de isolamento guiado por atividade biológica de modo a entender a relação entre substâncias químicas produzidas em um perspectiva ecológica.

Ensaio biológicos frente a outros simbioses precisam ser melhor investigados para confirmar a função ecológica dos metabólitos dos fungos negros nos ninhos das formigas. A ampliação do estudo em larga escala está sendo realizado para isolamento e revalidação dos experimentos realizados.

A relação dos fungos negros com os diferentes microrganismos simbioses das formigas da tribo Attini é um tema promissor a ser explorado, tanto para uma abordagem biológica e descritiva de novas espécies, ou para a ecologia química, em busca de entender como a comunicação química entre as leveduras negras e os demais simbioses ocorrem dentro dos ninhos das formigas, principalmente relacionado à função e atividade desses metabólitos.

Anexos

ANEXO A – Processamento de dados de LC-MS

A sequência de atividades listadas a seguir foi utilizada para a execução do trabalho e estão relacionados às análises e processamento de dados de LC-MS do capítulo 3 e 4. Essa sessão foi planejada como forma de facilitar a aquisição, processamento e análise de dados obtidos por LC-MS/MS em projetos relacionados a estudos de metabolômica, utilizando softwares e sites gratuitos e livres.

Esse tutorial foi organizado com o intuito de ajudar estudantes de graduação e pós-graduação que desejam realizar estudos comparativos de dados de LC-MS. O tutorial é escrito em uma linguagem bastante básica para facilitar a compreensão dos usuários. O planejamento do experimento é essencial para iniciar qualquer estudo. Antes de começar, enumere qual a pergunta que pode ser respondida com esse experimento e, somente depois dê continuidade aos experimentos.

Antes de começar a parte prática, um planejamento experimental (design of experiments, DoE) é uma importante etapa a ser realizada. Nesse caso, a fase de projeto experimental inclui a consideração de características e variáveis relevantes ao trabalho. Escolher a melhor metodologia de preparo de amostra, que inclui solvente, tempos e tipos de extração, são passos importantes para a montagem do experimento e para a otimização do trabalho, permitindo que comparações mais significativas entre os estudos possam ser feitas, além de evitar futuros problemas que possam vir a ocorrer durante a análise dos dados, como variações na repetibilidade das amostras.

A.1 Instalação de softwares e aberturas de contas

Antes de começar a aquisição dos dados é importante ter esses softwares salvos no computador e também se familiarizar com eles. Nos links, há tutoriais e artigos mostrando as infinitas possibilidades de aplicação dessas plataformas nas pesquisas. Os principais estão listados a seguir e exemplificados na Figura A.1:

- Criar a conta na plataforma do GNPS.
- Fazer o download do MS Convert do Proteowizard website: esse software é usado para converter os dados da Bruker e Thermo. Alguns outros equipamentos pedem

outros softwares de conversão. O site do GNPS oferece algumas informações a respeito.

- Baixar Filezila ou qualquer programa de FTP-VPN: usamos esse FTP para facilitar o carregamento dos dados do computador para a plataforma. É possível fazer manualmente, mas eu recomendo o FileZilla se houver grande número de amostras. Para o acesso à plataforma é necessário colocar o Host: **ccms-ftp01.ucsd.edu** e o usuário e senha utilizados no site do GNPS.
- Para analisar cada networking, você pode usar a plataforma online para uma visão em detalhes das famílias espectrais e no Cytoscape para edição visual do networking, como cores e tamanho dos nodos.
- Para as análises de processamento dos dados de LC-MS, utiliza-se o software MZmine que apresenta ampla aplicação e é de acesso livre. Nesse programa, etapas relacionadas ao pré-processamento dos dados serão feitas de acordo com os dados da amostra em análise.
- Para a aquisição das análises estatísticas (PCA, HCA, PLS-DA, Heat Map, etc), a plataforma Metaboanalyst pode ser utilizada. A organização dos dados e a análise dos resultados serão exemplificados nesse tutorial.

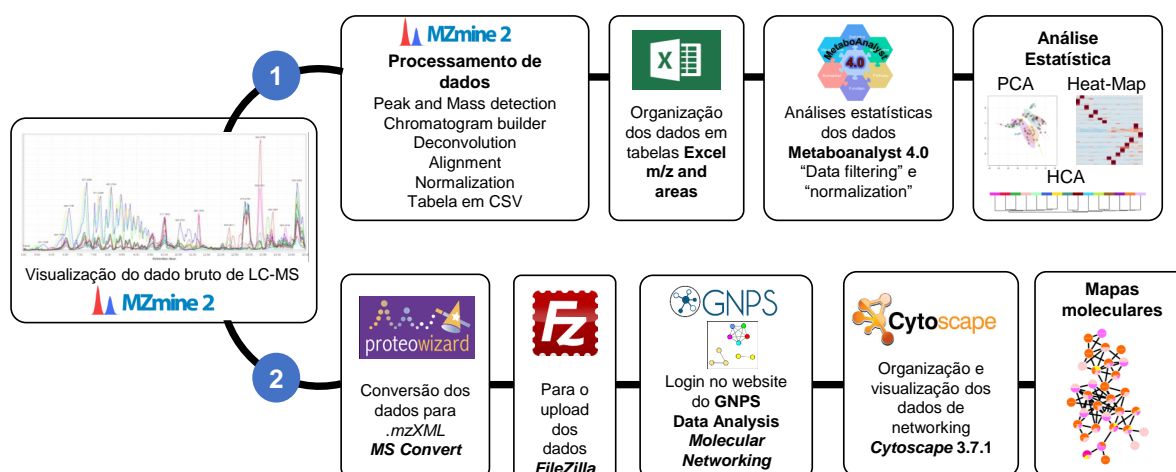


Figura A.1 – Workflow detalhado das etapas utilizadas no processamento dos dados na plataforma do GNPS para a construção dos mapas moleculares.

A.2 Preparo básico de amostra para LC-MS

As amostras para serem analisadas em LC-MS de alta resolução devem estar em baixa concentração (1 ou 2 mg · mL⁻¹). As amostras não podem conter precipitado na solução. Sempre verifique se as mesmas se apresentam completamente límpidas. Deve-se utilizar solventes compatíveis com o sistema cromatográfico. Como utilizamos fase reversa, pode-se usar metanol, acetonitrila ou água, acidificados ou não. Para garantir que não há precipitados, recomenda-se o uso de filtros de seringa ou algodão. Em caso de amostras mais complexas, recomenda-se uma pré-purificação por extração em fase sólida (SPE).

A.3 Aquisição de dados de LC-MS/MS

Os dados a serem adquiridos precisam ser otimizados em relação aos dados cromatográficos para adquirir uma boa resolução entre os picos. O método cromatográfico deve ser o mesmo entre todas as amostras a serem adquiridas, caso deseje comparar essas amostras entre elas. Pode-se comparar corridas adquiridas em modo positivo e em modo negativo de ionização, por exemplo. O método cromatográfico (composição da fase móvel, pH da fase móvel, fluxo de solvente, coluna utilizada, etc) escolhido depende da matriz estudada e da pergunta do trabalho. A separação cromatográfica é importante para a visualização dos dados, porém a fragmentação ajudará em casos em que não há boa separação cromatográfica. Especificamente para análises de cromatografia líquida a adição de ácidos e bases na fase móvel podem auxiliar na resolução dos picos cromatográficos, e também na ionização e, portanto, formação dos íons. No modo positivo de ionização, recomenda-se o uso de ácidos voláteis e, em modo negativo, uma base.

O método de aquisição do espectrômetro podem ser adquiridos em dois modos a) Aquisição Dependente de Dados (Data dependent acquisition, DDA), amplamente utilizado para metabolômica; ou b) Aquisição Independente de Dados (Data independent acquisition, DIA) bastante usando em proteômica. O modo DDA permite que um número determinado de picos seja selecionado em um espectro de varredura (full scan), usando regras determinadas (dependentes) nos parâmetros do equipamento, para um experimento de fragmentação, selecionando os sinais mais intensos no MS1, por exemplo, e realizando a fragmentação desses sinais. A configuração para esse tipo de aquisição depende de cada equipamento, mas ele é possível em qualquer espectrômetro de massas sequencial, ou seja, que realiza MS/MS.

A.4 Organização dos dados para análises

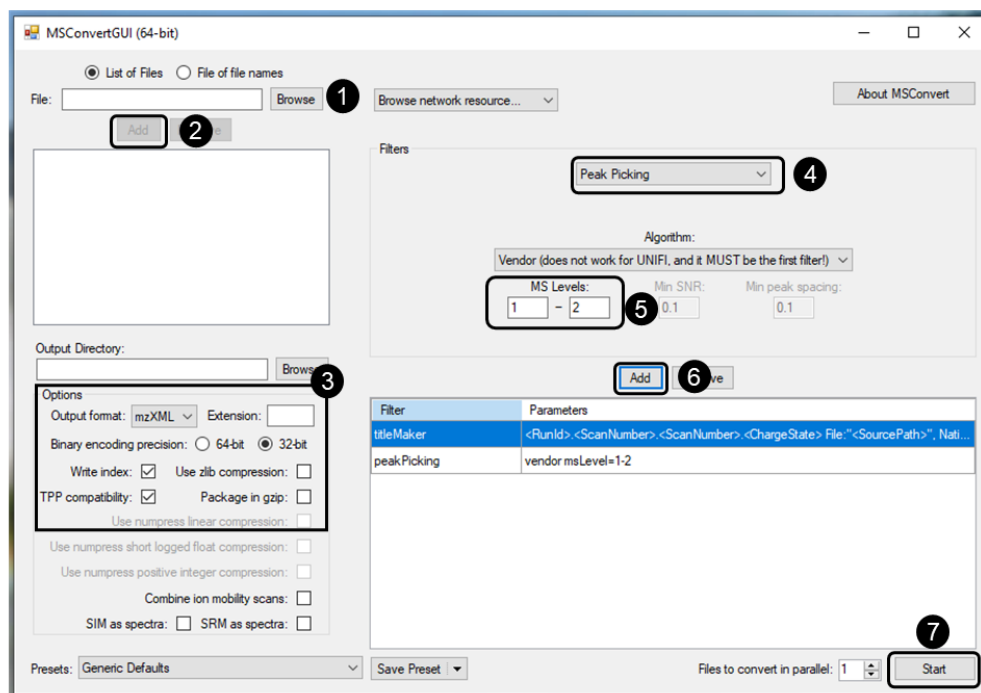
Para as demais etapas, a organização dos dados em tabelas é imprescindível. A maneira como irá interpretar os dados cabe somente ao pesquisador. Nessa etapa é importante saber separar as amostras em grupos de comparação, por exemplo. Não existe a necessidade de se realizar uma única análise de dados. Os dados podem ser organizados em partes para facilitar a interpretação dos resultados em grupos.

Por exemplo: Realizou-se diferentes tipos extrações de diferentes plantas e deseja verificar qual o extrato que mais diferenciou entre os demais: 1. Pode realizar uma análise de dados de todos os extratos de diferentes plantas, mas é importante ter consciência da complexidade desses dados no final; ou 2. Pode realizar a análise individual por espécie de plantas, no qual obterá vários grupos de resultados que poderão ser discutidos por partes. Organize tabelas, figuras, infográficos dessa parte e apresente aos colegas.

- Metadados ou *Metadata* - Organização dos dados A tabela de metadados (metadata, em inglês) é importante para a organização e descrição detalhadas dos dados que serão analisados. A tabela apresenta, além do nome do arquivo a ser processado, também informações extras como o nome da espécie de planta ou microrganismo, local de coleta, metodologia de extração, aquisição de dados, etc. A construção da tabela ajuda a compreender melhor os dados analisados e também contribui para o GNPS, colaborando com os dados e informações para a plataforma.

A.5 Convertendo os dados para mzXML ou mzML

Cada equipamento oferece um *output* em formato estabelecido pela empresa. Por exemplo, os dados da Agilent e Bucker tem a extensão .d, os dados da Waters e Thermo .raw. Essas extensões de arquivos estão de acordo com a compatibilidade que o software de cada companhia apresenta. Muitos dados não são compatíveis entre si e precisamos de softwares específicos para abrir o dado original. Para evitar quaisquer transtornos com licenças de programas, tende-se a utilizar softwares de leitura abertos. Nesse tutorial, será utilizado o MZMine para processar os dados adquiridos por LC-MS. Nesse software os arquivos precisam estar na extensão .mzXML ou .mzML e, portanto, precisam ser convertidos. O MSConvert é amplamente utilizado para a conversão desses dados. Os detalhes da conversão estão na Figura A.2.



- 1 **Browse:** Para buscar os arquivos originais em seu computador
- 2 **"Add":** Adicione arquivos originais para conversão
- 3 Escolha a extensão **mzXML**. Selecione **32 bit** e desmarque "use zlib compression"
- 4 Escolha a opção **"Peak peaking"**, para que a conversão seja no modo centróide
- 5 Os dados de LC-MS/MS serão utilizados **MS level 1-2**
- 6 **"Add"** = Adicione o modelo de conversão configurado
- 7 **"Start"** = Inicie a conversão

Figura A.2 – Workflow detalhado para conversão dos dados utilizando o MSConvert, de qualquer formato para *.mzXML*.

A.6 Processamento dos dados de LC-MS utilizando o MZMine

Para a realização dessa etapa, recomenda-se usar o software gratuito **MZmine**, para esse tutorial foi utilizado a versão 2.38. O workflow detalhado abaixo mostra como processar os dados de LC-MS. Após fazer o download do software, selecione o sistema operacional do seu computador (Windows, MAC ou Linux). Os detalhes ilustrados de cada etapa estão exemplificados na Figura A.3.

- 1. Importar os dados brutos para o MZMine

Nessa parte é importante selecionar os arquivos no formato *.mzXML* ou *.mzML* e os dados precisam ter um nome simples (sem acentos gráficos ou muitos números). Para as análises estatísticas é importante e recomendado que se tenha réplicas reais das amostras. Réplicas reais significam realizar réplicas do mesmo procedimento várias vezes e analisar os dados nas mesmas condições no LC-MS.

Raw data methods > Raw data import

Obs.: Nessa parte é importante selecionar os arquivos no formato .mzXML ou .mzML e os dados precisam ter um nome simples (sem acentos gráficos).

- 2. Organização da lista de massas (íons detectados) para cada *scan number* usando o *Mass Detector*

MS level 1 é usado para análises estatísticas (que serão abordadas no próximo tema do tutorial) e MS level 2 é utilizado para a criação de redes moleculares na plataforma do GNPS, como é o caso do Feature Based Molecular Networking (FBMN) que não será abordado neste tutorial. Mas em caso de MS 2, os dois devem ser realizados.

Peak detection > Mass detection

MS level 1 or MS level 2

Obs.: Para análises estatísticas usa-se MS level 1 e para o GNPS (FBMN) usa-se MS level 2.

Mass range: 50-1500

Obs.: Depende qual a faixa de massas você deseja observar ou em qual faixa foi adquirido os dados.

Scan number: Não precisa alterar esse parâmetro

Set filters: 2-30 min

Obs.: Geralmente exclui-se o volume morto da coluna e a parte de limpeza. Mas é necessário verificar manualmente os dados para que tenha certeza de que não se excluiu nada.

Mass detector: Centroid and Noise level: 1.0E3

Obs.: Verifique os dados originais para saber qual o nível de ruído das amostras. Clique em visualizar os dados para que tenha certeza dos sinais que estão sendo selecionados mais a etapa seguinte. Apenas os sinais em vermelho serão selecionados.

- 3. Detecção dos cromatogramas usando *Chromatogram builder*

Essa etapa está relacionada com a forma de aquisição dos dados espectrais no LC-MS. Selecione a lista de massas criada anteriormente chamada "MASSES" e verifique o "peak list" criado. O número de dados criados na sessão anterior é importante para verificar a qualidade dos parâmetros listados anteriormente. Se a lista de picos é

muito pequena, muito provavelmente o noise level” utilizado foi muito elevado, e vice-versa. Repita essa parte quantas vezes achar necessário antes de prosseguir. O peak list” formado mostrará a quantidade de bandas cromatográficas que foram detectadas.

Peak detection > Chromatogram builder

Min time span (min): 0.1

Min height: 6E3

m/z tolerance: 0.001 m/z or 0 ppm (apenas uma opção deve ser escolhida)

Essa etapa vai estar muito relacionada com a forma de aquisição dos dados espectrais. Selecione a lista de massas criada anteriormente chamada “MASSES” e verifique o “peak list” criado. O número de dados criados na sessão anterior é muito importante para verificar a qualidade dos parâmetros listados. Se a lista de picos é pequena, muito provavelmente o “noise level” utilizado foi muito elevado, e vice-versa. Repita essa parte quantas vezes achar necessário.

- 4. Deconvolução dos cromatogramas em picos individuais

Caso for ser realizado o FBMN, é necessário correlacionar os dados de MS1 e MS2. Para isso é preciso selecionar as caixas abaixo: m/z range for MS2 scan pairing (Da): A faixa de resolução de massa, para alta resolução recomenda-se 0.01 e para baixa resolução, pode ser 0.1 ou 1. RT range for MS2 scan pairing (min): Pode-se utilizar 0.1 para atribuir que sinais com essa diferença de tempo de retenção ainda são as mesmas substâncias, se tiverem o mesmo m/z .

Caso sejam realizadas apenas as análises estatísticas, não precisa selecionar essas duas caixas.

Peak list methods > Peak detection > Chromatogram deconvolution

Baseline cut-off

Minimum peak height= 2.1E3; Peak duration= 0.05 a 5.0; Baseline level= 2.0E3

Obs.: Verifique os picos coloridos que foram deconvoluídos. Essa etapa é importante para “separar” os picos de acordo com o tempo de retenção.

- 5. Remoção dos isótopos

Peak list methods > Isotopes > Isotopic peaks grouper

m/z tolerance: 0.001 m/z or 0 ppm (apenas uma opção deve ser escolhida)

Retention time tolerance: 0.1 min

Maximum charge: 2

Representative isotope: Most intense

Após essa etapa, recomenda-se verificar os dados individualmente, se os sinais estão separados. Para isso, basta clicar na amostra que deseja verificar. Uma nova aba mostrará as informações de m/z , tempo de retenção (RT), formato do pico (peak shape), além de informações como o “status”, onde verde significa a presença do íon, vermelho a ausência e amarelo, uma possível presença ou detecção; a altura do pico (height) e a área (area). Nessa etapa também pode-se buscar os íons de interesse, caso a análise realizada seja target. Essa verificação confere a possibilidade de retornar alguma etapa, caso esse íon de interesse tenha sido perdido em algum filtro utilizado.

- 6. Ordenar a lista de picos

Peak list export > order peaks lists

- 7. Alinhamento usando “Join aligne”

Peak list methods > Alignment > Join aligner and m/z tolerance: 0.001 m/z or 0 ppm

Obs.: Nessa etapa é preciso manter os mesmos parâmetros usados anteriormente.

Weight for m/z : 75

Obs.: O peso utilizado para m/z e para RT dependem do equipamento utilizado. Se for um equipamento de alta resolução, recomenda-se que se use 75% para m/z e 25% para o tempo de retenção, mas pode variar conforme a procedência dos dados.

Retention time tolerance: 0.1 min

Weight for RT: 25

- 8. Verifique manualmente a qualidade dos dados

Verifique manualmente a qualidade e quantidade de dados gerados na tabela : A tabela apresenta todas as informações necessárias para a validação da m/z , tempo de retenção, o pico característico e as amostras que apresentam aquela variável. Nessa etapa é importante fazer uma filtragem detalhada dos dados antes de seguir com a análise estatística, como por exemplo excluir os sinais do branco do solvente que aparentemente não é sinal cromatográfico e sim impurezas do solvente ou con-

taminação. Salve seu projeto para que possa retornar a ele, e a todas informações geradas pelo processamento, quando for necessário.

- 9. Exportar os dados: nessa etapa seleciona a m/z , o ID e a área de cada pico.
Peak list export > Export to CSV file → para análises estatísticas no Metaboanalyst;
ou
Feature list export > Export to Metaboanalyst

Peak list export > Export to GNPS-FBMN > mgf file and csv file → para a plataforma do GNPS.

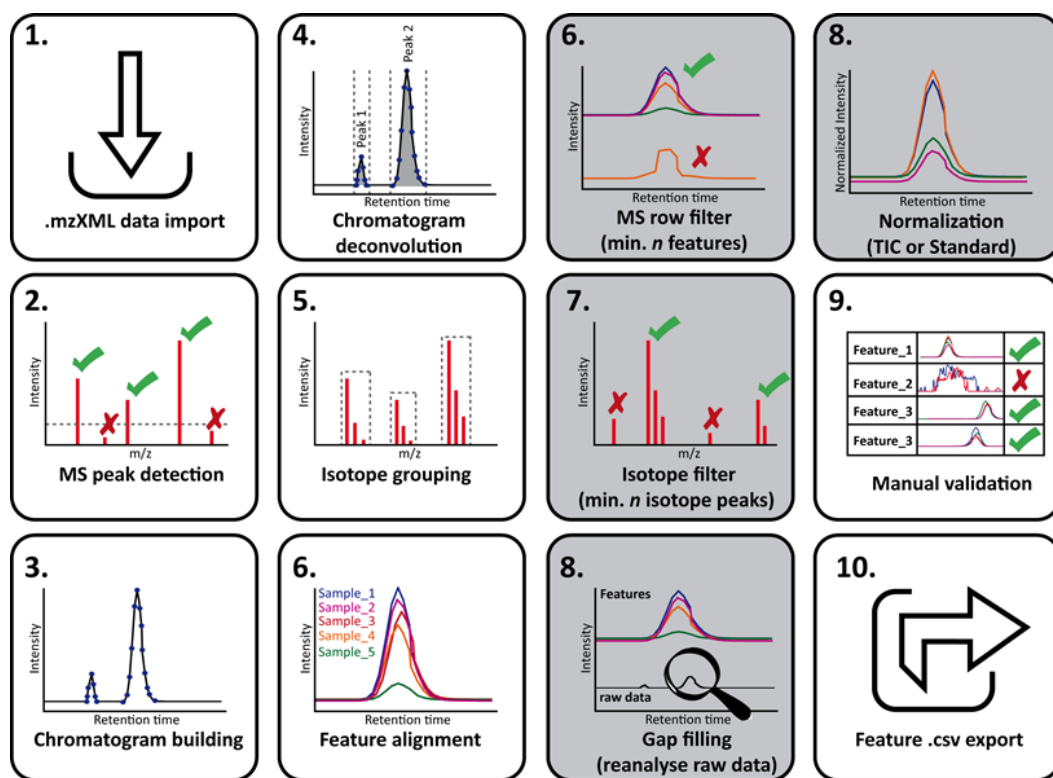


Figura A.3 – Workflow detalhado das etapas utilizadas no processamento dos dados no MZMine. Baseado em [1].

A.7 Organização dos dados para análises estatísticas no *Metaboanalyst*

Após a exportação dos dados em formato .csv, os dados precisam estar organizados em uma maneira válida para o processamento no Metaboanalyst.

- Montagem da planilha
 - O arquivo do Excel deve ser salvo com a extensão .csv - para que a separação dos decimais seja feita com vírgula;
 - Nos valores das variáveis (primeira coluna ou primeira linha) foi também usado vírgula, contudo suas células foram formatadas para estarem como “Texto”;
 - As variáveis, sejam elas as m/z ou o deslocamento químico (ppm) não podem repetir entre si, por isso recomenda-se o uso de uma sequência numérica que relacione com os valores das variáveis;
 - O nome das amostras deve conter somente letra e número (não pode ter símbolos, acentuação e ce-cedilha, parênteses, hífen, ou sinais);
 - O código de classificação dos grupos deve ir na segunda linha (se as amostras estiverem dispostas nas colunas) ou na segunda coluna (se as amostras estiverem dispostas nas linhas);
 - O arquivo deve ter menos de 50 Megabytes;
 - Valores de intensidade com Exponencial (Ex: 1.64E+6) são aceitos para análise.

- No site do *Metaboanalyst*

No site do Metaboanalyst, deve-se escolher a opção de “Statistical analysis”, selecionar a planilha do excel no formato adequado e selecionar a forma de organização da mesma: se as amostras estão em linhas ou colunas. Nessa etapa é importante que os dados estejam em replicatas, indicadas pelos números das réplicas (1, 2, 3, etc) e na linha abaixo o nome do grupo das amostras. Por exemplo, se você nomeou os dados em replicatas da “amostra” como “amostra 1”, “amostra 2” e “amostra 3”, na mesma linha abaixo desses nomes (enumerados de 1 a 3) deve ser indicado apenas por “Amostra”. “Amostra” é o nome dado ao grupo das réplicas. Nessa planilha também não pode haver repetições das variáveis, por isso, recomenda-se que use os IDs das m/z e busque os valores das razões m/z no projeto do MZMine ou no arquivo original do Excel. Todo o procedimento está organizado na Figura A.4. As etapas estão descritas abaixo [2].

- 1. Clique em começar.

MetaboAnalyst - statistical, functional and integrative analysis of metabolomics data

Welcome >> [click here to start cc](#)

1.

2.

3.

	Amostra1	Amostra2	Amostra3
	Amostra	Amostra	Amostra
1	Área do pico	Área do pico	Área do pico
2	Área do pico	Área do pico	Área do pico
3	Área do pico	Área do pico	Área do pico

4.

1) Upload your data

A plain text file (.txt or .csv):

Data Type: Concentrations Spectral bins Peak intensity table

Format: Samples in columns (unpaired) Samples in rows (paired)

Data File: Nenhum arquivo selecionado

5.

6.

7.

8. Resultado das análises

Univariate Analysis
 Fold Change Analysis T-tests Volcano plot
[One-way Analysis of Variance \(ANOVA\)](#)
[Correlation Analysis](#) [Pattern Searching](#)

Chemometrics Analysis
[Principal Component Analysis \(PCA\)](#)
[Partial Least Squares - Discriminant Analysis \(PLS-DA\)](#)
[Sparse Partial Least Squares - Discriminant Analysis \(sPLS-DA\)](#)
 Orthogonal Partial Least Squares - Discriminant Analysis (orthoPLS-DA)

Feature Identification
[Significance Analysis of Microarray \(and Metabolites\) \(SAM\)](#)
 Empirical Bayesian Analysis of Microarray (and Metabolites) (EBAM)

Cluster Analysis
 Hierarchical Clustering: [Dendrogram](#) [Heatmap](#)
 Partitional Clustering: [k-means](#) [Self-Organizing Map \(SOM\)](#)

Classification & Feature Selection
[Random Forest](#)
 Support Vector Machine (SVM)

1. Clique aqui para começar
 2. Análises estatísticas
 3. Organize sua tabela no **Excel** com as réplicas na primeira linha
 4. Faça o upload do arquivo
 5. Selecione o formato: se as amostras estão em linhas ou colunas
 6. Filtro de dados se tem mais de 5 mil variáveis
 7. A normalização/escalamento do dado: Auto-scaling ou Pareto

Figura A.4 – Workflow detalhado das etapas utilizadas no processamento dos dados no site do *Metaboanalyst*.

- 2. Diferentes opções de análise podem ser realizadas dentro do Metaboanalyst. Escolha a opção “Statistical analysis” .
- 3. As planilhas no Excel precisam estar organizadas da forma exemplificada em A.7. No mínimo três réplicas são necessárias para a efetiva análise dos dados. Além disso, na segunda linha deve estar o nome dos grupos das amostras. Sem essa informação ocorrerá um erro na leitura dos dados.
- 4. Faça o upload do arquivo do seu computador para a plataforma no formato *.csv*.
- 5. Selecione a forma de organização da planilha: se as amostras estão em linhas ou em colunas. E utilize a forma de análise em “Concentrations”.
- 6. O filtro dos dados precisa ser realizado apenas se houver mais de 5 mil variáveis, o que não é o caso dos dados de LC-MS.
- 7. A normalização dos dados depende de como foi feita a aquisição, se são pontos de um cromatograma, por exemplo, “auto-scaling” é o método mais

- adequado, mas se são contínuos, é melhor escolher “mean-centering”.
- 8. Os resultados da análise serão listados e podem ser escolhidos de acordo com o que deseja comparar: PCA, PLS, HCA. Dentro de cada opção pode-se escolher os gráficos de “scores” ou amostras e “loadings” ou variáveis.
 - 9. Todas as análises escolhidas ao longo do processamento são salvas e podem ser baixadas na aba “Download”. As figuras e as tabelas referentes aos dados também são encontrados nessa aba.
- **Interpretação geral dos dados estatísticos** Para as análises estatísticas, os dados processados de LC-MS podem ser comparados entre si através de diferentes metodologias. Dentre eles pode-se destacar: (I) estudos de análises univariadas dos dados, através da construção da ANOVA, tabela de teste-T e mapa de correlação dos dados, (II) utilização de análise multivariada de dados com estudos de PCA (análise de componentes principais) ¹ e PLS-DA (análise discriminante por mínimos quadrados parciais)² que permitem verificar o grau de similaridade entre as amostras e saber quais as variáveis responsáveis por essa separação através dos gráficos biplots e, por último, (III) utilização de análises de agrupamento através de estudos de HCA (análise de agrupamento hierárquico)³ associados a mapas de calor (heat map)⁴, com a organização por grupos relacionando as amostras analisadas aos metabólitos associados.

A.8 Construção dos mapas moleculares na plataforma GNPS

Após a organização dos dados, é necessário saber quantos grupos serão analisados pelo Molecular Networking [3], se for mais de seis diferentes grupos, é necessário fazer a organização dos dados em uma lista do bloco de notas e adicionar o arquivo como “Group mapping”. O tutorial a seguir é válido apenas para até seis grupos de amostras (Fig. A.5).

- 1. Na página inicial, após a realização do *login*, escolha a opção Data Analysis > Create Molecular Network.
- 2. Escolha o nome do projeto e lembre-se de especificar o máximo possível para não confundir com outros “jobs”.
- 3. Adicione manualmente os arquivos por Grupos, de 1 - 6, ou;

1. **Create Molecular Network**

2. **Title:** _____

3. **Spectrum Files** (Required) Select Input Files

4. **Adicione nos grupos** (Ou 4. **Arquivos do meu computador**)

5. **Advanced Network Options** (Minimum Matched Fragment Ion: 4, Minimum Cluster Size: 2)

6. **Workflow Submission** (Email me at: alanake@gnps.gov)

7. **Visualização do Job** (Default Molecular Networking Results Views, Network Visualizations, Export/Download Network Files, Advanced Views - Metadata Views, Advanced Views - Global Public Dataset Matches, Advanced Views - External Visualization, Advanced Views - Networking Graphs/Histograms, Advanced Views - Misc Views, Advanced Views - Make Dataset Public, Advanced Views - Experimental Views, Advanced Views - qiime2 Views)

Figura A.5 – Workflow detalhado das etapas utilizadas no processamento dos dados na plataforma GNPS para a construção dos mapas moleculares.

- 4. Utilize algum software de FTP para fazer o upload dos arquivos do computador. Nesse trabalho, o software FileZila foi utilizado, porém muitos outros estão disponíveis de forma gratuita online.
- 5. Os parâmetros que são alterados estão relacionados principalmente à configuração do espectrômetro de massas: “Precursor ion mass tolerance” e “fragment ion mass tolerance”. Se os parâmetros não estiverem definidos no equipamento que você utilizou, as instruções de cada etapa são explicadas na própria plataforma.
- 6. Adicione o e-mail que será avisado quando as análises finalizarem e submeta o

projeto.

A visualização das análises pode ser explorada detalhadamente dentro da plataforma. Para ver as anotações das substâncias, escolha “View All Library Hits” e para ver as famílias espectrais e os networkings, escolha “View spectral Families”. Os detalhes dos parâmetros de análise são encontrados em “Workflow Written Description”. E para a edição do networking, baixe o arquivo utilizando “Direct Cytoscape Preview/Download”.

- **Anotação dos metabólitos:** A identificação das substâncias por MS/MS vem crescendo ao longo dos anos, porém o nível de confiança dessas identificações podem variar de acordo com diferentes estudos. Muitas comprovações exigem isolamento, síntese das substâncias, outros experimentos espectrais como ressonância magnética nuclear (RMN). Para padronizar as anotações dos metabólitos, algumas sugestões dos níveis de anotação existem na literatura e facilita essa busca. Diante das informações obtidas com as análises, diferentes níveis de anotação dos metabólitos utilizando MS/MS foram enumerados. O nível mais alto de anotação/identificação refere-se a confirmação dos metabólitos pela massa exata, pelos fragmentos e comparação ao padrão, verificando tempo de retenção. O nível 2 de anotação sugere a possível estrutura, baseada em bibliotecas de fragmentação disponíveis online. O nível 3 refere-se a tentativa de anotação ou anotação putativa, baseada na massa e nos fragmentos. O nível 4 permite a comprovação da fórmula molecular, com cálculo do erro baseado em massa teórica e experimental. O nível 5, e último, em que comprova apenas a m/z experimental, com baixo erro em Da ou ppm, não levantando nenhuma hipótese sobre o metabólito, mas indicando ser algo interessante a ser pesquisado ou isolado, por exemplo.

A.9 Organização dos mapas moleculares utilizando o Cytoscape

Após o download do arquivo para o Cytoscape no formato *.cys*, o networking completo pode ser editado nesse software. As cores e tamanhos dos nodos, as conexões entre os clusteres, as famílias espectrais, toda a disposição visual e as informações que se deseja visualizar podem ser editadas da maneira mais conveniente e adequada. Os dados e gráficos podem ser importados como imagem e como tabela na opção “Export”. Nessa

etapa é importante ter claro como se deseja verificar os dados e as comparações entre os dados.

A.10 Análise geral das informações obtidas

A conciliação de diferentes ferramentas utilizadas nesse tutorial pode facilitar estudos de comparação entre amostras de plantas, de microrganismos ou biológicas. A representação visual é mais didática e facilita a compreensão do leitor do texto. O processamento automático pelo MZMine possibilita uma rápida leitura de muitos espectros de MS/MS e podem ser comparados entre si utilizando o Metaboanalyst, através de análise multivariada dos dados. O molecular networking na plataforma GNPS possibilita a anotação de metabólitos automaticamente e contribui para focar os estudos em tópicos que são realmente importante. Essas ferramentas não substituem abordagens tradicionais de isolamento e identificação estrutural, mas podem evitar desperdício de tempo e de materiais com projetos que aparentemente podem não ser tão promissores. A definição das perguntas do projeto de pesquisa são muito importantes nessa fase: O que essas análises vão auxiliar no seu trabalho? Qual o objetivo do seu estudo e onde se deseja chegar com essa análise de dados? - Esses importantes questionamentos precisam ser levantados e discutidos para dar continuidade à pesquisa que se deseja realizar.

A.11 Referências

- [1] Nothias LF, Petras D, Schmid R, Duhrkop K, Rainer J, Sarvepalli A, et al. Feature-based molecular networking in the GNPS analysis environment. *Nature Methods*. 2020;17(9):905–908.
- [2] Pang Z, Chong J, Li S, Xia J. MetaboAnalystR 3.0: Toward an optimized workflow for Global Metabolomics. *Metabolites*. 2020;10(5):186.
- [3] Wang M, Carver J, Phelan V, Sanchez L, Garg N, Peng Y, et al. Sharing and community curation of mass spectrometry data with Global Natural Products Social Molecular Networking. *Nature Biotechnology*. 2016 05;34:828–837.

ANEXO B – Supplementary Information - Chapter 3

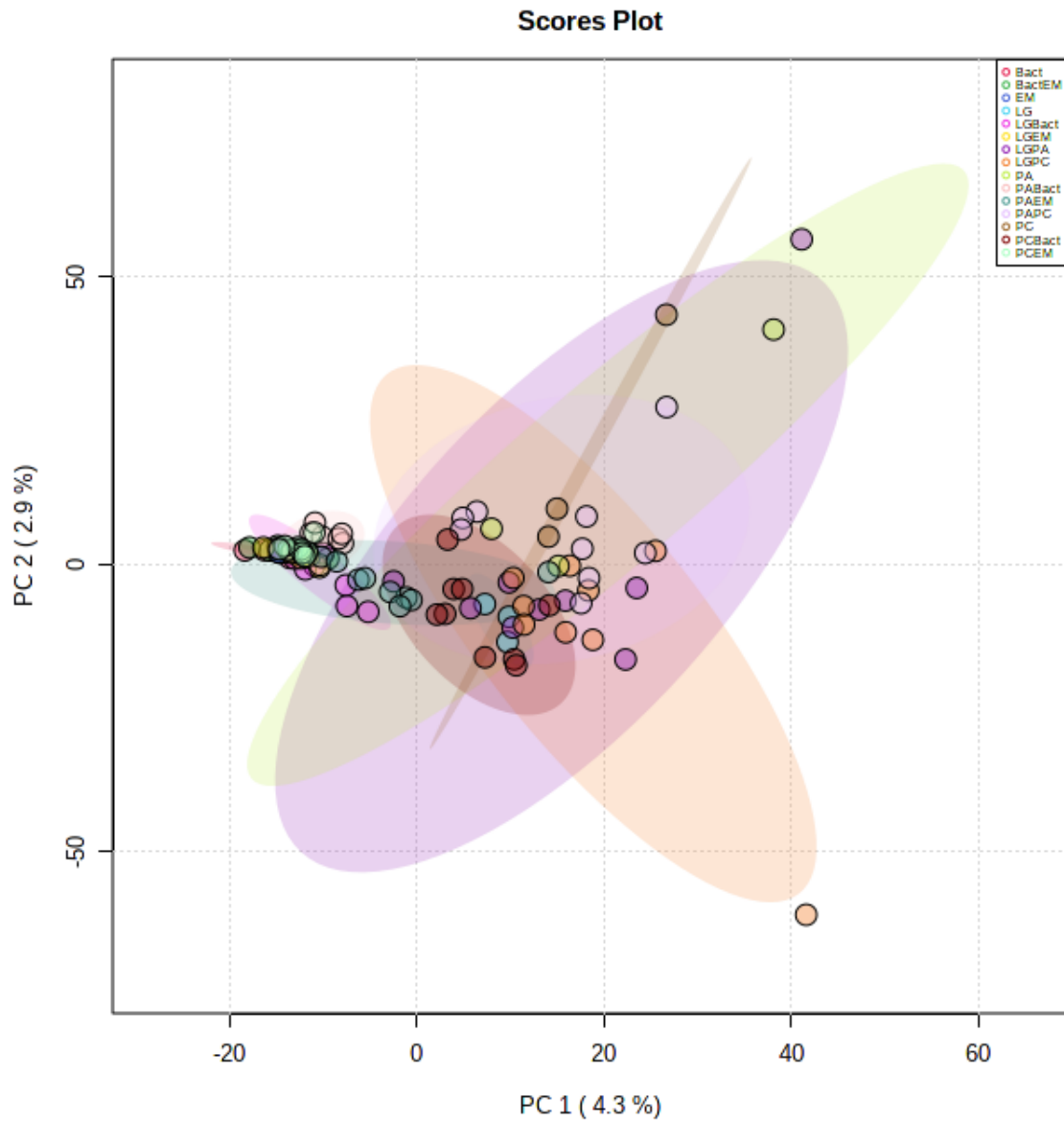


Figura B.1 – PCA analysis: Scores plot between the PC 1 (4.3%) and PC 2 (2.9%).

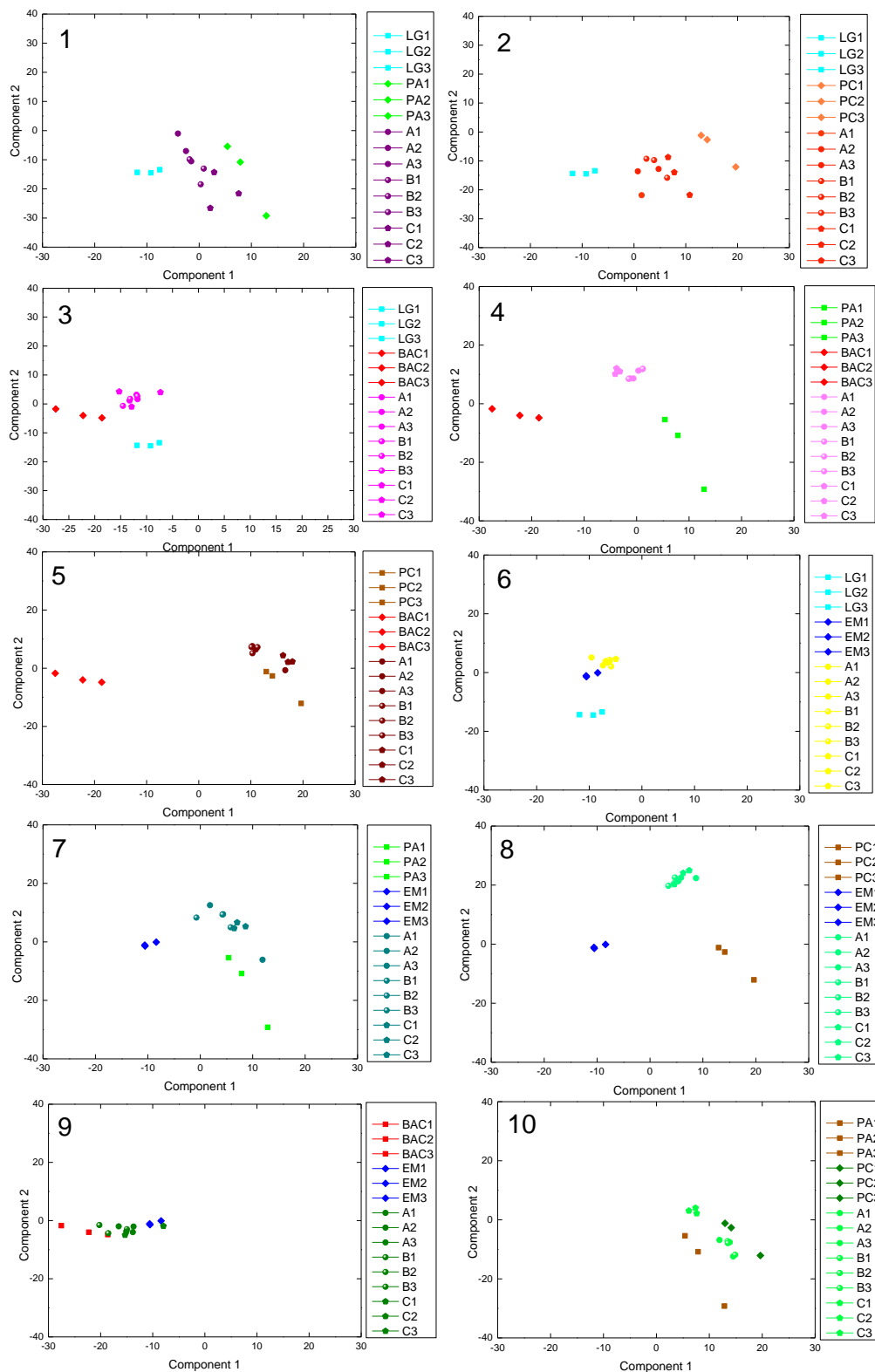


Figura B.2 – PLS-DA supervised analysis: Scores plot between the Component 1 (4.3%) and Component 2 (2.9%), with 7.2% of variance. (1) The mutualist (LG) and BY *P. attae* (PA), (2) the mutualist (LG) and black yeast (BY) *P. capiguarae* (PC), (3). the mutualist (LG) and the actinomycete (Bac), (4) the BY *P. attae* (PA) and actinomycete (Bac), (5) the BY *P. capiguarae* (PC) and actinomycete (Bac), (6) the mutualist (LG) and the parasite (EM), (7) the BY *P. attae* (PA) and the parasite (EM), (8) the BY *P. capiguarae* (PC) and the parasite (EM), (9) the actinomycete (Bac) and the parasite (EM) and (10) both BYs (PA and PC).

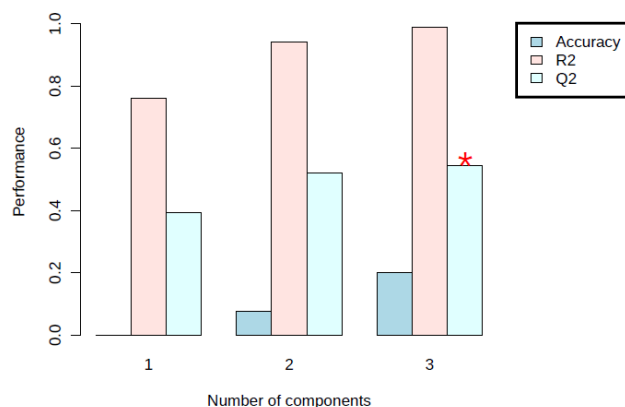


Figura B.3 – PLS-DA classification using different number of components. The red star indicates the best classifier in Component 3. In this validated model, R^2 is ~ 0.9 and $Q^2 \leq 0.5$.

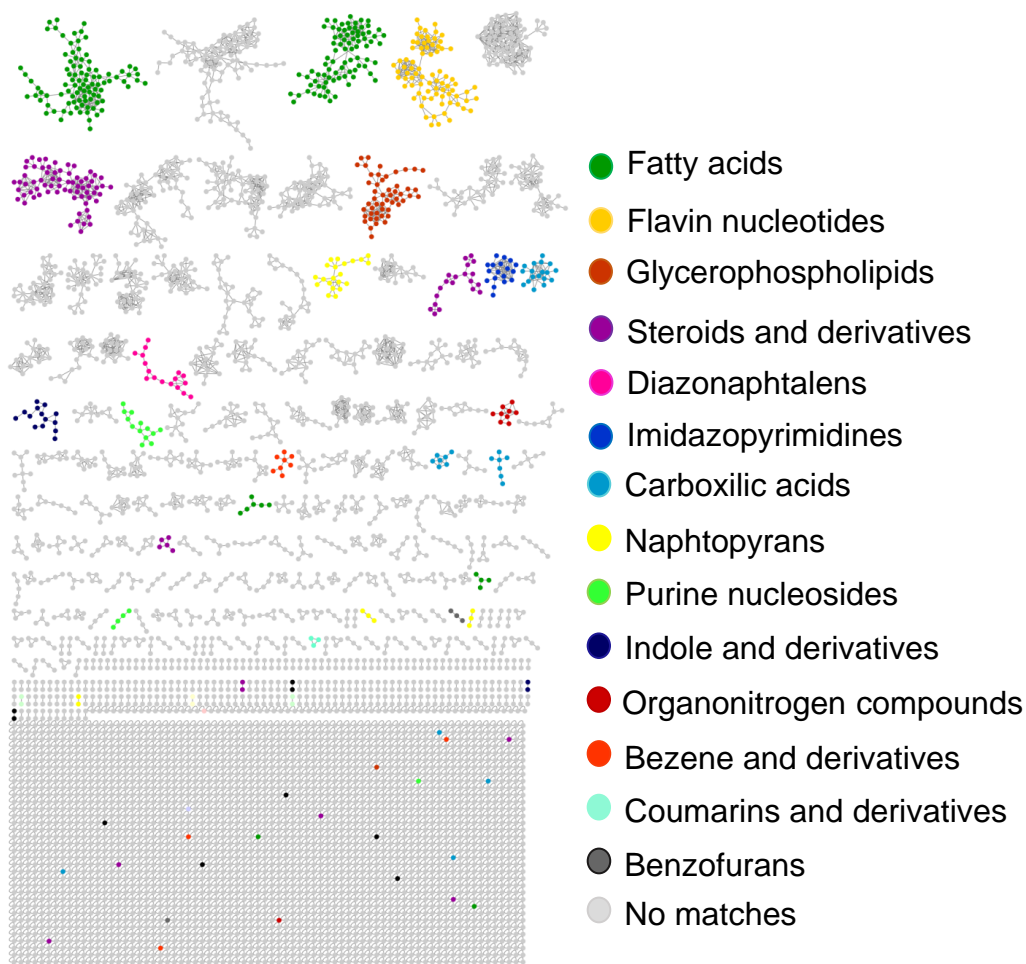


Figura B.4 – MolNetEnhancer used to identify the chemical structural information obtained for co-cultures and mono-cultures metabolites. Structural annotation for molecular families was suggested based on MS fragments using the *in silico* tool. The class of metabolites is highlighted and a complete metabolites class overview is summarized at this network.

Tabela B.1 – Main MS spectral matches of GNPS library (Continuation)

N	Compound	Instrument	Precursor ion	MQSScore	Class
1	1-Hexadecanoyl-glycerol	QqQ	683.543	0.95736	N/A
2	(6E)-heptadeca-6,16-diene-1,2,4-triol	qTof	591.462	0.956743	Fatty Acyls
3	Norharmane from NIST14	Q-TOF	169.075	0.945218	N/A
4	phenylethylamide 205	qTof	206.153	0.936005	N/A
5	4-methoxy-6-2-(4-methoxyphenyl)ethyl-pyran-2-one	qTof	543.199	0.933829	N/A
6	Tris(2-butoxyethyl) phosphate	QqQ	819.501	0.930594	N/A
7	N-acetyltyramine	ESI-QFT	180.102	0.930407	Phenols
8	ADENINE	Orbitrap	136.062	0.925523	Imidazopyrimidines
9	Umbelliferone	LC-ESI-QTOF	163.04	0.924826	Coumarins and derivatives
10	Indole-3-carboxyaldehyde	LC-Q-TOF/MS	146.061	0.924645	Indoles and derivatives
11	Inosine 5'-monophosphate	HCD	349.055	0.923998	N/A
12	Adenosine	QqQ	268.109	0.918336	N/A
14	"methyl pentanoate"	qTof	827.543	0.915944	Steroids and steroid derivatives
15	Leucine - chenodeoxycholic acid	qToF	1033.74	0.913426	Steroids and steroid derivatives
16	Dodecylbenzenesulfonic acid	QqQ	719.335	0.910908	N/A
17	Sorbitane Monopalmitate	qTof	402.36	0.905972	Fatty Acyls
18	N-Acetylphenylalanine	Q-TOF Bruker	208.097	0.90469	Carboxylic acids and derivatives
19	Phytosphingosine	Q-TOF	318.301	0.899362	Organonitrogen compounds
Main MS spectral matches of GNPS library (Continuation)					

Tabela B.1 – Main MS spectral matches of GNPS library

N	Compound Name	Instrument	Precursor ion	MQSScore	Class
20	N-Acetyl-L-tyrosine	QQQ	224.092	0.899004	Carboxylic acids and derivatives
21	Phytosphingosine	Q-TOF	318.301	0.896112	Organonitrogen compounds
22	Cordycepin	HCD	252.109	0.888625	N/A
23	Sorbitane Monopalmitate - Polysorbate 40	qTof	402.36	0.888565	Fatty Acyls
24	Glycero-3-phosphocholine	LC-ESI-QTOF	258.111	0.887642	Glycerophospholipids
25	2,4-dihydroxyheptadec-16-enyl acetate	qTof	679.518	0.88512	Fatty Acyls
26	Benzenepropanamide	Q-TOF Bruker	445.212	0.882716	Carboxylic acids and derivatives
27	Diethyltoluamide	qTof	192.138	0.882528	Benzene and substituted derivatives
28	Dimethyldioctadecylammonium cation	IT/ion trap	550.64	0.881506	N/A
29	Hesperidin	LC-ESI-QTOF	611.198	0.877308	Flavonoids
30	Adenosine 3',5'-cyclic monophosphate	HCD	330.059	0.876347	N/A
31	Naringenin	LC-ESI-QTOF	273.076	0.868038	Linear 1,3-diarylpropanoids
32	Shearinine D	Q-Tof	600.34	0.76	N/A
33	Sorbitane Monostearate - Polysorbate 60	qTof	430.38	0.867819	Fatty Acyls
34	sulfanylpropanoic acid	qTof	631.184	0.865963	Fatty Acyls
35	Sorbitane Monostearate	qTof	430.38	0.86155	Fatty Acyls
36	Avobenzene	Q-TOF	311.165	0.859544	Linear 1,3-diarylpropanoids
37	Tyr-Leu	Q-TOF	295.165	0.852991	N/A
38	5'-Deoxy-5'-(methylsulfinyl)adenosine	qTof	314.09	0.851825	N/A
Main MS spectral matches of GNPS library (Continuation)					

Tabela B.1 – Main MS spectral matches of GNPS library

N	Compound Name	Instrument	Precursor ion	MQSScore	Class
39	Sorbitane Monopalmitate	qTof	402.36	0.848874	Fatty Acyls
40	Aspartame	LC-ESI-ITFT	295.129	0.842135	Carboxylic acids and derivatives
41	DL-Phenylalanine	QqQ	166.086	0.836769	N/A
42	L-phenylalanine	qTof	166.086	0.836746	Carboxylic acids and derivatives
43	Decaethylene glycol	QqQ	459.286	0.829802	N/A
44	Coproporphyrin I	HCD	655.27	0.829678	N/A
45	Coproporphyrin I	HCD	328.142	0.807899	N/A
46	Nonaethylene glycol	QqQ	415.253	0.804271	N/A
47	2,2-dimethyl-1,3-dihydroquinazolin-4-one	Q-TOF Bruker	177.102	0.803229	Diazanaphthalenes
48	dimethoxy-myricetin-3-O-pentoside	qTof	479.121	0.801826	N/A
Main MS spectral matches of GNPS library (Continuation)					

ANEXO C – Supplementary Information - Chapter 4

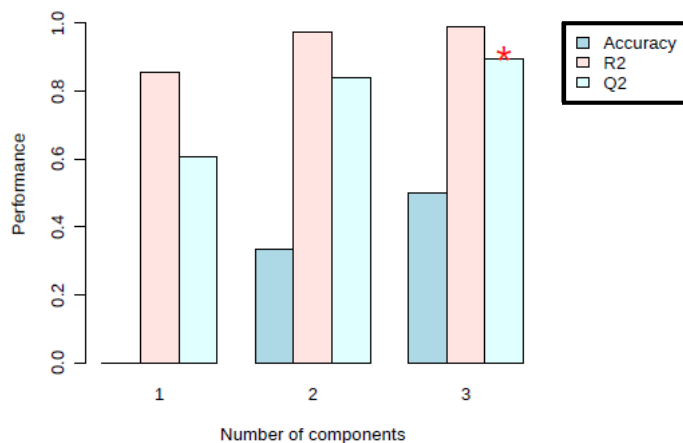


Figura C.1 – PLS-DA classification using different number of components (1, 2 and 3). The red star indicates the best classifier in Component 3. In this validated model, $R^2 \sim 0.9$, $Q^2 \leq 0.85$ and the accuracy $\sim 50\%$.

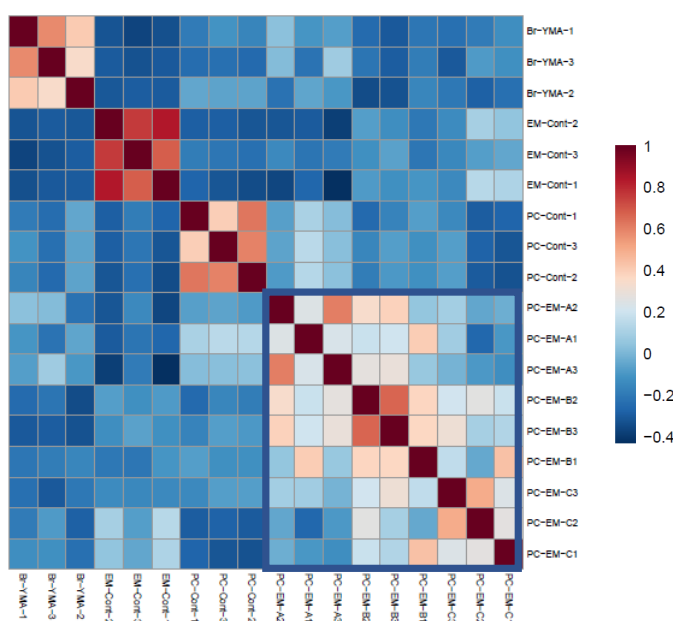


Figura C.2 – The correlation heatmap analysis can be used to visualize the overall correlations between different features. All the co-cultures samples are correlated (highlighted in a blue square). The mono-cultures are related to the replicates which also means good reproducibility. Dark red squares are related to high similarity and dark blue to high distinction.

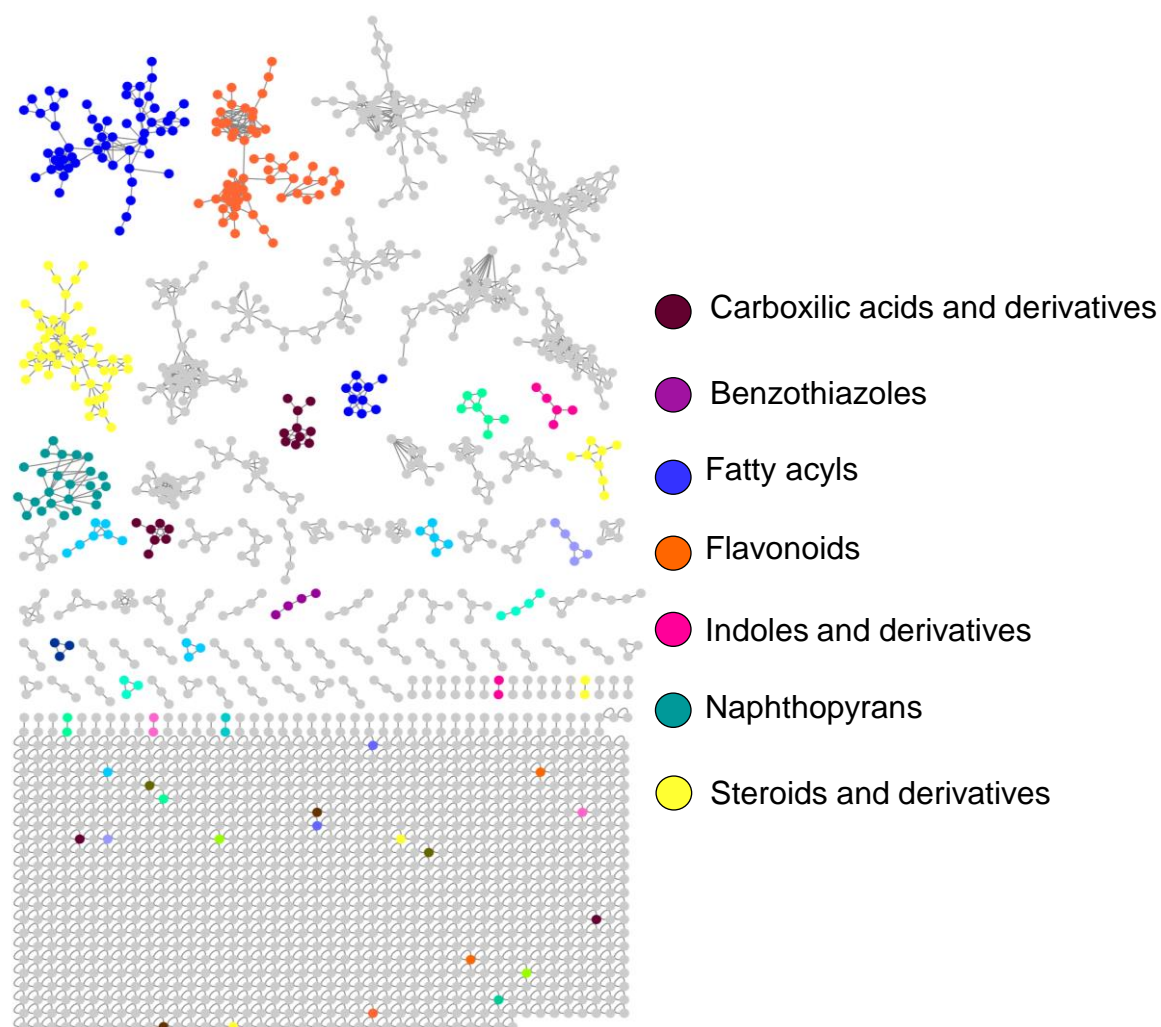


Figura C.3 – MolNetEnhancer: Enhanced molecular networks by integrating metabolome mining and annotation tools of LC-HRMS data of interaction between *P. capiguarae*, the black yeast, and the parasite *Escovopsis*. Different natural products classes were categorized: carboxylic acids (in brown), benzothiazoles (in purple), fatty acyls (in blue), flavonoids (in orange), indoles and derivatives (in pink), naphthopyrans (in green) and steroids and derivatives (in yellow). The non-match compounds are in grey.

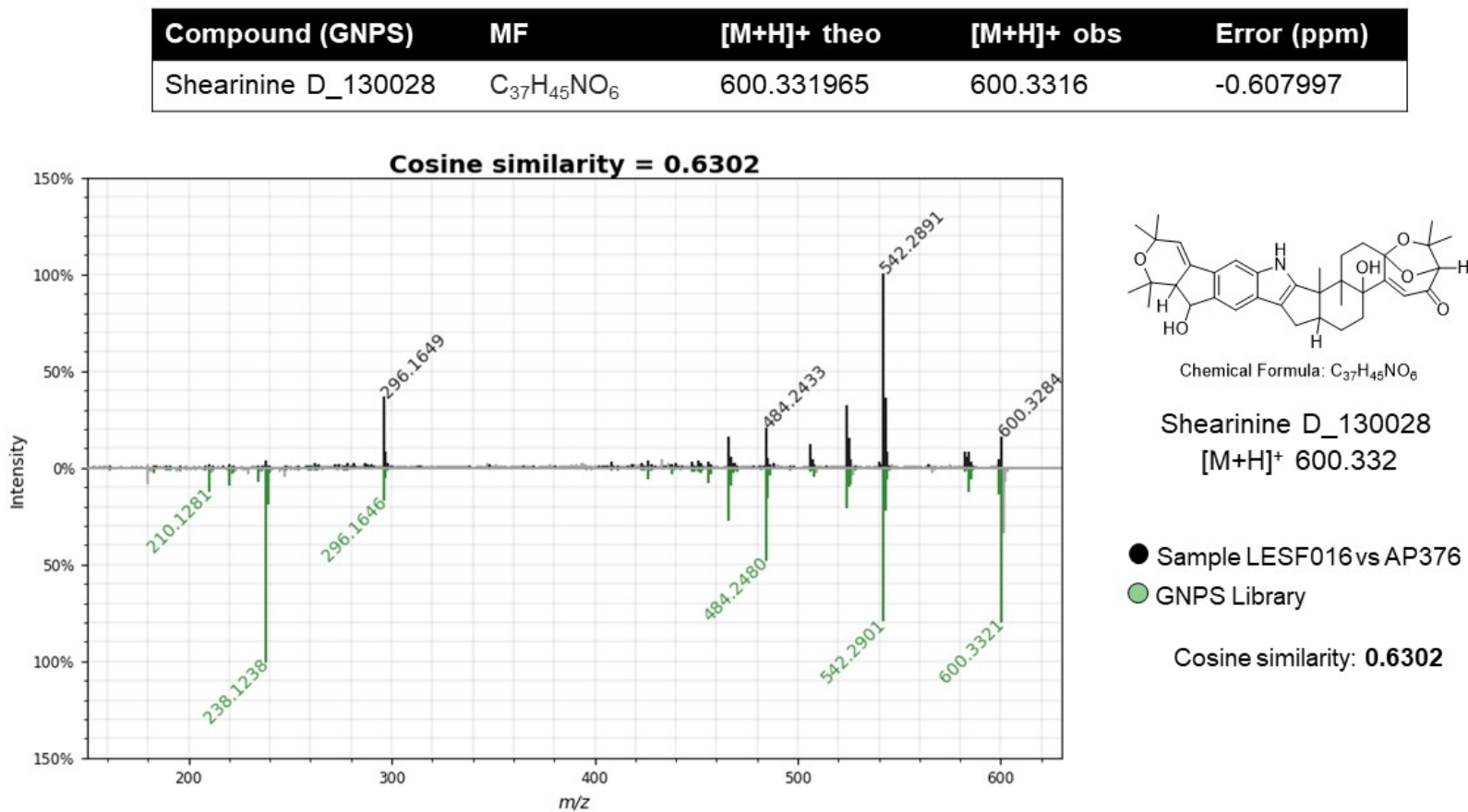


Figura C.4 – MS/MS comparison of compound 1 shearinine D from the extract of co-culture between AP376 with LESF016 (Silver spectrum) from GNPS spectral library (CCMSLIB00000478066) with 0.63 of cosine.

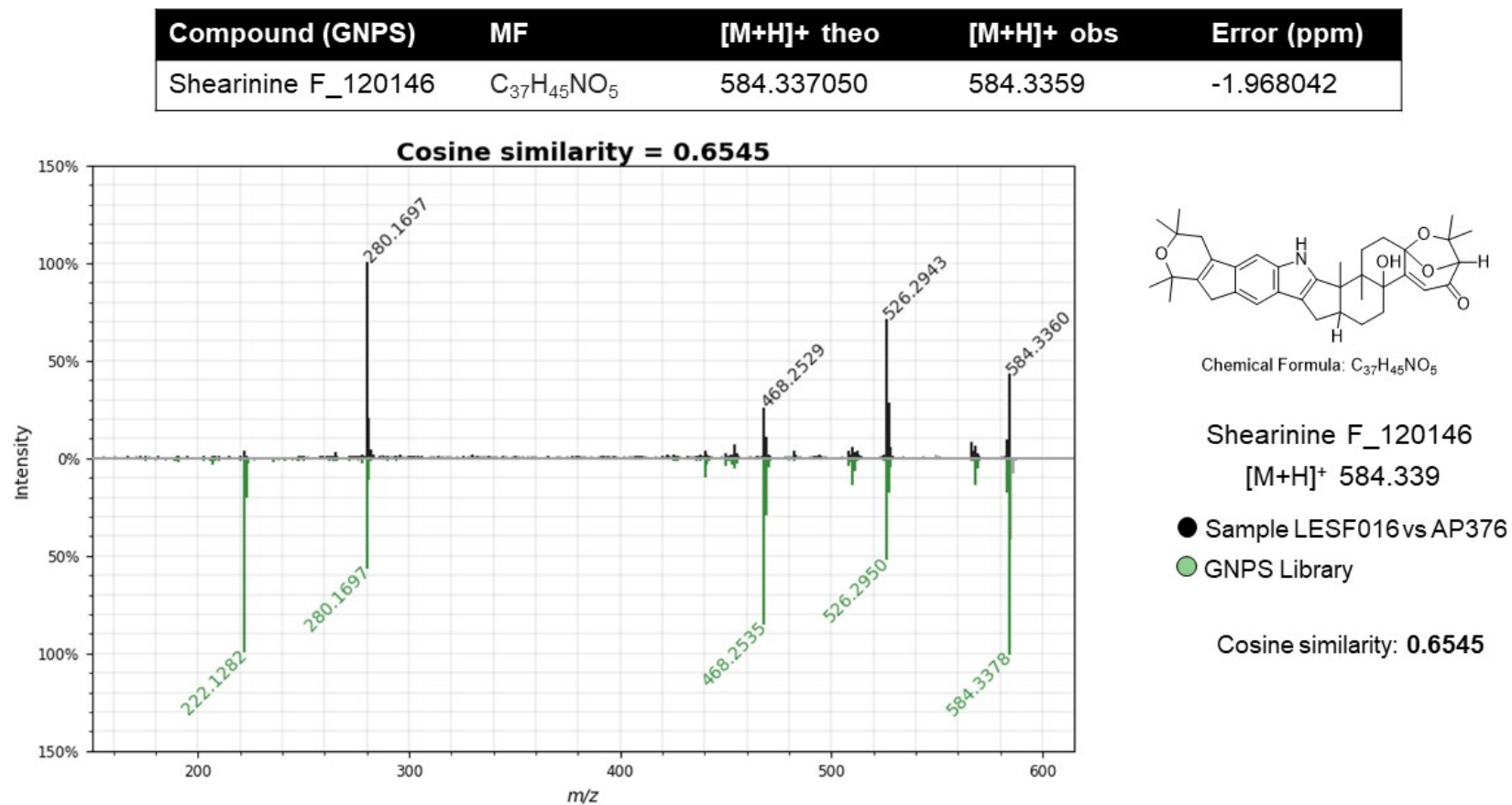


Figura C.5 – MS/MS comparison of compound 2 shearinine F from the extract of co-culture between AP376 with LESF016 (Silver spectrum) from GNPS spectral library (CCMSLIB00000478461) with 0.65 of cosine.

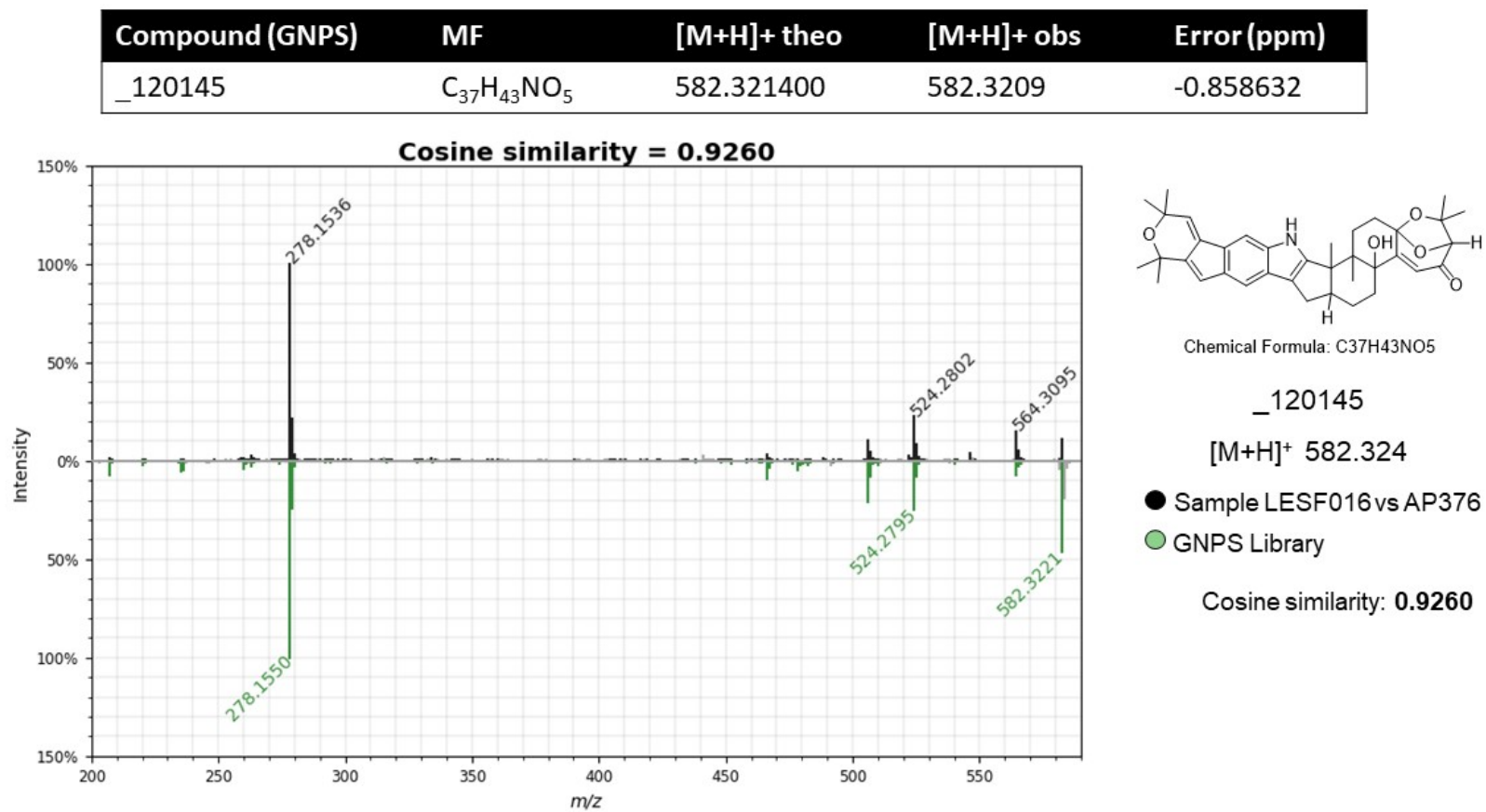


Figura C.6 – MS/MS comparison of compound 3 22,23-dehydro-shearinine A from the extract of co-culture between AP376 with LESF016 (Silver spectrum) from GNPS spectral library (CCMSLIB00000478065) with 0.92 of cosine.

Tabela C.1 – Shearinines MS spectral matches of GNPS library and analogous compounds. The retention time (RT), compound name, GNPS m/z , the precursor m/z , cosine, correlation to the annotated compound, Delta m/z in comparison to the annotated compound, molecular formula of and the metabolite class are detailed in the table below. n/a is the non-annotated compounds.

	RT (min)	Compound Name	GNPS m/z	precursor m/z	cosine	Correlation	MSI presence	Neutral molecular formula
1	21.06	Shearinine D	600.348	600.3311	0.63	-	-	C ₃₇ H ₄₅ NO ₆
2	24.88	Shearinine F	584.346	584.3442	0.65	-	-	C ₃₇ H ₄₅ NO ₅
3	19.18	22,23-dehydro-shearinine A	582.324	582.3223	0.92	-	-	C ₃₇ H ₄₃ NO ₅
4	20.61	n/a	748.4	748.4036	n/a	1	yes	-
5	21.85	n/a	736.361	736.3575	n/a	2	yes	-
6	12.89	n/a	785.402	786.3691	n/a	3	yes	-

	MSI m/z	Proposal Molecular formula	Theoretical [M+H] ⁺	MS/MS	Error (ppm)
1	-	-	600.331965	524 [100], 466 [54], 540 [39], 296 [36], 482 [9]	-0.61
2	-	-	584.33705	280 [100], 526 [53], 584 [28], 468 [19], 566 [13]	-1.97
3	-	-	582.3214	524 [100], 466 [21], 438 [19], 451 [8], 278 [7]	-0.85
4	748.48317	C ₄₈ H ₆₂ NO ₉	748.480975	690 [100], 386 [41], 466 [40], 524 [29], 632 [26]	5.3
5	736.35732	C ₄₄ H ₅₀ NO ₉	736.359242	678 [100%], 432 [91], 734 [72], 356 [56], 602 [36]	7.1
6	785.40475	C ₄₈ H ₅₁ NO ₉	785.403453	785 [100], 727 [65], 699 [24], 641 [15], 670 [10]	4.9

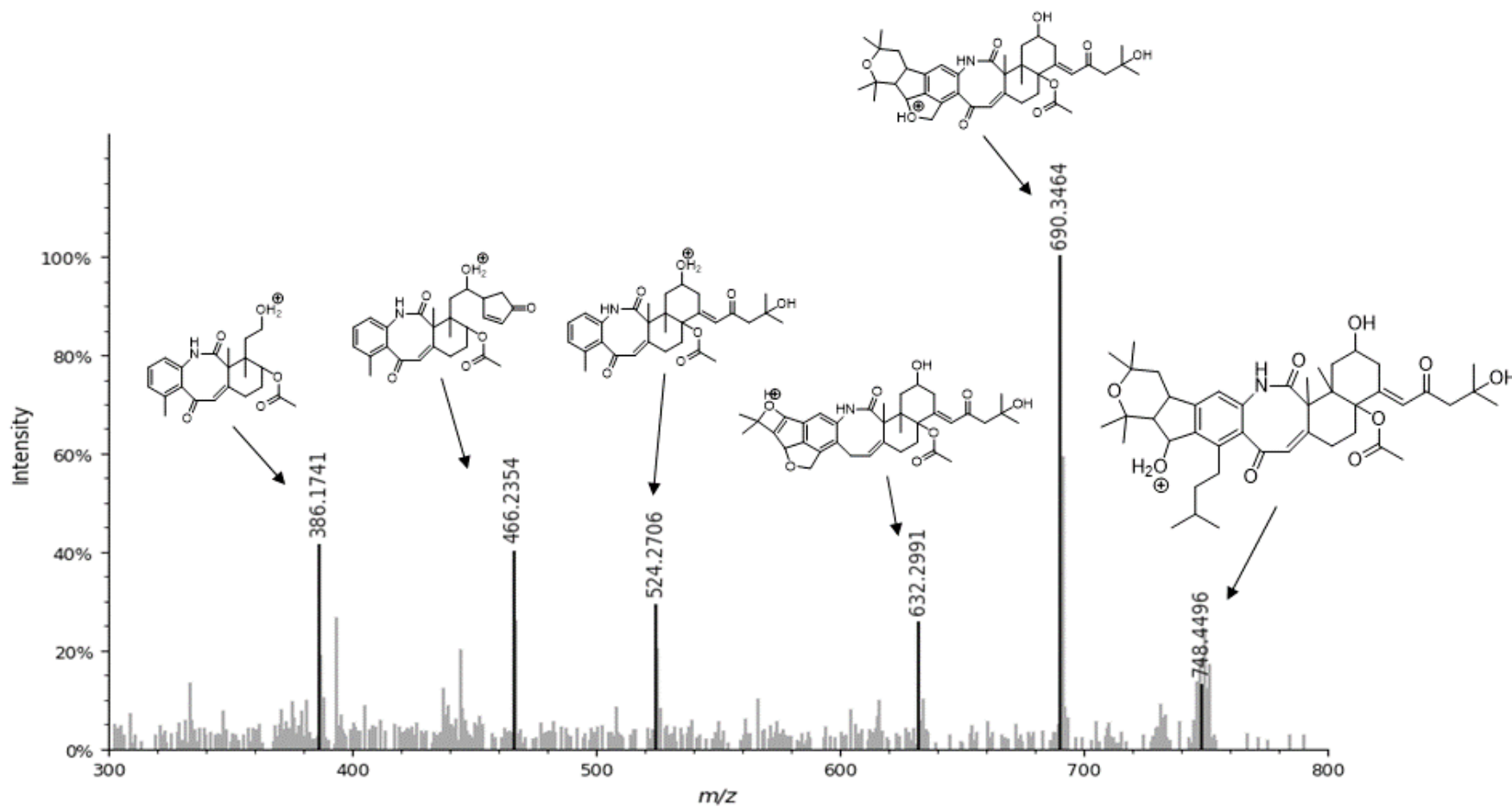


Figura C.7 – MS/MS fragmentation of compound m/z 748 from the extract of co-culture between PC (AP376) with EM (LESF016).

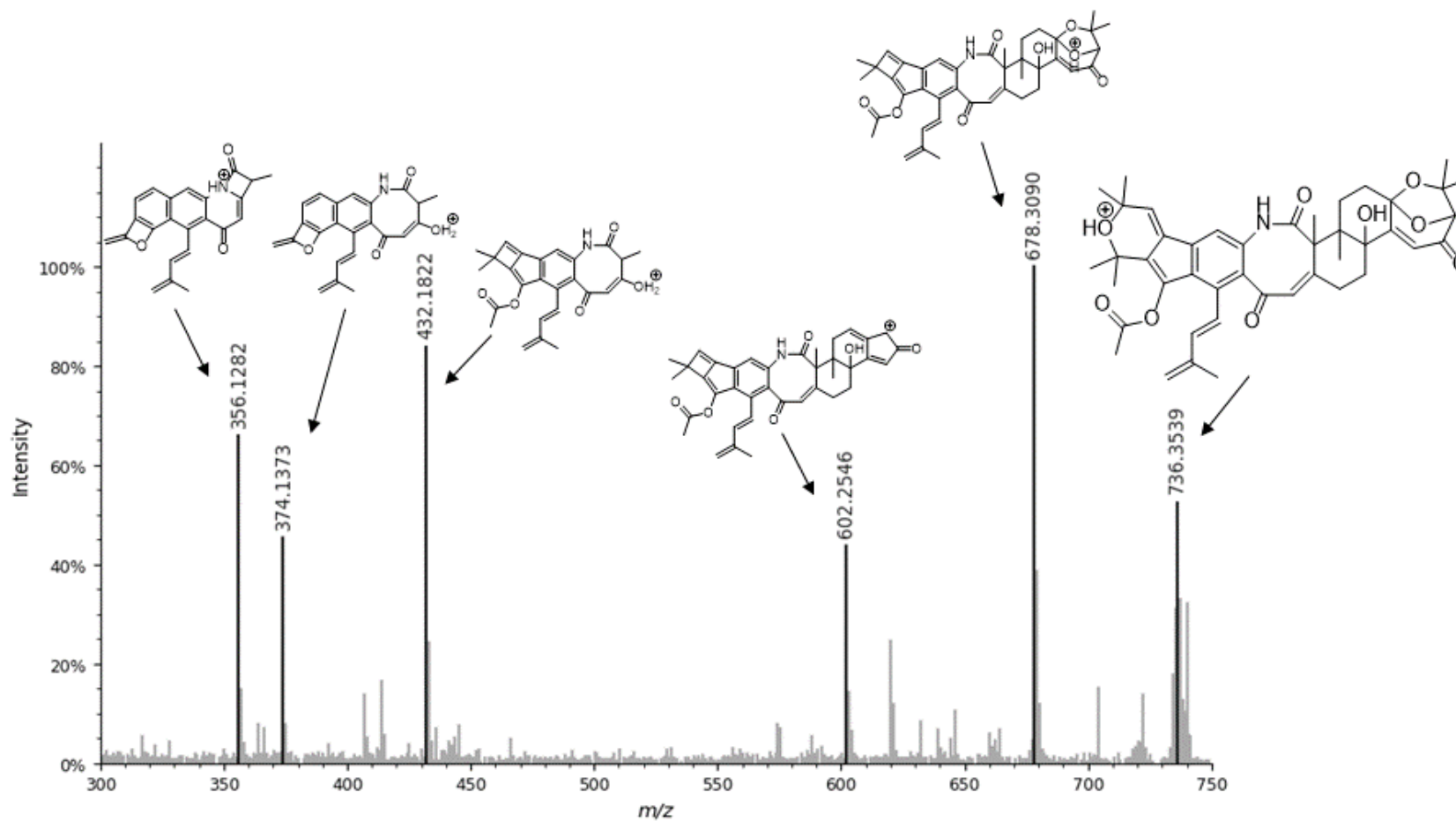


Figura C.8 – MS/MS fragmentation of compound m/z 736 from the extract of co-culture between PC (AP376) with EM (LESF016).

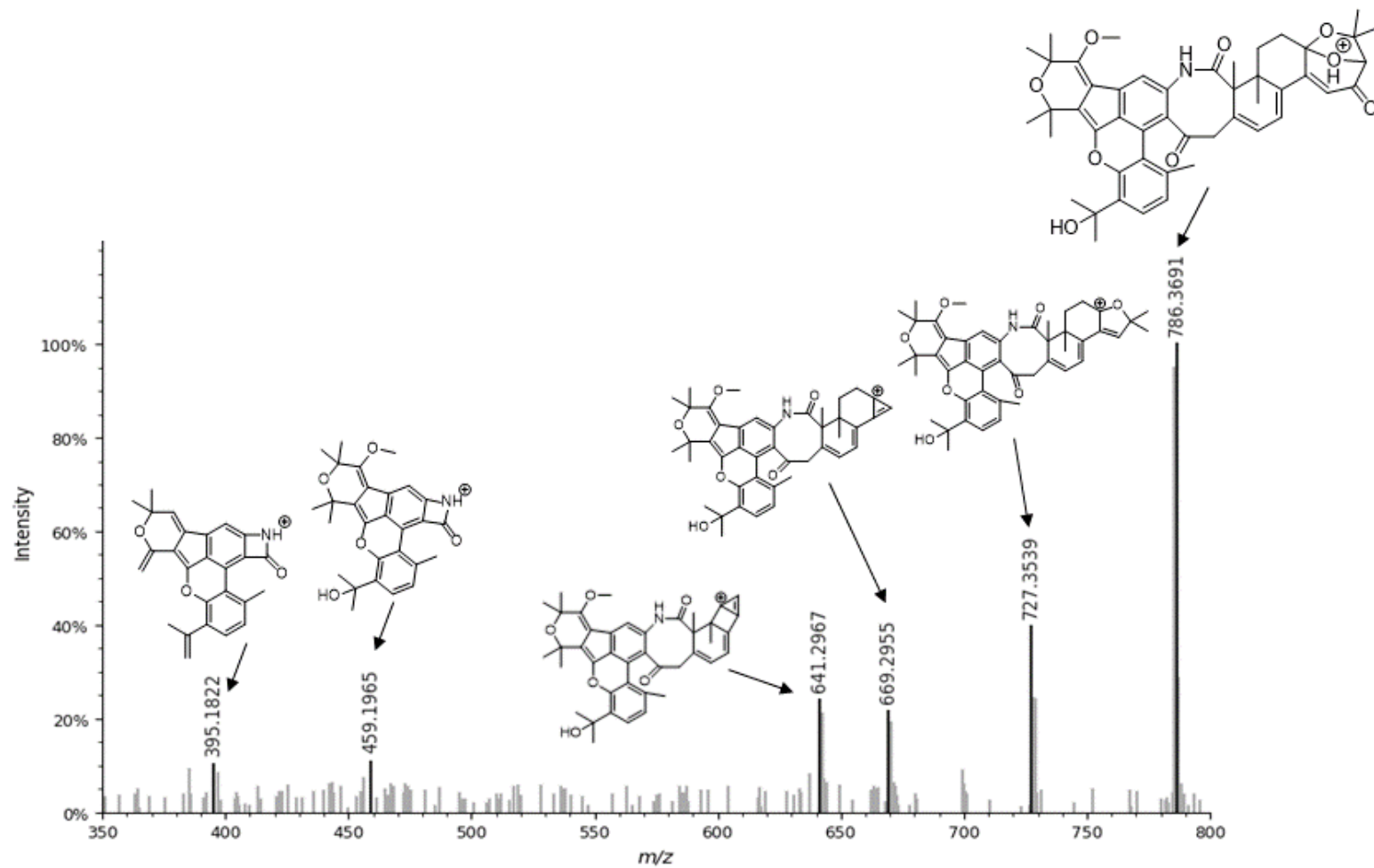


Figura C.9 – MS/MS fragmentation of compound m/z 786 from the extract of co-culture between PC (AP376) with EM (LESF016).

ANEXO D – Supplementary Information - Chapter 5

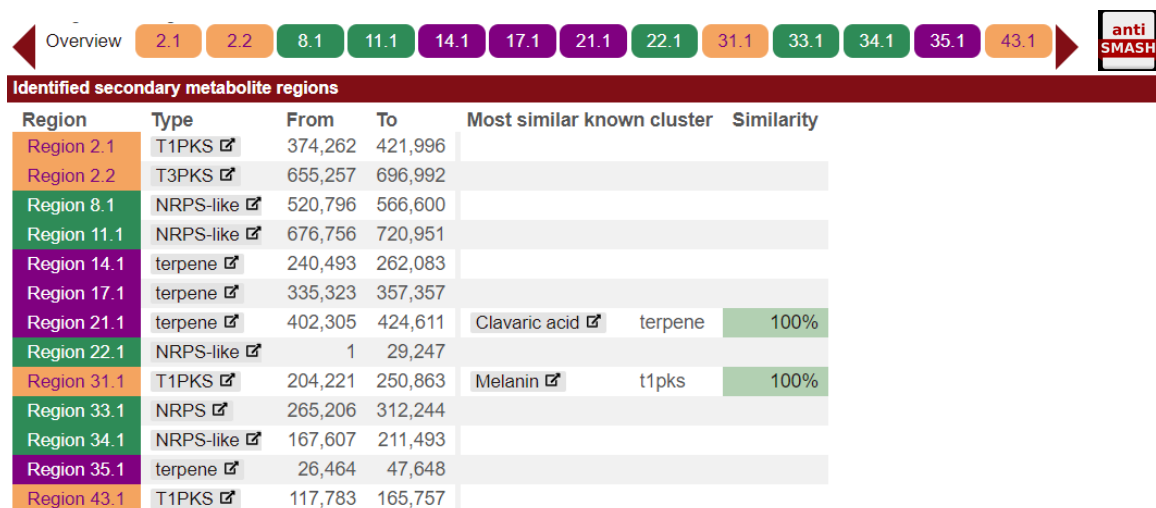


Figure D.1 – Antismash analysis of *P. atiae* strain in NCBI data bank. This strain presents NRPS, terpene and PKS types of secondary metabolites. Metabolites as clavarinic acid and melanin were identified by gene cluster comparison.

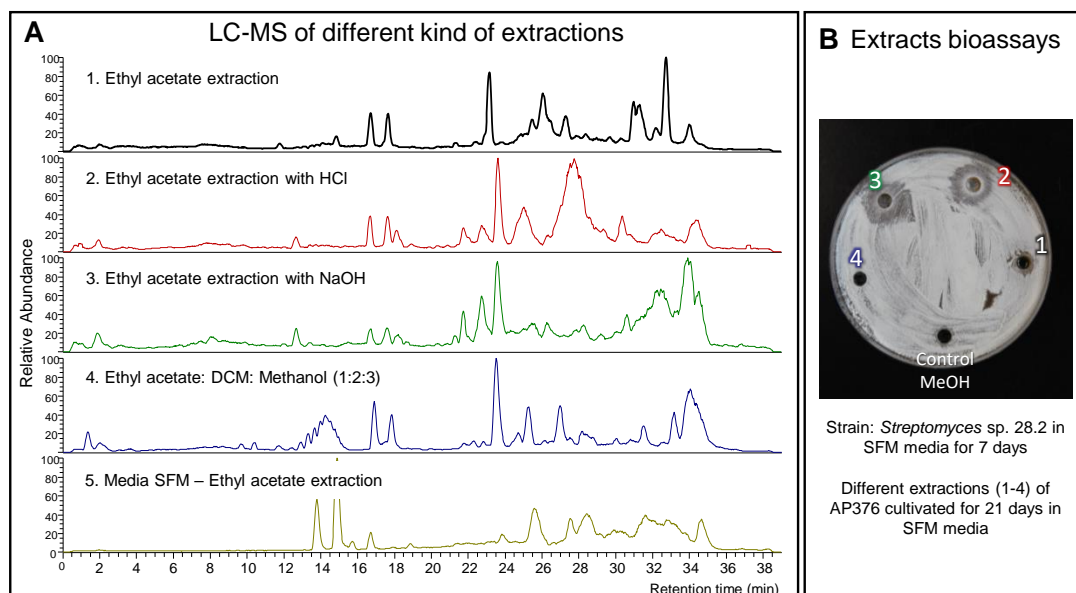


Figure D.2 – A) LC-profile of different extractions: ethyl acetate (EA) extraction (1), acid EA extraction (2), basic EA extraction (3), ethyl acetate: dichloromethane: methanol (3:2:1). B) bioactivity against *Streptomyces* sp. The extracts were solubilized in methanol (MeOH) and the negative control was performed in this solvent.



Figura D.3 – Differences between the bioassay against *Streptomyces* 28.2 and *Pseudonocardia* W3 according to the time. The inhibition disappeared in 3 days in the bioassay against *Streptomyces* 28.2 (in the left) and the inhibition zone remained the same even after a month of incubation (in the right). This kind of bioactivity means that extract activity does not change or degrade over time.

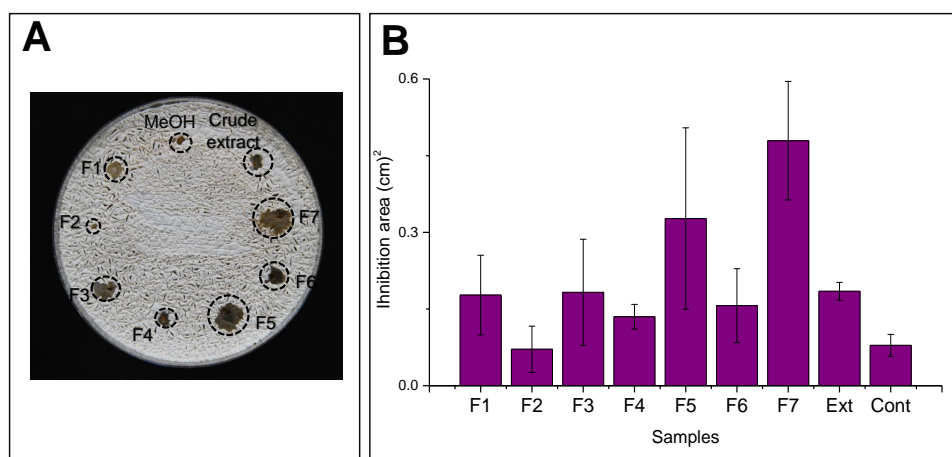


Figura D.4 – A) The bioassays against *Pseudonocardia* W3 sp. using the different fractions 1 to 7. B) Statistic analysis based in inhibition zone area observed on AP376 extracts bioassays. Bioassays shows a clear inhibition zone in F5 and F7. The material referent of F7 was not enough to proceed with purification.

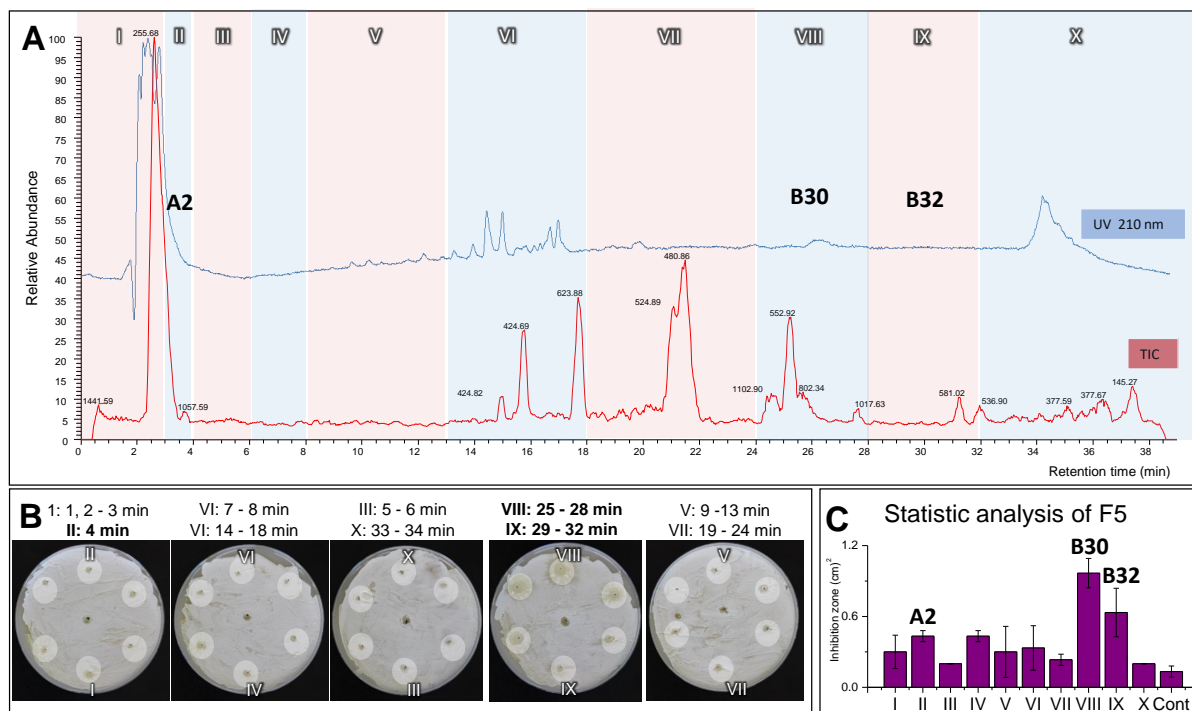


Figura D.5 – A) Base peak and UV (250 nm) chromatogram of the RP C18 HPLC separation of bioactive silica column F5. The red and blue sections is related to the collecting time using semi-prep-HPLC. B) The subfractions were tested against the actinomycete. C) Statistical analysis of the subfractions.

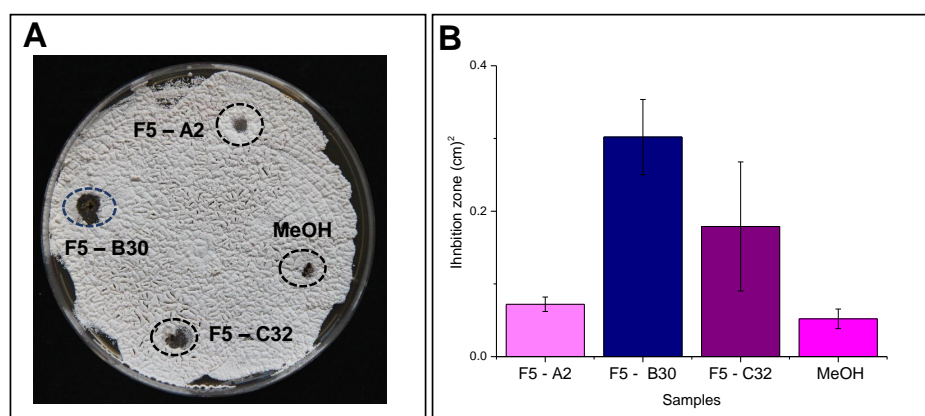


Figura D.6 – A) Bioassays of the three different sub-fractions of fraction 5 (F5) and statistical analysis of bioactivity against *Pseudonocardia* sp. W3. F5-A2 was collected in 2 min, F5-B30 in 30 and F5-32 in 32 min over LC-run. B) Statistic analysis based in inhibition zone area observed on different sub-fractions of F5 bioassays. *The inhibitions are showed based on the area of inhibition. The samples names are based on the retention time (min) and the M means the media of the inhibition zone area.

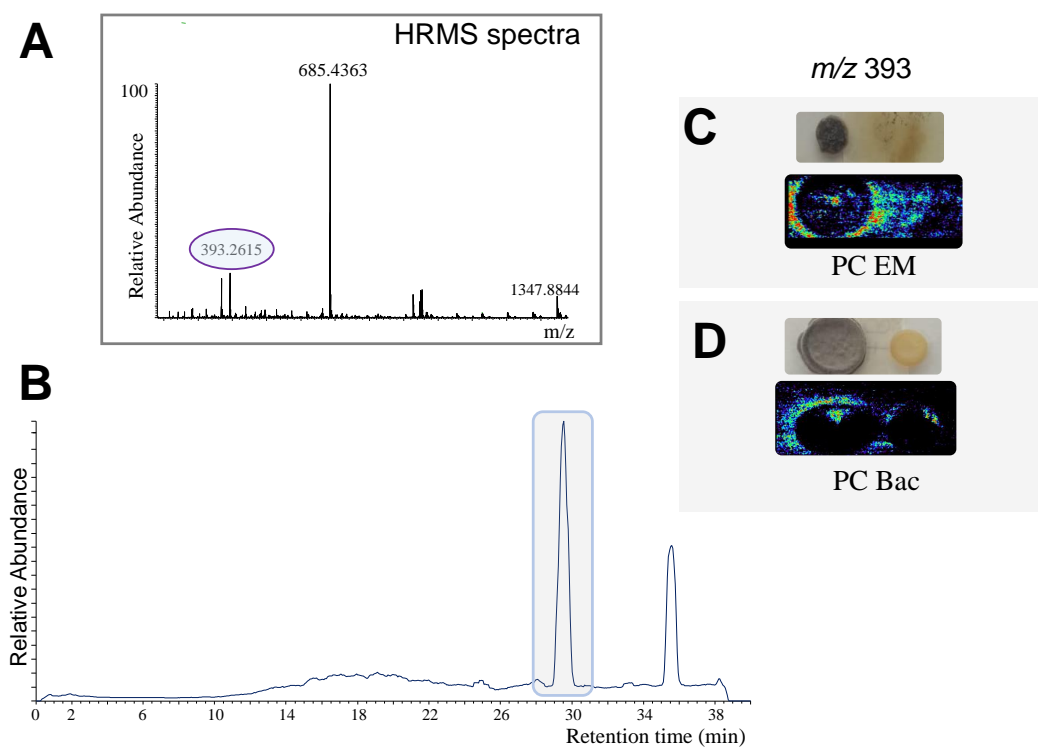


Figura D.7 – Compound F5-30 isolated of black yeast *P. capiguarae*. A) HRMS info can be seen in m/z 393. B) LC profile of the compound. C) MSI between the black yeast (PC) and parasite *Escovopsis* (EM) D) MSI between the black yeast (PC) and actinobacterium *Pseudonocardia* sp. (Bac).

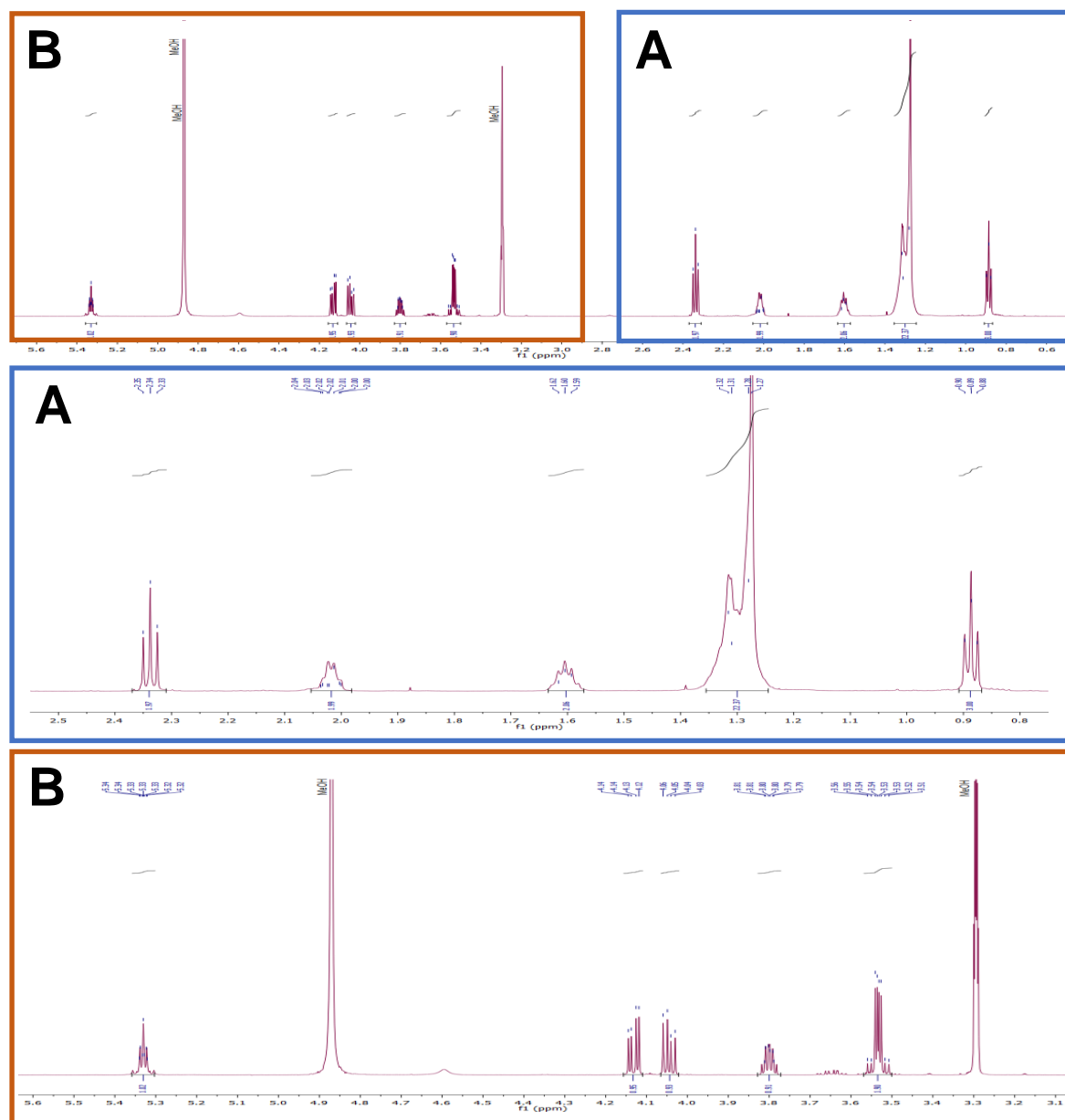


Figure D.8 – ^1H NMR spectrum of F5-B30 in methanol- d_4 (600 MHz). The spectra above is the complete 0 to 6 ppm. (A) Detail view from spectrum region of 0 to 2.5 ppm and (B) Detail view from spectrum region of 3 to 5.6 ppm.

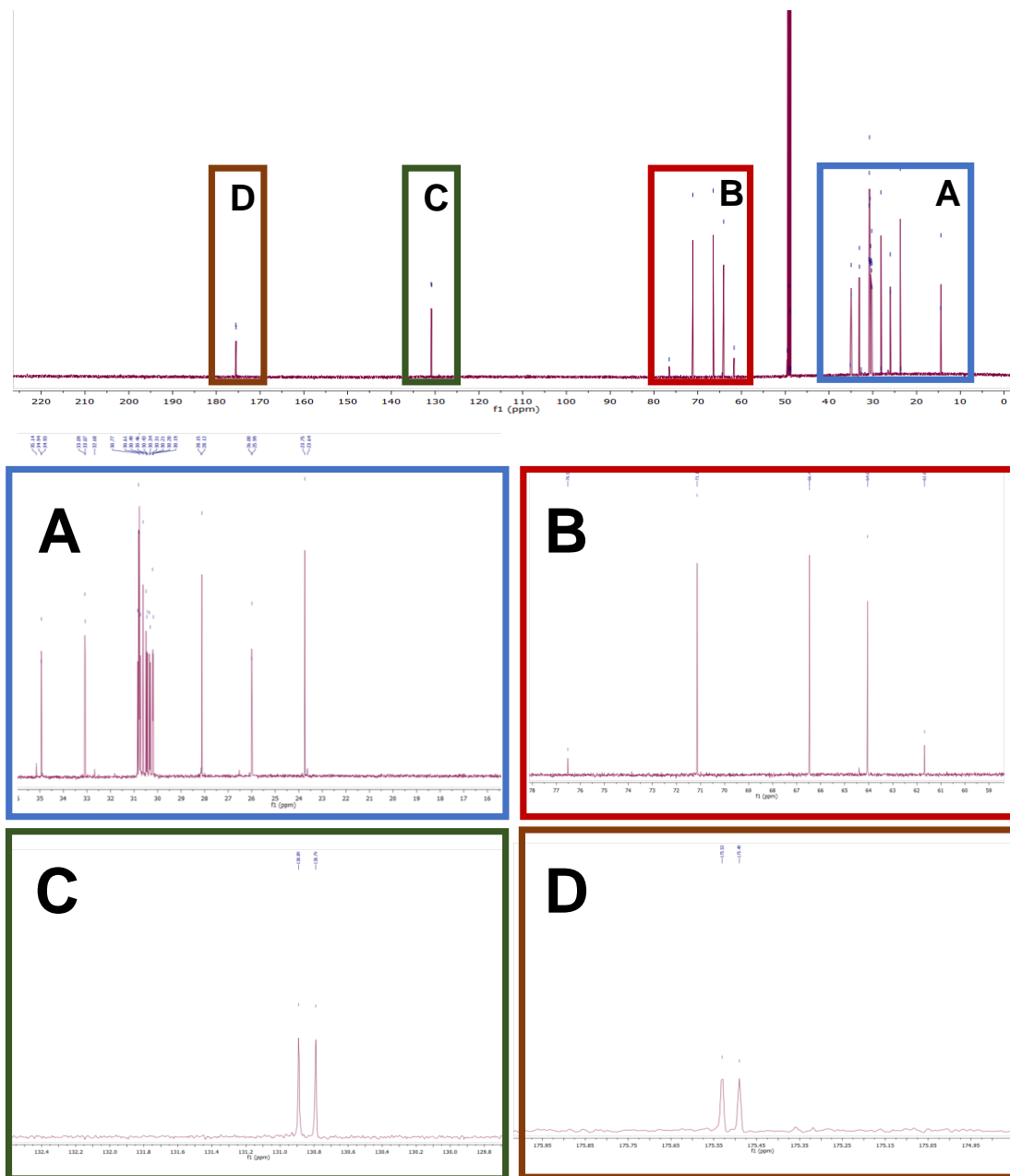


Figure D.9 – ^{13}C NMR spectrum of F5-B30 in methanol- d_4 (150 MHz). The complete spectra is shown above. (A) Detail view from spectrum region of 0 to 35 ppm. (B) Detail view from spectrum region of 60 to 78 ppm. (C) Detail view from spectrum region of 174 to 175 ppm.

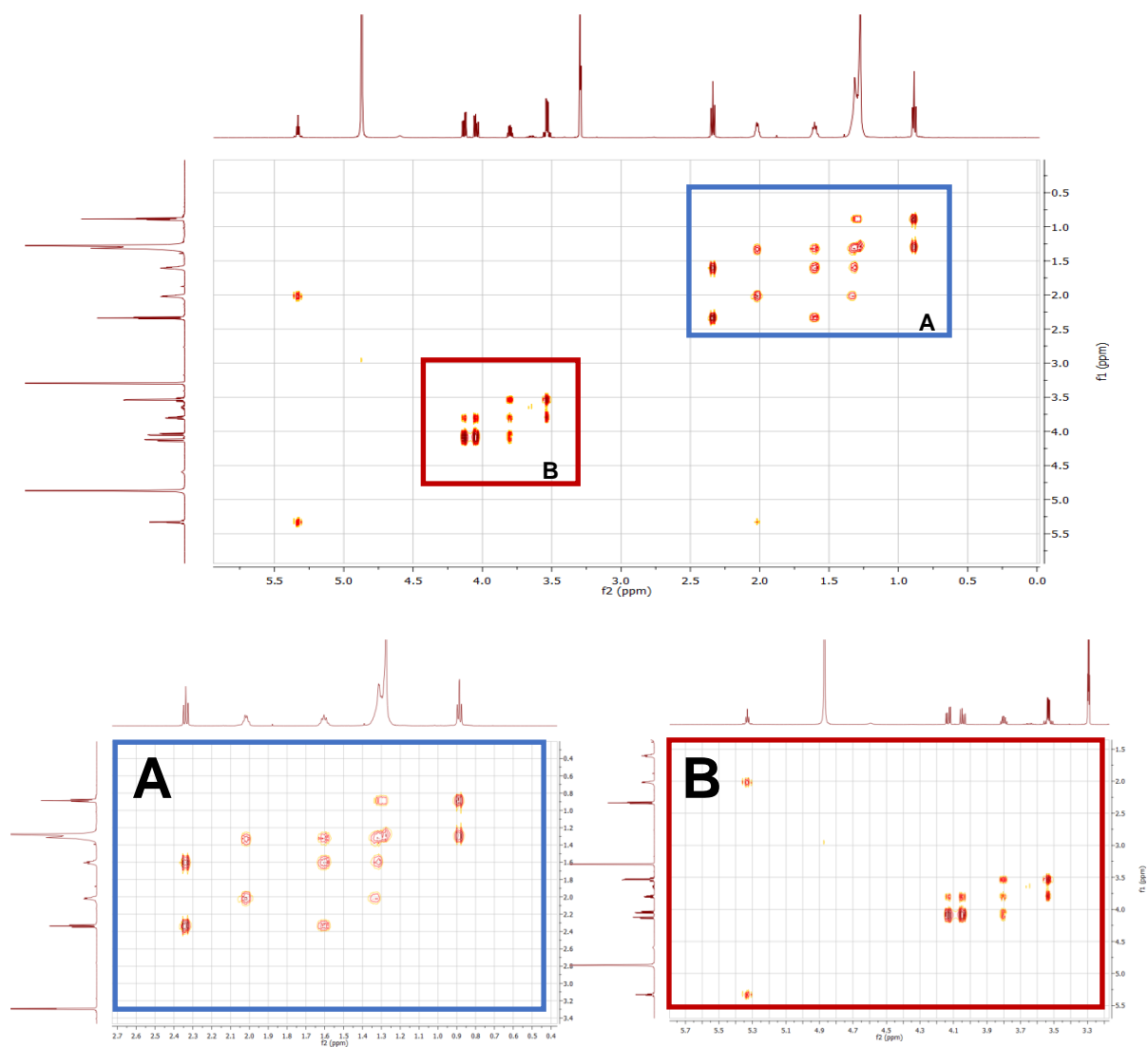


Figura D.10 – ^1H - ^1H COSY NMR spectrum of F5-B30 in methanol- d_4 (600 MHz).

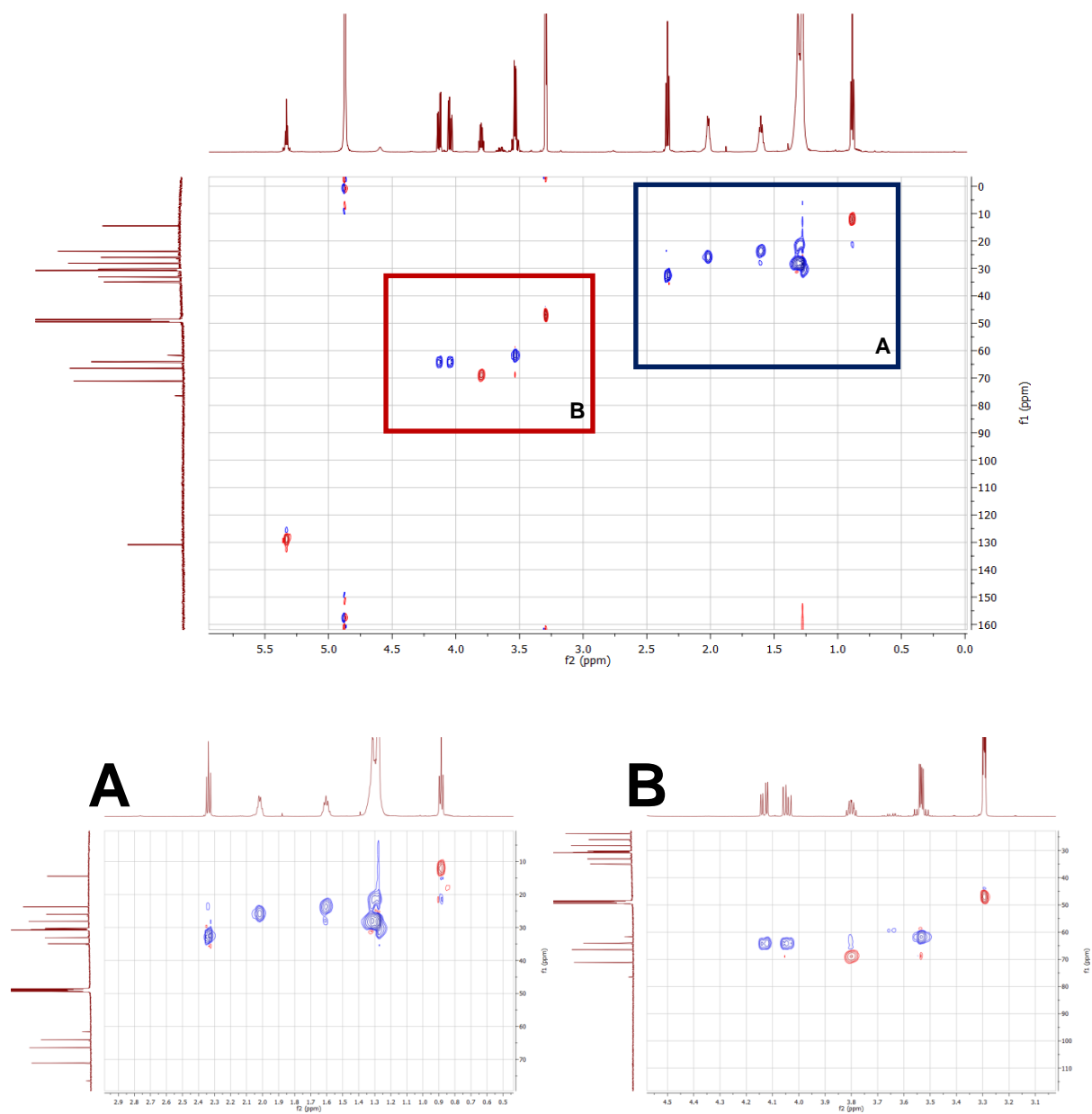


Figura D.11 – HSQC NMR 2D spectrum of F5-B30 in methanol- d_4 (600 MHz). Expansion HSQC NMR spectrum of F5-B30 of the aliphatic part.

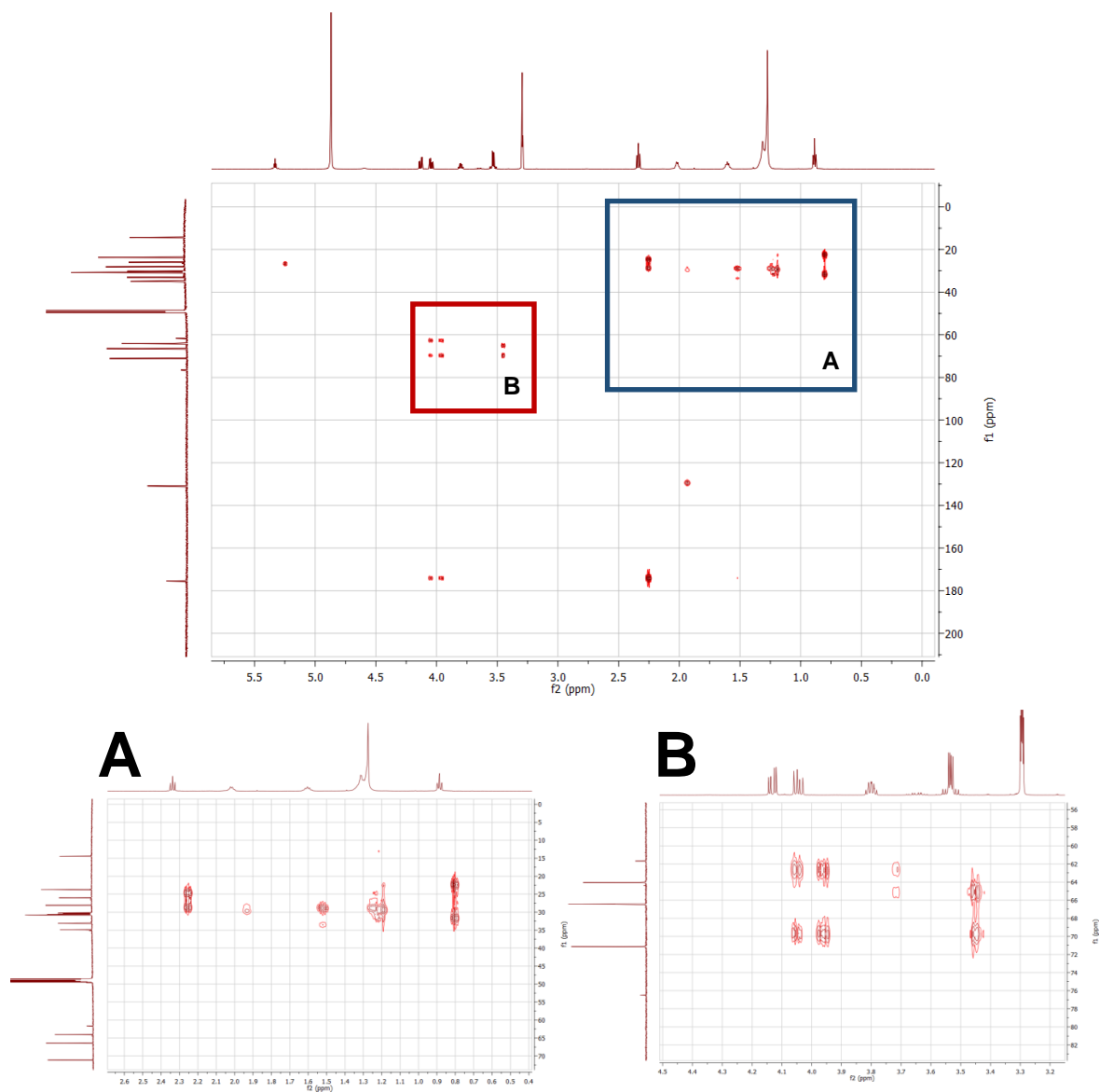


Figura D.12 – HMBC NMR 2D spectrum of F5-B30 in methanol- d_4 (600 MHz). (A) Expansion of HMBC NMR spectrum of F5-B30 of the aliphatic part.